

# Tessellations and Speiser graphs arising from meromorphic functions on simply connected Riemann surfaces

Alvaro Alvarez–Parrilla<sup>a</sup>, Jesús Muciño–Raymundo<sup>b</sup>

<sup>a</sup>Grupo Alximia SA de CV, Ryerson 1268, Ensenada, 22800, Baja California, México

<sup>b</sup>Centro de Ciencias Matemáticas, Universidad Nacional Autónoma de México, Morelia, Michoacán, México

---

## Abstract

Motivated by W. P. Thurston, we ask: What is the shape of a meromorphic function on a simply connected Riemann surface  $\Omega_z$ ? We consider Speiser functions, *i.e.* meromorphic functions on a simply connected Riemann surface, that have a finite number  $q \geq 2$  of singular (critical or asymptotic) values. As a first result, we make precise the correspondence between: Speiser functions  $w(z)$ , Speiser Riemann surfaces  $\mathcal{R}_{w(z)}$ , Speiser  $q$ –tessellation, and analytic Speiser graphs of index  $q$ . As the second main result, we characterize tessellations with alternating colors (equivalently abstract pre–Speiser graphs) that are realized by Speiser functions on  $\Omega_z$ . The characterization is in terms of the  $q$ –regular extension problem of bipartite planar graphs. As third main results, the Speiser Riemann surface  $\mathcal{R}_{w(z)}$  can be constructed by isometric glueing of a finite number of types of sheets, where each sheet is a maximal domain of single–valuedness of  $w^{-1}(z)$ . Furthermore, a unique decomposition of  $\mathcal{R}_{w(z)}$  into maximal logarithmic towers and a soul is provided. Using vector fields we recognize that logarithmic towers come in two flavors: exponential or  $h$ –tangent blocks, directly related to the exponential or the hyperbolic tangent functions on the upper half plane. The surface  $\mathcal{R}_{w(z)}$  of a finite Speiser function is characterized by surgery of a rational block and a finite number of exponential or  $h$ –tangent blocks.

**Keywords:** Riemann surfaces, Speiser functions, tessellations, Speiser graphs, essential singularities, logarithmic singularities, vector fields

**2020 MSC:** Primary: 30D30, Secondary: 32S65, 34M05

---

## Contents

<b>1</b>	<b>Introduction</b>	<b>2</b>
1.1	Brief statement of the results	2
1.2	Accurate results and comments	3
1.3	Epilogue	6
<b>2</b>	<b>Singularities of the inverse for meromorphic functions</b>	<b>7</b>
<b>3</b>	<b>Speiser functions</b>	<b>8</b>
3.1	Speiser functions: notation for singular values and singular points	10
3.2	$N$ –functions: only a finite number of logarithmic singularities and no algebraic singularities	11
<b>4</b>	<b>Speiser Riemann surfaces</b>	<b>12</b>
4.1	Surgery of Riemann surfaces	12
<b>5</b>	<b>Schwarz–Klein–Speiser tessellations</b>	<b>15</b>
5.1	Schwarz–Klein–Speiser’s algorithm	18

<b>6 Speiser graphs</b>	<b>23</b>
6.1 Duality: Tessellations and Speiser graphs . . . . .	24
6.2 Speiser graphs for $N$ -functions . . . . .	26
<b>7 A complete correspondence</b>	<b>29</b>
<b>8 When does a pre-Speiser graph represent a Speiser function?</b>	<b>30</b>
8.1 Certain constraints on the extension of pre-Speiser graphs to Speiser graphs. . . . .	31
8.2 Necessary and sufficient conditions for a pre-Speiser graph to be extendable to a Speiser graph of index $q$ . . . . .	33
8.3 W. P. Thurston <i>et al.</i> 's approach . . . . .	34
8.4 J. Tomasini's approach . . . . .	35
<b>9 Geometrical decomposition of Speiser functions</b>	<b>37</b>
9.1 The pieces: flat $p$ -gons, maximal logarithmic towers, the soul . . . . .	37
9.2 Characterization of finite Speiser functions on $\Omega_z = \mathbb{C}_z, \widehat{\mathbb{C}}_z$ . . . . .	46
<b>10 Examples</b>	<b>46</b>

## 1. Introduction

### 1.1. Brief statement of the results

Let  $w(z) : \Omega_z \longrightarrow \widehat{\mathbb{C}}_w$  be a meromorphic function on the simply connected Riemann surface  $\Omega_z$ , *i.e.* the Riemann sphere  $\widehat{\mathbb{C}}_z$ , the complex plane  $\mathbb{C}_z$ , or the Poincaré unit disk  $\Delta_z$ . Allow us first to summarize the main results.

A) On  $\Omega_z$ , we provide a bijective correspondence between:

- 1) *Speiser functions* with  $q \geq 2$  singular values.
- 2) *Speiser Riemann surfaces*.
- 3) *Speiser  $q$ -tessellations*.
- 4) *Analytic Speiser graphs of index  $q$* .

B) We answer the question

*What is the shape of a Speiser function on  $\Omega_z$ ?*

by characterizing when an abstract *pre-Speiser graph* represents a Speiser function. The solution presented in terms of Hall-type inequalities arises from the *bipartite transportation problem*.

C) We provide a decomposition of Speiser Riemann surfaces into *maximal logarithmic towers* and a *soul*. This decomposition is unique and provides another answer to Question (B):

*the shape of a Speiser function is its soul.*

Moreover,

*finite Speiser functions are those that can be constructed by surgery of maximal logarithmic towers and a soul arising from a rational function.*

A few words on the above is in order.

Most of (A) is classical, we fill in the details to provide a structured and modern approach that allows us to prove (B) and (C).

Question (B) was first answered by W. P. Thurston for the generic<sup>1</sup> rational functions on  $\widehat{\mathbb{C}}_z$ , we present an answer valid for all Speiser functions (which of course include rational functions).

Decomposition (C) is reminiscent of the dichotomy between Fatou and Julia sets; in the sense of presenting regions where a function behaves *tame*  $\longleftrightarrow$  maximal logarithmic towers, or *wild*  $\longleftrightarrow$  soul. It is to be noted that maximal logarithmic towers arise from considering the accurate behaviour of exponential or hyperbolic tangent functions near the essential singularity at  $\infty \in \widehat{\mathbb{C}}_z$ .

---

<sup>1</sup>Generic means that it only has simple critical points.

## 1.2. Accurate results and comments

Recalling W. P. Thurston's question on rational functions on  $\widehat{\mathbb{C}}_z$ , see [1], [2], it is natural to extend it to:

*What is the shape of a meromorphic function on  $\Omega_z$ ?*

In order to answer the above question, we restrict ourselves to the family of *Speiser functions*, which are meromorphic functions  $w(z)$  on  $\Omega_z$  with a finite set of  $q \geq 2$  distinct singular values in  $\widehat{\mathbb{C}}_w$ . This is a large family that includes rational functions on  $\widehat{\mathbb{C}}_z$ , and many transcendental functions on  $\Omega_z = \mathbb{C}_z$  or  $\Delta_z$ .

As an appropriate first answer to the “shape of a Speiser function”, we propose a *Speiser  $q$ -tessellation*, which is the output of the *Schwarz–Klein–Speiser's algorithm* (see §5.1), with roots in the works of H. A. Schwarz [3], F. Klein [4], A. Speiser [5]; as far as we known, studied by R. Nevanlinna [6]. We briefly describe the algorithm as follows. Let  $\gamma$  be a Jordan path through the cyclically ordered singular values  $\mathcal{W}_q \doteq [w_1, \dots, w_q]$ , and consider the pullback graph

$$w^*(\gamma) = \widehat{\Gamma}_q.$$

Then, the underlying Speiser  $q$ -tessellation, Definition 5.10, is

$$\mathcal{T}_\gamma(w(z)) = (\Omega_z \cup \partial_I \Omega_z) \setminus \widehat{\Gamma}_q = \underbrace{T_1 \cup \dots \cup T_\alpha \cup \dots}_{n \text{ blue tiles}} \cup \underbrace{T'_1 \cup \dots \cup T'_\alpha \cup \dots}_{n \text{ grey tiles}}, \quad 2 \leq n \leq \infty,$$

with a *consistent  $q$ -labelling*  $\mathcal{L}_{W_q}$  of the vertices of the graph  $\widehat{\Gamma}_q$ , where  $\partial_I \Omega_z$  denotes the *ideal boundary* of  $\Omega_z$  depending on  $w(z)$ , namely see Proposition 3.3. Summarizing,

given a Speiser function  $w(z)$ , provided with a cyclic order  $\mathcal{W}_q$ ,  
on its singular values, the Schwarz–Klein–Speiser's algorithm determines  
a Speiser  $q$ -tessellation  $(\underbrace{\mathcal{T}_\gamma(w(z))}_{\text{tessellation}}, \underbrace{\mathcal{L}_{W_q}}_{\substack{\text{consistent} \\ \text{q-labelling}}})$ .

The tessellation consists of tiles that are topological  $q$ -gons with alternating colors, see [7], [2], [8] and [9]. It provides a simple and straightforward visual description of the Speiser function  $w(z)$ ; in particular, if  $\gamma = \mathbb{R} \cup \{\infty\}$ , then it is clear that set theoretically  $\widehat{\Gamma}_q$  is a real analytic curve simply given by  $\{\Im(w(z)) = 0\}$ .

We call the naturally associated underlying graph  $\widehat{\Gamma}_q$  an *A-map*. Thus, the Speiser  $q$ -tessellation is equivalent to

$$(\widehat{\Gamma}_q, \mathcal{L}_{W_q}).$$

A clear understanding of this structure, naturally leads, through duality, to *analytic Speiser graphs of index  $q$* ,

$$(\underbrace{\mathfrak{S}_{w(z)}}_{\text{graph}}, \underbrace{\mathcal{L}_{W_q}}_{\substack{\text{consistent} \\ \text{q-labelling}}}).$$

In plain words, an analytical Speiser graph of index  $q$  in  $\Omega_z$ , is a countable, connected, bipartite, planar multigraph<sup>2</sup> with vertices  $\times$  and  $\circ$ , each with valence  $q$ , whose  $w_j$ -faces in  $\Omega_z$  are labelled cyclically with  $\mathcal{L}_{W_q}$ , so that the labelling follows a clockwise order around  $\times$  and anticlockwise order around  $\circ$ ; see [6] and [10] ch. 4 for examples. Furthermore, it is required that for each  $w_j \in \mathcal{W}_q$  at least one  $w_j$ -face is not a digon. See Definitions 6.1 and 6.5 for full details.

The analytical Speiser graph  $\mathfrak{S}_q$  of index  $q$  structure provides an equivalent answer to the “shape of a Speiser function”. The Speiser 3-tessellations on  $\widehat{\mathbb{C}}_z$  with  $\mathcal{W}_3 = [0, 1, \infty]$  are naturally equivalent to the celebrated dessins d'enfants, see [11] for that theory.

Furthermore, the *Speiser Riemann surface*

$$\mathcal{R}_{w(z)} \doteq \{(z, w(z))\} \subset \Omega_z \times \widehat{\mathbb{C}}_w,$$

associated to a Speiser function  $w(z)$ , see Definition 3.1.2, is a powerful tool towards understanding the “shape of a Speiser function”. All this allows us to prove the correspondence (A) previously announced.

<sup>2</sup>A *multigraph* is a graph that admits multiple edges between the same pair of vertices.

**Theorem 7.1** (Main Correspondence). *Let  $\Omega_z$  be a simply connected Riemann surface, and let  $q \geq 2$ . There exists a one to one correspondence between:*

1) *Speiser functions*

$$w(z) : \Omega_z \longrightarrow \widehat{\mathbb{C}}_w,$$

*provided with a cyclic order  $\mathcal{W}_q$  for its  $q$  singular values.*

2) *Speiser Riemann surfaces*

$$\mathcal{R}_{w(z)} \subset \Omega_z \times \widehat{\mathbb{C}}_w,$$

*provided with a cyclic order  $\mathcal{W}_q$  for the  $q$  projections of its branch points on  $\widehat{\mathbb{C}}_w$ .*

3) *Speiser  $q$ -tessellations*

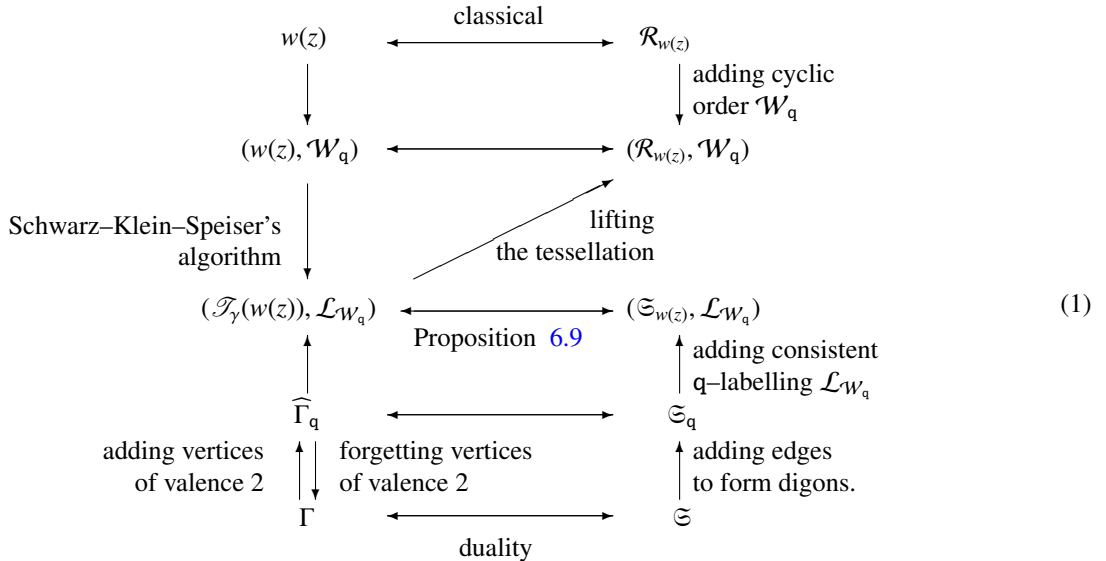
$$\left( \underbrace{\mathcal{T}_\gamma(w(z))}_{\text{tessellation}}, \underbrace{\mathcal{L}_{\mathcal{W}_q}}_{\substack{\text{consistent} \\ q\text{-labelling}}} \right).$$

4) *Analytic Speiser graphs of index  $q$*

$$\left( \underbrace{\mathcal{S}_{w(z)}}_{\text{graph}}, \underbrace{\mathcal{L}_{\mathcal{W}_q}}_{\substack{\text{consistent} \\ q\text{-labelling}}} \right).$$

As a useful consequence of the Main Correspondence, a tessellation or Speiser graph with a chosen consistent  $q$ -labelling  $\mathcal{L}_{\mathcal{W}_q}$  produces a family of Speiser functions parametrized by  $\text{Aut}(\Omega_z) \times \text{Stab}(\mathcal{W}_q)$ , where  $\text{Stab}(\mathcal{W}_q) \subset \text{Aut}(\widehat{\mathbb{C}}_w)$  is the isotropy group of the cyclic order  $\mathcal{W}_q$ . Very roughly speaking,  $\mathcal{W}_q$  provides the complex analytic information for tessellations and Speiser graphs. See Lemma 5.19.

The proof of the Main Correspondence follows by showing that rows two and three of the following diagram commute



Thus, from our point of view/perspective, the notion of “shape of a Speiser function” is given by the third row of the above diagram: a Speiser  $q$ -tessellation or equivalently an analytic Speiser graph of index  $q$ .

It is interesting to note that in Diagram 1.

- The top two rows contain analytical objects/information.
- Rows two and three contain pairs, whose second entry is essentially the cyclic order  $\mathcal{W}_q$  of the singular values of  $w(z)$ .
- In order to complete the whole picture and gain a better understanding of “shape of a Speiser function”, we introduce the two last rows, containing topological and combinatorial objects, and information related to *topological branched coverings of  $\Omega_z$* .

- In the fifth row of the above diagram, we have the the most basic objects which can be completed with some structure so that they characterize a Speiser function: *t-graphs*  $\Gamma$  and their duals *pre-Speiser graphs*  $\mathfrak{S}$ . Consider a tessellation of  $\Omega_z$  with alternating colors whose tiles are topological  $\rho$ -gons, where  $\rho \leq q$  depends on the tile. The boundary of its  $\rho$ -gons, is by definition a graph, called a *t-map*  $\Gamma$ . See Definitions 5.2 and 6.2 for details.

Formally, Question (B) can be restated as the following inverse problem:

*Characterize tessellations  $(\Omega_z \cup \partial_I \Omega_z) \setminus \Gamma$  with alternating colors and  
not necessarily homogeneous tiles,  
that are realized by topological branched coverings of  $\Omega_z$ ,  
hence by Speiser functions.*

In these terms, the above inverse problem can be translated in our language as follows.

Question: *is it possible to characterize whether a t-graph  $\Gamma$ ,  
or equivalently a pre-Speiser graph  $\mathfrak{S}$ , represents a Speiser function?* (2)

- Going from the bottom to the fourth row in Diagram 1, a certain homogenization procedure is required: the A-map  $\widehat{\Gamma}$  is homogeneous (each polygon of the tessellation  $\mathcal{T}_y(w(z))$  has  $q$  edges, *i.e.* it is a  $q$ -gon) and the Speiser graph  $\mathfrak{S}_q$  is regular (all its vertices have valence  $q$ ); however the t-graph  $\Gamma$  is not necessarily homogeneous and the pre-Speiser graph not necessarily regular.

As an advantage of Speiser graphs, the study of Question (2) is more lucid using them, this motivates our notion of pre-Speiser graph. The solution arises from the equivalent problem: the *bipartite transportation problem* associated to planar graphs, in our case the pre-Speiser graph  $\mathfrak{S}$ , see §8.2.

**Theorem 8.5.** *provides the solution, in terms of Hall-type inequalities, it is valid for finite and infinite pre-Speiser graphs; hence it solves*

- *the elliptic case, when  $\mathfrak{S}$  is finite,  $\Omega_z = \widehat{\mathbb{C}}_z$ , and also*
- *the parabolic and hyperbolic cases when  $\mathfrak{S}$  is infinite,  $\Omega_z = \mathbb{C}_z$  or  $\Delta_z$ .*

Finally in §9, the decomposition (C), an answer to the “shape of a Speiser function”, is provided by the *soul*<sup>3</sup>. The motivation comes from Speiser graphs: the notions of *logarithmic ends* and their complement the *nucleus*; Definition 6.18.1 and 6.18.2. In the context of Riemann surfaces, the above gives rise to *maximal logarithmic towers* and their complement the *soul*; Definitions 9.8 and 9.10.

**Theorem 9.12.** *provides a unique decomposition of  $\mathcal{R}_{w(z)}$  into*

- $0 \leq p \leq \infty$  maximal logarithmic towers and
- *their complement, the soul.*

*Conversely, since the soul can be geometrically recognized as a flat  $p$ -gon, then we can glue (maximal) logarithmic towers to it to “recover” the Riemann surface  $\mathcal{R}_{w(z)}$ .*

Furthermore, logarithmic towers come in two flavors exponential or  $h$ -tangent blocks. They are directly related to the exponential  $\exp(z)$  or the hyperbolic tangent  $\tanh(z)$  on the upper half plane  $\mathbb{H}$ . Since the behavior of  $w(z)$  is tame on the towers, the soul carries the essential information of  $w(z)$ . The proof of Theorem 9.12 uses the Main Correspondence, Theorem 7.1, and a decomposition of Riemann surfaces into maximal domains of single-valuedness, Proposition 4.7.

As a corollary, we provide a constructive characterization of *finite*<sup>4</sup> Speiser functions. Note that, for finite Speiser functions, the hyperbolic case,  $\Omega_z = \Delta_z$ , does not appear; moreover, the only finite Speiser functions in the elliptic case,  $\Omega_z = \widehat{\mathbb{C}}_z$ , are the rational functions. This leaves the parabolic case  $\Omega_z = \mathbb{C}_z$  as the only one left to consider.

In Definitions 9.4 and 9.6, we introduce the elementary blocks arising from the soul and the maximal logarithmic towers:

- a) *rational-block*,  $R(z) : \overline{\mathcal{P}} \subset \widehat{\mathbb{C}}_z \longrightarrow \widehat{\mathbb{C}}_w$ , for a Jordan domain  $\mathcal{P}$ ,

<sup>3</sup>To fix ideas, the usual plane polygons in  $\mathbb{C}$  are examples of souls.

<sup>4</sup>Functions  $w(z)$  whose Riemann surface  $\mathcal{R}_{w(z)}$  only have a finite number of branch points.

b) *exponential block*,  $\exp(z) : \overline{\mathbb{H}} \subset \widehat{\mathbb{C}}_z \rightarrow \widehat{\mathbb{C}}_w$ , Figure 13.a,  
 c) *h-tangent block*,  $\tanh(z) : \overline{\mathbb{H}} \subset \widehat{\mathbb{C}}_z \rightarrow \widehat{\mathbb{C}}_w$ , Figure 13.b.

With the above blocks we obtain the following characterization, see Corollary 9.14.

*Finite Speiser functions are those that can be constructed by surgery of a rational block with  $2 \leq p < \infty$  exponential and h-tangent blocks.*

A well studied subfamily of the finite Speiser functions are the Nevanlinna functions  $w(z)$ , denoted in [12] as  $N$ -functions; functions that have  $2 \leq p < \infty$  logarithmic singularities and no algebraic singularities of the inverse function<sup>5</sup>  $w^{-1}(z)$ , see [13] §8, [6] p. 301, [14], [15]. An immediate consequence of Corollary 9.14 is that,

*$N$ -functions are those that can be constructed by surgery of a rational block, without interior singular points, with  $2 \leq p < \infty$  exponential and h-tangent blocks.*

Figure 10 illustrates the construction. The  $N$ -functions coincide with the meromorphic functions on  $\widehat{\mathbb{C}}_z$  with exactly one essential singularity at  $\infty$ , having  $2 \leq p < \infty$  logarithmic singularities and no other transcendental singularities of  $w^{-1}(z)$ . In plain words,  $N$ -functions are the simplest meromorphic functions on  $\widehat{\mathbb{C}}_z$  with one essential singularity.

The introduction of the h-tangent elementary blocks extends the previous work of M. Taniguchi [16], [17] to a natural/larger framework. As valuable and advantageous mechanisms, we recognize the rational, exponential and h-tangent blocks, arising from the *sharp tools of singular complex analytic vector fields* canonically associated to meromorphic functions  $w(z)$ ,

$$X_{w(z)}(z) \doteq \frac{1}{w'(z)} \frac{\partial}{\partial z}, \quad (3)$$

see the “Dictionary” [18] prop. 2.5.

- The first is a tool that allows easy glueing and pasting of Riemann surfaces and functions, as in §4.1 and §9.
- The second is that, visualizing the phase portraits of the  $X_{w(z)}(z)$  associated to  $w(z)$ , improves the global understanding of  $w(z)$ . The behaviour which is lost in the tessellations can readily be observed with the visualization<sup>6</sup> of  $X_{w(z)}(z)$ , e.g. simple poles of  $w(z)$  can be clearly described as dipoles of the vector fields.
- In particular, tessellations or Speiser graphs, because of their topological nature, can not distinguish between the (holomorphic) exponential block and the strictly meromorphic h-tangent block. An advantage of vector fields is that it allows us to easily distinguish between them, as can be observed in Remark 9.7 and in Figure 13. See [19], [20], [21], [18], [15] for further details, references and applications.

In §10 we have collected a number of examples of the Main Correspondence (A): Speiser functions with a cyclic order  $\mathcal{W}_q$ , the decomposition of  $\mathcal{R}_{w(z)}$  into

- maximal domains of single-valuedness (Proposition 4.7),
- maximal logarithmic towers and soul (Corollary 9.14),
- Speiser  $q$ -tessellations, and analytic Speiser graphs of index  $q$ .

### 1.3. Epilogue

The underlying theme of several of our previous works has been the study of essential singularities of functions and vector fields, see [20], [19], [21], [18], [15]. As a concluding remark of this introduction, we would like to point out that,

*the simplest functions  $w(z)$  with a unique essential singularity on the Riemann sphere are those whose soul has no algebraic singularities, and has  $2 \leq q < \infty$  exponential and h-tangent blocks (i.e.  $N$ -functions).*

As an immediate consequence of Equation (3),

*the simplest complex analytic vector fields  $X_{w(z)}(z)$  with a unique essential singularity on the Riemann sphere are those whose distinguished parameter  $w(z)$  is a single-valued  $N$ -function as above.*

<sup>5</sup>Equivalently, that the Riemann surface  $\mathcal{R}_{w(z)}$  associated to  $w(z)$  only has  $p$  infinitely ramified branch points.

<sup>6</sup>Throughout this entire work, the phase portrait of  $X_{w(z)}(z)$  means the phase portrait of the real vector field  $\Re(X_{w(z)}(z))$ .

## 2. Singularities of the inverse for meromorphic functions

Let  $w(z) : \Omega_z \rightarrow \widehat{\mathbb{C}}_w$  be a meromorphic function.

**Remark 2.1** (Natural boundary of  $w(z)$ ). Throughout this work,  $\Omega_z$  is either  $\widehat{\mathbb{C}}_z$ ,  $\mathbb{C}_z$  or  $\Delta_z \doteq \{|z| < 1\}$ . In the cases  $\mathbb{C}_z$  or  $\Delta_z$ , we assume that  $\infty$  or  $\{|z| = 1\}$  are natural boundaries of  $w(z)$ , i.e.  $w(z)$  can not be analytically extended as a meromorphic function across these boundaries.

**Definition 2.2** (Singularities of  $w^{-1}(z)$ ; [22], [14], [23]). Take  $w \in \widehat{\mathbb{C}}_w$  and denote by  $D(w, \rho) \subset \widehat{\mathbb{C}}_w$  the disk of radius  $\rho > 0$  (in the spherical metric) centered at  $w$ . For every  $\rho > 0$ , choose a component  $U_w(\rho) \subset \Omega_z$  of  $w^{-1}(D(w, \rho))$  in such a way that  $\rho_1 < \rho_2$  implies  $U_w(\rho_1) \subset U_w(\rho_2)$ . Note that the function  $U_w : \rho \rightarrow U_w(\rho)$  is completely determined by its germ at 0.

The two possibilities below can occur for the germ of  $U_w$ .

- 1)  $\cap_{\rho > 0} U_w(\rho) = \{z_k\}$ ,  $z_k \in \Omega_z$ . In this case,  $w = w(z_k)$ .

Moreover, if  $w \in \mathbb{C}_w$  and  $w'(z_k) \neq 0$ , or  $w = \infty$  and  $z_k$  is a simple pole of  $w(z)$ , then  $z_k$  is called an *ordinary point*.

On the other hand, if  $w \in \mathbb{C}_w$  and  $w'(z_k) = 0$ , or if  $w = \infty$  and  $z_k$  is a multiple pole of  $w(z)$ , then  $z_k$  is called a *critical point* and  $w$  is called a *critical value* of  $w(z)$ . We also say that the critical point  $z_k$  *lies over*  $w$ . In this case,  $U_w : \rho \rightarrow U_w(\rho)$  defines an *algebraic singularity* of  $w^{-1}(z)$ .

- 2)  $\cap_{\rho > 0} U_w(\rho) = \emptyset$ . We then say that our choice  $\rho \rightarrow U_w(\rho)$  defines a *transcendental singularity* of  $w^{-1}(z)$  and that the transcendental singularity  $U_w$  *lies over*  $w$ .

In both cases, the open set  $U_w(\rho) \subset \Omega_z$  is called a *neighbourhood of the singularity*  $U_w$ . Therefore, when  $\zeta_m \in \Omega_z$ , we say that  $\zeta_m \rightarrow U_w$  if for every  $\rho > 0$  there exists  $m_0 \in \mathbb{N}$  such that  $\zeta_m \in U_w(\rho)$ , for  $m \geq m_0$ .

A transcendental singularity  $U_w$ , i.e. the germ in Definition 2.2 case (2), can be understood as the addition, to  $\Omega_z$ , of an ideal point  $U_w$ , together with its corresponding family of neighbourhoods  $\{U_w(\rho)\} \subset \Omega_z$ . If we perform the above for all the transcendental singularities of  $w^{-1}(z)$ , then a completion/compactification of  $\Omega_z$  is constructed. See [24] Ch. I § 6, for the general construction.

### Definition 2.3.

- 1) An *ideal point*  $U_w$  of  $w(z)$  is a transcendental singularity of  $w^{-1}(z)$ .
- 2) The set of ideal points is the *ideal boundary* of  $\Omega_z$ , denoted as

$$\partial_I \Omega_z.$$

The ideal boundary of  $\Omega_z$  is totally disconnected, separable and compact, see for instance [24] Ch. I § 6, or [25] proposition 3.

### Definition 2.4.

- 1) Let  $U_w$  be a transcendental singularity of  $w^{-1}(z)$ . An *asymptotic value*  $w \in \widehat{\mathbb{C}}_w$  of  $w(z)$  means that, for sufficiently small  $\rho > 0$ , there exists a  $C^1$  *asymptotic path*  $\alpha_w(\tau) : [0, \infty) \rightarrow U_w(\rho) \subset \Omega_z$ ,  $\alpha_w(0) = z_0 \in \Omega_z \setminus \mathcal{S}$ , tending to  $z_\ell \in \partial_I \Omega_z$  with well defined slope at the limit  $\tau \rightarrow \infty$ , such that

$$w = \lim_{\tau \rightarrow \infty} w(\alpha_w(\tau)) \in \widehat{\mathbb{C}}_w. \quad (4)$$

We shall not distinguish between individual members  $\alpha_w$  of the class of asymptotic paths  $[\alpha_w]$  giving rise to the same transcendental singularity  $U_w$  over  $w$  of  $w^{-1}(z)$ . By Equation (4), the asymptotic path  $\alpha_w(\tau)$  ends at the transcendental singularity  $z_\ell = U_w$ .

- 2) A pair  $(\alpha_w, w)$  is a *branch point* of the Riemann surface  $\mathcal{R}_{w(z)}$  of  $w(z)$ .

**Remark 2.5.** There is a bijective correspondence between the following:

- i) classes  $[\alpha_w(\tau)]$  of asymptotic<sup>7</sup> paths  $\alpha(\tau)$ , with asymptotic value  $w$ ,
- ii) transcendental singularities  $U_w$  of  $w^{-1}(z)$  over  $w$ , and
- iii) ideal points  $U_w \in \partial_I \Omega_z$  of  $w(z)$ ,
- iv) branch points  $(\alpha_w, w)$  of  $\mathcal{R}_{w(z)}$ .

<sup>7</sup>A slight abuse of notation is made here, when  $U_w$  is algebraic, the path  $\alpha_w(\tau) \rightarrow z_\ell$  is not an asymptotic path, it is just a path arriving to the critical point  $z_\ell$ .

According to Definition 2.2, throughout all this work the points and singularities of  $w(z)$  are of the following kinds:

- simple zeros and poles are ordinary points in  $\Omega_z$ ,
- critical points (in particular zeros and poles of order at least two), are algebraic singularities of  $w^{-1}(z)$ , in  $\Omega_z$ ,
- transcendental singularities of  $w^{-1}(z)$ , in  $\partial_I \Omega_z$ .

**Definition 2.6.**

- 1) A *singular value*  $w_j \in \mathcal{SV}_w \subset \widehat{\mathbb{C}}_w$  of  $w(z)$  is either a critical value or an asymptotic value.
- 2) A *singular point*  $z_t \in \mathcal{SP}_w \subset \Omega_z \cup \partial_I \Omega_z$  of  $w(z)$  is either
  - a critical point  $z_t \in \Omega_z$  of  $w(z)$  that lies over the critical value  $w_j$ , or
  - a transcendental singularity  $z_t \in \partial_I \Omega_z$  of  $w^{-1}(z)$  that lies over the asymptotic value  $w_j$ .
- 3) The *cosingular points* of  $w(z)$  are

$$CS_w \doteq w^{-1}(\mathcal{SV}_w) \setminus \mathcal{SP}_w \subset \Omega_z,$$

i.e. the points in the preimage of  $\mathcal{SV}_w$  that are not singular points of  $w(z)$ .

In all that follows, we assume that  $w(z)$  has non empty singular value set  $\mathcal{SV}_w$ .

Note that if  $z_t$  is a critical point and  $w_j$  is its corresponding critical value, then of course  $w_j = w(z_t) = \lim_{\tau \rightarrow \infty} w(\alpha_{w_j(\tau)}(\tau))$ , for any path  $\alpha_{w_j(\tau)}(\tau) \rightarrow z_t$ . Thus, using Definition 2.6.2 and abusing notation, we shall sometimes write  $w(z_t)$  for the singular value associated to the singular point  $z_t$ , instead of the more cumbersome  $\lim_{\tau \rightarrow \infty} w(\alpha_{w_j(\tau)}(\tau))$ .

### 3. Speiser functions

We now introduce the family of functions that will be the main subject in this work.

**Definition 3.1.**

- 1) A meromorphic function  $w(z) : \Omega_z \rightarrow \widehat{\mathbb{C}}_w$  with a finite set of distinct singular values  $\mathcal{SV}_w = \{w_1, \dots, w_j, \dots, w_q\}$ ,  $q \geq 2$ , is a *Speiser function with  $q$  singular values*, also known as a *Speiser function of index  $q$* .
- 2) The corresponding Riemann surface

$$\mathcal{R}_{w(z)} = \{(z, w(z))\} \subset \Omega_z \times \widehat{\mathbb{C}}_w$$

is a *Speiser Riemann surface with  $q$  singular values*.

- 3) A meromorphic function  $w(z)$  with a finite number of singularities of  $w^{-1}(z)$  is a *finite Speiser function*<sup>8</sup>.

**Example 3.1** (Speiser functions and finite Speiser functions). Speiser functions (of the appropriate index  $q$ ) comprise a large family of useful functions. Some examples are:

1. Rational functions. Since rational functions of degree  $2 \leq n < \infty$  have a finite set of  $2 \leq r \leq 2n - 2$  critical points and  $2 \leq q \leq 2n - 2$  critical values, then they belong to both the Speiser and finite Speiser class.
2. Functions with an infinite number of critical points and no transcendental singularities of  $w^{-1}(z)$ . The Weierstrass  $\wp(z)$  function, see [9] example 5.1, is a Speiser function with (generically) 4 critical values and zero asymptotic values; however it has an infinite number of critical points, hence it is not a finite Speiser function.
3. Functions with zero critical values and a finite number  $p < \infty$  of asymptotic values. These are called  $N$ -functions, in honor of the Nevanlinna brothers. As examples we mention:
  - a) The simplest cases are  $w(z) = e^z$ , with asymptotic values  $\{0, \infty\}$ , and  $w(z) = \tanh(z)$  with asymptotic values  $\{-1, 1\}$ . Each has two logarithmic singularities of  $w^{-1}(z)$ . See Example 9.1 for full details.
  - b) Quotients of Airy functions, say  $w(z) = \frac{\text{Bi}(z)}{\text{Ai}(z)}$ , that has 3 logarithmic singularities over 3 distinct asymptotic values. See Example 10.1 for full details.
4. The function  $w(z) = \exp(\exp(z))$  is a Speiser function with 3 singular values, namely  $\{0, 1, \infty\}$ ; however it is not a finite Speiser function since it has an infinite number of logarithmic singularities of  $w^{-1}(z)$ . Further details can be found in Example 10.3. See Figure 16.a for the Speiser 3-tessellation and Figure 16.b for the Speiser graph of index 3.
5. Functions with both critical and asymptotic values.

<sup>8</sup>In this case  $\Omega_z$  is either  $\widehat{\mathbb{C}}_z$  or  $\mathbb{C}_z$ .

- a) Consider  $w(z) = \int_0^z P(\zeta) e^{E(\zeta)} d\zeta$  with  $P, E \in \mathbb{C}[z]$  polynomials of degree  $0 \leq r < \infty$  and  $0 < p/2 < \infty$  respectively. These functions have (generically)  $r$  critical values and  $p$  asymptotic values, thus they are in the Speiser class. Moreover they also are in the finite Speiser class since they have a finite number of singular points. See for instance [21] and [18].
- b) The function  $w(z) = \cos \sqrt{z}$  is in the Speiser family since its singular values are  $\{-1, 1, \infty\}$ : the critical values are  $\{-1, 1\}$  associated to an infinite number of critical points, and it has one transcendental singularity of  $w^{-1}(z)$  over the asymptotic value  $\{\infty\}$ . Clearly it is not a finite Speiser function. See also [10] p. 360.
- c) Another example is  $w(z) = e^{\sin(z)}$ , in this case the critical values are  $\{e, e^{-1}\}$  and the asymptotic values are  $\{0, \infty\}$ ; thus it is a Speiser function with 4 distinct singular values. On the other hand, it has an infinite number of critical points and an infinite number of transcendental singularities of  $w^{-1}(z)$  over each of the the asymptotic values  $\{0, \infty\}$ ; thus it is not a finite Speiser function. See Example 10.4 for more details.

Speiser functions are simple in the following aspect: the transcendental singularities of the inverse belong to the simplest kind.

**Definition 3.2.** A transcendental singularity  $U_{w_j}$  of  $w^{-1}(z)$  over  $w_j$  is a *logarithmic singularity over  $w_j$*  if

$$w(z) : U_{w_j}(\rho) \subset \Omega_z \longrightarrow D(w_j, \rho) \setminus \{w_j\} \subset \widehat{\mathbb{C}}_w$$

is a universal covering for small enough  $\rho$ .

**Proposition 3.3.** Let  $w(z)$  be an Speiser function.

- 1) The singular values of  $w(z)$  are isolated, hence the singularities of  $w^{-1}(z)$  are either
  - i) logarithmic or
  - ii) algebraic.
- 2) Depending on  $w(z)$ , the following cases for  $\Omega_z \cup \partial_I \Omega_z$  appear:
  - i) the Riemann sphere  $\widehat{\mathbb{C}}_z$ ,
  - ii) a non Hausdorff compactification

$$\mathbb{C}_z \cup \{\infty_1, \dots, \infty_p\},$$

with  $2 \leq p \leq \infty$  ideal points,

- iii) a Hausdorff compactification with an infinite number of ideal points

$$\Delta_z \cup_{\sigma=1}^{\infty} \{e^{i\theta_\sigma}\}.$$

*Proof.* Assertion (1) follows from the classical theorem of Nevanlinna on isolated asymptotic values, [6] Ch. XI, §1.3, also see [15] theorem 4.4.

The general construction for (2) is in [24] Ch. I § 6. In particular, regarding case (ii), the ad hoc construction of the non-Hausdorff compactification of  $\mathbb{C}_z$ , for  $N$ -functions (see §3.2) and for the family of functions  $\{w(z) = \int^z P(\zeta) e^{E(\zeta)} d\zeta\}$ , appeared in [18] p. 12. For (iii) the ideal points originate from classes  $[\alpha_{w_j}(\tau)]$  of asymptotic paths as usual in the boundary of the hyperbolic disk  $\Delta_z$ .  $\square$

**Corollary 3.4.** For  $w(z)$  a Speiser function, its domain is  $\Omega_z = \widehat{\mathbb{C}}_z$  if and only if  $w(z)$  is a rational function.  $\square$

Because of Proposition 3.3.1.i, from this point forward, we convene that whenever we are considering Speiser functions with transcendental singularities, the terms,

$$\begin{array}{ccc} \text{logarithmic singularity} & \longleftrightarrow & \text{transcendental singularity} \\ \text{of } w^{-1}(z) & & \text{of } w^{-1}(z) \\ & & \longleftrightarrow \\ & & \text{ideal point} \\ & & \text{of } w(z) \end{array}$$

are referring to the same object.

The Riemann surfaces  $\mathcal{R}_{w(z)}$  are valuable tools, they have natural projections  $\pi_1$  and  $\pi_2$  as in the following commutative diagram. Note that  $\pi_1$  is in fact a biholomorphism.

$$\begin{array}{ccc}
 \Omega_z & \xleftarrow{\pi_1} & \mathcal{R}_{w(z)} \subset \Omega_z \times \widehat{\mathbb{C}}_w \\
 & \searrow w(z) & \downarrow \pi_2 \\
 & & \widehat{\mathbb{C}}_w.
 \end{array} \tag{5}$$

If  $w \in \widehat{\mathbb{C}}_w$  is an asymptotic value of  $w(z)$ , then there is at least one logarithmic singularity  $U_w$  of the inverse  $w^{-1}(z)$  over  $w$ . Certainly, there can be many (finite or even infinite) different logarithmic singularities as well as critical and ordinary points over the same singular value  $w$ .

**Definition 3.5.** Let  $w(z)$  be a Speiser function, and consider the singularities of the inverse  $w^{-1}(z)$ .

- 1) The *multiplicity*  $m$  of an ordinary point point  $z \in \Omega_z$  is 1.
- 2) The *multiplicity*  $m_i$  of an algebraic singularity or critical point  $z_i \in \Omega_z$  is the number  $2 \leq m_i < \infty$  such that  $w(z)$  is locally equivalent to  $\{z \mapsto z^{m_i}\}$ .
- 3) The *multiplicity*  $m_i$  of a logarithmic singularity  $z_i \in \partial_I \Omega_z$  of  $w^{-1}(z)$  is  $\infty$ .
- 4) In all the cases the multiplicity is also known as the *ramification index*.

**Definition 3.6.** The *multiplicity*  $\mu_j \in \mathbb{N} \cup \{\infty\}$  of a singular value  $w_j$ , is the number of branch points of the Riemann surface  $\mathcal{R}_{w(z)}$  that project via  $\pi_2$  to  $w_j$ .

The *total number of branch points* of  $\mathcal{R}_{w(z)}$  is

$$\delta = \mu_1 + \dots + \mu_q \in \mathbb{N} \cup \{\infty\}.$$

**Remark 3.7** (The existence of non-trivial multiplicities of the singular values makes enumerating singular points a non-trivial issue). In order to enumerate singular points and values, consider the following.

1. Choose a singularity of  $w^{-1}(z)$ , thus we either have:

- a critical point (algebraic singularity of  $w^{-1}(z)$ ),  $z_i \in \Omega_z$ , or
- an ideal point (logarithmic singularity of  $w^{-1}(z)$ ),  $z_i \in \partial_I \Omega_z$ .

2. We can then obtain its corresponding singular value  $w_{j(i)} = w(z_i)$ .

3. So, a branch point of  $\mathcal{R}_{w(z)}$ , namely the pair  $(\alpha_{w_{j(i)}}, w_{j(i)})$ , can be naturally identified with the pair

$$(z_i, w_{j(i)}) = \left( \underbrace{z_i = \lim_{\tau \rightarrow \infty} \alpha_{w_{j(i)}}(\tau)}_{\in \Omega_z \cup \partial_I \Omega_z}, \underbrace{w_{j(i)} = w(z_i)}_{\in \widehat{\mathbb{C}}_w} \right).$$

4. Finally, a reordering of the singular points  $\{z_i\} \subset \Omega_z \cup \partial_I \Omega_z$  so that the singular values  $w_{j(i)}$  are grouped together, provides the relationship

$$j(i) = \begin{cases} 1 & \text{for } i = 1, \dots, \mu_1, \\ 2 & \text{for } i = \mu_1 + 1, \dots, \mu_1 + \mu_2, \\ \vdots & \\ q & \text{for } i = \mu_1 + \dots + \mu_{q-1} + 1, \dots, \delta, \end{cases} \quad (6)$$

between the singular values, identified by  $j(i)$ , and the corresponding branch point identified by the unique index  $i \in \{1, \dots, \delta\}$ .

5. Additionally, letting  $m_i \in \mathbb{N} \cup \{\infty\}$  denote the ramification index of  $w(z)$  at  $(z_i, w_{j(i)})$ , we can use the triplet

$$(z_i, w_{j(i)}, m_i),$$

to easily distinguish between algebraic and logarithmic singularities of  $w^{-1}(z)$ .

The triplet  $(z_i, w_{j(i)}, m_i)$  represents an

$$\begin{aligned} \text{algebraic} &\quad \iff \quad 2 \leq m_i < \infty \quad \iff \quad z_i \in \{z_\kappa\} \subset \Omega_z \\ \text{singularity of } w^{-1}(z) &\quad \text{for some } \kappa \in \{1, \dots, r\}, \\ \text{logarithmic} &\quad \iff \quad m_i = \infty \quad \iff \quad z_i \in \{z_\sigma\} \subset \partial_I \Omega_z \\ \text{singularity of } w^{-1}(z) &\quad \text{for some } \sigma \in \{1, \dots, p\}. \end{aligned} \quad (7)$$

### 3.1. Speiser functions: notation for singular values and singular points

Summarizing, the distinct singular values of  $w(z)$  shall be denoted as

$$\mathcal{SV}_w = \sum_{j=1}^q \mu_j w_j = \{(w_1, \mu_1), \dots, (w_j, \mu_j), \dots, (w_q, \mu_q)\}, \quad (8)$$

where  $1 \leq \mu_j \leq \infty$  indicates the multiplicity of the singular value  $w_j$ .  
The singular points of  $w(z)$  are

$$\mathcal{SP}_w = \{z_1, \dots, z_\ell, \dots, z_\delta\} \subset \Omega_z \cup \partial_I \Omega_z, \text{ where } 2 \leq \delta \leq \infty. \quad (9)$$

The corresponding branch points of  $\mathcal{R}_{w(z)}$  are as follows.

$$\begin{aligned} \mathcal{BP}_w = & \left\{ \underbrace{(z_1, w_1, m_1), (z_2, w_1, m_2), \dots, (z_{\mu_1}, w_1, m_{\mu_1}),}_{\mu_1} \right. \\ & \quad \underbrace{(z_{\mu_1+1}, w_2, m_{\mu_1+1}), (z_{\mu_1+2}, w_2, m_{\mu_1+2}), \dots, (z_{\mu_1+\mu_2}, w_2, m_{\mu_1+\mu_2}),}_{\mu_2} \\ & \quad \vdots \\ & \quad \underbrace{(z_{\mu_1+\dots+\mu_{j-1}+1}, w_j, m_{\mu_1+\dots+\mu_{j-1}+1}), (z_{\mu_1+\dots+\mu_{j-1}+2}, w_j, m_{\mu_1+\dots+\mu_{j-1}+2}), \dots, (z_{\mu_1+\dots+\mu_j}, w_j, m_{\mu_1+\dots+\mu_j}),}_{\mu_j} \\ & \quad \vdots \\ & \quad \left. \underbrace{(z_{\delta-\mu_q+1}, w_q, m_{\delta-\mu_q+1}), (z_{\delta-\mu_q+2}, w_q, m_{\delta-\mu_q+2}), \dots, (z_\delta, w_q, m_\delta)}_{\mu_q} \right\} \\ & = \{(z_1, w_1, m_1), \dots, (z_\ell, w_{j(\ell)}, m_\ell), \dots, (z_\delta, w_q, m_\delta)\} = \sum_{\ell=1}^{\delta} (z_\ell, w_{j(\ell)}, m_\ell). \quad (10) \end{aligned}$$

Each type of branch point is identified by the value of its ramification index  $m_\ell$ , as in (7). Our notation is:

$q$  is the number of distinct singular values,

$p = \#\{m_\ell = \infty\}$  is the total number of logarithmic singularities of  $w^{-1}(z)$ ,

$r = \#\{2 \leq m_\ell < \infty\}$  is the total number of algebraic singularities (counted with multiplicity), and hence

$\delta = p + r$  is the total number of singularities of  $w^{-1}(z)$ .

Note that  $2 \leq q < \infty$ ,  $0 \leq p \leq \infty$ , and  $0 \leq r \leq \infty$ .

**Remark 3.8.** As is usual in the literature, we shall denote a singular value by  $a_{j(\ell)}$  when we want to emphasize that it is an asymptotic value. Otherwise it will be denoted by  $w_{j(\ell)}$ .

We provide some features for the simplest families of Speiser functions.

**Remark 3.9** (Rational functions). For rational  $R(z)$  only a finite number of algebraic singularities appear and no logarithmic singularities of  $R^{-1}(z)$ . Of course, the algebraic singularities of the inverse are the critical points of the function.

### 3.2. $N$ -functions: only a finite number of logarithmic singularities and no algebraic singularities

The original definition of an  $N$ -function is due to R. Nevanlinna who considered functions  $w(z)$  on  $\mathbb{C}_z$ , that are solutions to the Schwarzian differential equation

$$Sw\{w, z\} = P(z), \quad (11)$$

where  $P(z)$  is a polynomial, and

$$Sw\{f, z\} \doteq \frac{f'''(z)}{f'(z)} - \frac{3}{2} \left( \frac{f''(z)}{f'(z)} \right)^2,$$

is the usual Schwarzian derivative. It is a deep, and classical, result that the above is equivalent to having only a finite number of logarithmic singularities and no algebraic singularities, see [13], [6] and [12]. Since there are no critical values, then according to Remark 3.8, the  $q$  distinct singular values are asymptotic values denoted by:

$$\mathcal{AV}_w = \sum_{j=1}^q \mu_j a_j = \{(a_1, \mu_1), \dots, (a_j, \mu_j), \dots, (a_q, \mu_q)\}, \quad a_j \in \widehat{\mathbb{C}}_w, \quad q \geq 2.$$

The singular points are now asymptotic points denoted by

$$\mathcal{AP}_w = \{\infty_1, \dots, \infty_\sigma, \dots, \infty_p\} \subset \mathbb{C}_z \setminus \{\infty_1, \dots, \infty_\sigma, \dots, \infty_p\}.$$

The corresponding branch points are all infinitely ramified, so  $m_\sigma = \infty$  for  $\sigma \in \{1, \dots, p\}$ :

$$\mathcal{BP}_w = \{(\infty_1, a_1, \infty), \dots, (\infty_{\mu_1}, a_1, \infty), \dots, (\infty_\sigma, a_{j(\sigma)}, \infty), \dots, (\infty_{p-\mu_p}, a_q, \infty), \dots, (\infty_p, a_q, \infty)\} = \sum_{\sigma=1}^p (z_\sigma, a_{j(\sigma)}, \infty),$$

thus there are finitely many, namely  $p = \delta = \sum_{j=1}^q \mu_j$  infinitely ramified branch points (logarithmic singularities of  $w^{-1}(z)$ ). Once again  $q < p$  if and only if at least one  $\mu_j \geq 2$ .

See Examples 9.1.a, 10.1.a, 10.2.a for  $N$ -functions with index  $q = 2, 3, 3$  respectively. For an example of a (non finite) Speiser function of index  $q = 4$ , that is not an  $N$ -function, consider Example 10.4.a.

#### 4. Speiser Riemann surfaces

As in Definition 3.1, a *Speiser Riemann surface* is

$$\mathcal{R}_{w(z)} = \{(z, w(z)) \mid z \in \Omega_z\} \subset \Omega_z \times \widehat{\mathbb{C}}_w,$$

where  $w(z)$  is a Speiser function with  $q$  singular values.

Each  $\mathcal{R}_{w(z)}$  is simply connected with branch points as previously described in Diagram (5). Roughly speaking,  $\mathcal{R}_{w(z)}$  is the domain where the inverse function  $w^{-1}(z)$  is single-valued. In fact, considering Diagram (5),  $\pi_1$  “is the inverse” of the Speiser function  $w(z)$ .

Recall that in  $\mathcal{R}_{w(z)}$ , the  $2 \leq \delta \leq \infty$  branch points can be described, when displayed in the notation of a “divisor”, as

$$\sum_{\iota=1}^{\delta} (z_\iota, w_{j(\iota)}, m_\iota), \quad \text{with } j(\iota) \in \{1, \dots, q\}, \quad q \geq 2, \quad (12)$$

so that  $w_{j(\iota)} \in \widehat{\mathbb{C}}_w$  indicates over which singular value the branch point lies over, and  $2 \leq m_\iota \leq \infty$ , as in (7), indicates the ramification index of the corresponding branch point.

**Remark 4.1.** 1. In order to specify the location (in  $\mathcal{R}_{w(z)}$ ) of a branch point, the ramification index  $m_\iota$  is not needed, thus it will sometimes be omitted.

2. Note that only one subindex, namely  $\iota$ , is needed to identify the branch points, however the other indices are sometimes convenient for what follows. A shorthand notation for the branch point shall be

$$\langle \iota \rangle \doteq (z_\iota, w_{j(\iota)}, m_\iota).$$

A natural question to ask about Riemann surfaces of meromorphic functions  $w(z)$  is:

*Can  $\mathcal{R}_{w(z)}$  be expressed in terms of maximal domains of single-valued branches of  $w^{-1}(z)$ ?*

In order to answer this we shall need the following.

##### 4.1. Surgery of Riemann surfaces

In the Riemann surfaces category, surgery tools are widely used, v.g. [26] p.56 “welding of surfaces”, [27], or [28] §3.2.–3.3 for general discussion on geometric structures. Let  $w(z)$  be a Speiser function, the singular complex analytic vector field

$$X_{w(z)}(z) \doteq \frac{1}{w'(z)} \frac{\partial}{\partial z}$$

is canonically associated to it; see the “Dictionary” [18] prop. 2.5. Moreover, a complex analytic vector field  $X$  on a Riemann surface  $M$  has an associated singular flat metric  $g_X$  on  $M^0$ , the surface minus the singular points of the metric. The real trajectories of  $\Re(X)$  are unitary geodesics on  $(M^0, g_X)$ ; see [20] lemma 2.6 and the singular complex analytic dictionary [18] prop. 2.5. Throughout the entire work

$$(\widehat{\mathbb{C}}_w, \frac{\partial}{\partial w})$$

denotes the Riemann sphere furnished with the holomorphic vector field  $\frac{\partial}{\partial w}$ . Equivalently, this pair denotes the flat Riemannian metric with a singularity at  $\infty$  on  $\widehat{\mathbb{C}}_w$ . The concepts of unitary geodesics, euclidean segments and trajectories of the real vector field  $\operatorname{Re}(e^{i\theta}\frac{\partial}{\partial w}) = \cos(\theta)\frac{\partial}{\partial x} + \sin(\theta)\frac{\partial}{\partial y}$  (which are circles through  $\infty$  in  $\widehat{\mathbb{C}}_w$ ), are used in the same way.

The use of vector fields allows us to isometrically glue Riemann surfaces, as in the following Corollary, whose proof can be found in the above references.

**Corollary 4.2** (Surgery of flat surfaces). *Let  $(M^0, g_x), (N^0, g_y)$  be two flat surfaces arising from two singular complex analytic vector fields  $X$  and  $Y$ . Assume that both spaces  $M^0, N^0$  have as geodesic boundary components of the same length: the trajectories  $\sigma_1(\tau), \sigma_2(\tau)$  of  $\operatorname{Re}(X)$  and  $\operatorname{Re}(Y)$ ,  $\tau \in I \subset \mathbb{R}$ , respectively. Then, the isometric glueing of them along these geodesic boundary, is well defined, and provides a new flat surface on  $M^0 \cup N^0$  arising from a new complex analytic vector field  $Z$  that extends  $X$  and  $Y$ .  $\square$*

The notion of a segment of  $(\widehat{\mathbb{C}}_z, \frac{\partial}{\partial w})$  passing through the singular point  $\infty$  will be useful.

**Definition 4.3.** Given two distinct points  $w_\alpha, w_\beta \in \widehat{\mathbb{C}}_w$ , a geodesic segment in  $(\widehat{\mathbb{C}}_w, \frac{\partial}{\partial w})$  is defined as follows.

1) If  $w_\alpha, w_\beta \in \mathbb{C}_w$ , as

- i) the oriented straight line segment  $\overline{w_\alpha w_\beta} \subset \mathbb{C}_w$ , or
- ii) the oriented arc of a circle in  $\widehat{\mathbb{C}}_w$ , starting at  $w_\alpha$ , passing through  $\infty$  and ending at  $w_\beta$ ; it is denoted by  $\overline{w_\alpha \infty w_\beta}$ .

Note that  $\overline{w_\alpha \infty w_\beta} \cup \overline{w_\beta w_\alpha}$  is the unique circle in  $\widehat{\mathbb{C}}_w$  passing through  $w_\alpha, \infty$  and  $w_\beta$ .

2) If  $w_\alpha = \infty$  and  $w_\beta \in \mathbb{C}_w$ , as one of the oriented arcs of a circle in  $\widehat{\mathbb{C}}_w$  with  $\operatorname{Im}(w) = \operatorname{Im}(w_\beta)$ , denoted by  $\pm \overline{\infty w_\beta}$ .

3) If  $w_\alpha \in \mathbb{C}_w$  and  $w_\beta = \infty$ , as one of the oriented arcs of a circle in  $\widehat{\mathbb{C}}_w$  with  $\operatorname{Im}(w) = \operatorname{Im}(w_\alpha)$ , denoted by  $\pm \overline{w_\alpha \infty}$ .

Note that for any pair  $w_\alpha, w_\beta$  there are two choices of geodesics segments between them.

As usual, a *branch cut* is the operation of removing from  $\widehat{\mathbb{C}}_w$  a geodesic segment  $\overline{w_{j(a)} w_{j(r)}}$  in  $(\widehat{\mathbb{C}}_w, \frac{\partial}{\partial w})$ .

**Definition 4.4.** A sheet with branch cuts is

$$\mathcal{Q}_\Xi = \widehat{\mathbb{C}}_w \setminus \left( \bigcup_{j(a), j(r) \in \Xi} \overline{w_{j(a)} w_{j(r)}} \right), \quad (13)$$

such that

- i) the subindex  $\Xi = \{\overline{w_{j(a)} w_{j(r)}} \mid j(a) \neq j(r)\} \neq \emptyset$  enumerates the particular collection of branch cuts,
- ii) the geodesic segments  $\overline{w_{j(a)} w_{j(r)}}, \overline{w_{j(a')} w_{j(r')}}$  intersect at most at their endpoints,
- iii)  $\mathcal{Q}_\Xi$  is simply connected.

In particular if both  $w_{j(a)}, w_{j(r)} \in \mathbb{C}_w$  we use the usual geodesic segment with length  $|w_{j(a)} - w_{j(r)}|$ . In case either  $w_{j(a)}$  or  $w_{j(r)}$  is  $\infty \in \widehat{\mathbb{C}}_w$ , we shall choose  $\overline{w_{j(a)} w_{j(r)}}$  as an appropriate geodesic segment in  $(\widehat{\mathbb{C}}_w, \frac{\partial}{\partial w})$  that ensures that condition (iii) of Definition 4.4 is satisfied.

**Lemma 4.5.** *Given a distinct set  $\{w_1, \dots, w_q\} \subset \widehat{\mathbb{C}}_w$  of  $q$  singular values, there are a finite number of types  $\mathcal{Q}_\Xi$  (i.e. non isometric sheets with branch cuts, understood as translation surfaces) that can be formed.*

*Proof.* Let  $K_q$  be the complete graph with  $q$  vertices formed by the set  $\{w_1, \dots, w_q\} \subset \widehat{\mathbb{C}}_w$  of distinct  $q$  values. Clearly the number of possible sheets is less than the number of subgraphs of  $K_q$ , which is finite.  $\square$

**Definition 4.6.**

1) A segment  $\Delta_{\theta\alpha\tau} \subset \mathcal{R}_{w(z)}$  is a diagonal of  $\mathcal{R}_{w(z)}$  when

- i) the projection

$$\pi_2(\Delta_{\theta\alpha\tau}) = \overline{w_{j(a)} w_{j(r)}}$$

- is a geodesic segment in  $(\widehat{\mathbb{C}}_w, \frac{\partial}{\partial w})$ ,
- ii) the interior of  $\pi_1(\Delta_{\theta\alpha\tau})$  is in  $\Omega_z$ , and
- iii) the endpoints,  $z_\alpha$  and  $z_\tau$ , of  $\pi_1(\Delta_{\theta\alpha\tau})$  are algebraic or logarithmic singularities of  $w^{-1}(z)$ .

2) An oriented diagonal  $\Delta_{\vartheta ar}$  starts at the branch point  $\textcircled{a} = (z_a, w_{j(a)}, m_a)$  and ends at the branch point  $\textcircled{r} = (z_r, w_{j(r)}, m_r)$ . In this case, we shall say that the branch points,  $\textcircled{a}$  and  $\textcircled{r}$ , share the sheet identified<sup>9</sup> by the diagonal  $\Delta_{\vartheta ar}$  in  $\mathcal{R}_{w(z)}$ .

From the above definitions, notation, and the repeated use of isometric glueing (*i.e.* Corollary 4.2) between sheets along their branch cuts, the following result is clear.

**Proposition 4.7** (Decomposition of  $\mathcal{R}_{w(z)}$  into maximal domains of single-valuedness). *Let  $w(z)$  be a Speiser function with  $q \geq 2$  distinct singular values.*

1) *The Riemann surface  $\mathcal{R}_{w(z)}$  associated to  $w(z)$  can be constructed by isometric glueing of sheets, denoted by  $\sim$ , as follows*

$$\mathcal{R}_{w(z)} = \left[ \bigcup_{\vartheta} \mathfrak{L}_{\Xi, \vartheta} \right] / \sim = \left[ \bigcup_{\vartheta} \left( \widehat{\mathbb{C}}_w \setminus \left( \bigcup_{j(a), j(r) \in \Xi} \overline{w_{j(a)} w_{j(r)}} \right) \right)_{\vartheta} \right] / \sim, \quad (14)$$

*In the above expression the following conventions are observed.*

- *The singular values of  $w(z)$  are denoted by  $\{w_{j(i)}\}_{i=1}^{\delta}$ , recall Equation (10).*
- *The index  $\Xi$  indicates the type of sheet, *i.e.* the particular collection*

$$\{\overline{w_{j(a)} w_{j(r)}} \mid j(a) \neq j(r)\}$$

*that is considered on each sheet  $\vartheta$ , a finite number of types of sheets  $\mathfrak{L}_{\Xi}$  appears.*

2) *The number of sheets in (14) is  $n = |\{\vartheta\}|$ , with  $2 \leq n \leq \infty$ . Note that  $n < \infty$  if and only if  $w(z)$  is a rational function of degree  $n \geq 2$ .*

□

Note that the decomposition is in no way unique. Also note that this answers the question posed at the end of last subsection.

**Corollary 4.8.** *Each sheet  $\mathfrak{L}_{\Xi}$  is a maximal domain in which  $w^{-1}(z)$  admits a single-valued branch.*

□

**Remark 4.9** (The relevance of the sheets and of the decomposition of  $\mathcal{R}_{w(z)}$ ). Even though the sheets  $\mathfrak{L}_{\Xi}$ , as in (4.4), appear to be very innocent (they are only copies of the Riemann sphere with certain branch cuts), when they are “mounted” on the Riemann surface  $\mathcal{R}_{w(z)}$  they gain relevance in the sense that:

- they are now maximal domains where  $w^{-1}(z)$  admits a single-valued branch,
- they also inherit the vector field structure of  $\mathcal{R}_{w(z)}$  provided by  $\pi_2^* \frac{\partial}{\partial w}$  (see Diagram (5)).

For examples of decomposition of  $\mathcal{R}_{w(z)}$  in sheets, see Example 9.1.b for the simplest case of an  $N$ –function, Examples 10.1.b and 10.2.b for a presentation of two non-trivial cases of  $N$ –functions when  $q = 3$ ; Examples 10.4.b and 10.5.b show Speiser functions of index  $q = 4$  that are not  $N$ –functions.

The Riemann surface  $\mathcal{R}_{w(z)}$  of a Speiser–function  $w(z)$ , has:

- $0 \leq r \leq \infty$  finitely ramified branch points, and
- $0 \leq p \leq \infty$  infinitely ramified branch points

over  $q$  distinct singular values (with  $2 \leq q \leq r + p$ ).

**Remark 4.10** (Features of some families of functions). 1. Let  $w(z) = R(z)$  be a rational function of degree  $n \geq 2$ . The surface  $\mathcal{R}_{w(z)}$  has  $r < \infty$  finitely ramified branch points over  $2 \leq q \leq 2n - 2$  distinct critical values.

2. Consider a polynomial  $w(z) = P(z)$  of degree  $n \geq 2$ , then  $\mathcal{R}_{w(z)}$  has a finitely ramified branch point of ramification index  $n - 1$  over  $\infty \in \widehat{\mathbb{C}}_w$  and whose projection via  $\pi_1$  is  $\infty \in \widehat{\mathbb{C}}_z$ , and up to  $n - 1$  finitely ramified branch points over  $q - 1$  distinct finite critical values.

3. Given an  $N$ –function  $w(z)$ , its surface  $\mathcal{R}_{w(z)}$  has:

- $p < \infty$  infinitely ramified branch points (logarithmic singularities of  $w^{-1}(z)$ ) over  $q \leq p < \infty$  distinct asymptotic values, and
- no finitely ramified branch points (algebraic singularities of  $w^{-1}(z)$ ).

<sup>9</sup>In this case, the index  $\vartheta$  enumerates the sheets that share the branch points  $\textcircled{a}$  and  $\textcircled{r}$ . Also if two diagonals have the same  $\vartheta$  then their corresponding branch points share the same sheet.

## 5. Schwarz–Klein–Speiser tessellations

We roughly follow the classical works of H. A. Schwarz [3], F. Klein [4], [7], R. Nevanlinna [6] ch. XI §2, and A. Speiser [5]. However, we make some precisions<sup>10</sup> that we consider improve the presentation and our understanding. We develop, in an axiomatic way, tessellations, their associated graphs and certain labellings associated to them.

Let  $\Omega_z$  be a simply connected Riemann surface. For our purposes, we shall require the compactifications of  $\Omega_z$  provided by Proposition 3.3.2.ii–iii. Namely,

$$(\Omega_z \cup \partial_I \Omega_z) \doteq \begin{cases} \widehat{\mathbb{C}}_z \\ \mathbb{C}_z \cup \{\infty_1, \dots, \infty_p\} \\ \Delta_z \cup_{\sigma=1}^{\infty} \{e^{i\theta_\sigma}\} \end{cases}$$

as the case may arise.

### Definition 5.1.

1) A *tessellation* of a surface  $\Omega_z$  is a collection of alternating colored tiles

$$\mathcal{T} = \underbrace{T_1 \cup \dots \cup T_\alpha \cup \dots \cup T'_1 \cup \dots \cup T'_\alpha \cup \dots}_{n \text{ blue tiles}} \subset \Omega_z \cup \partial_I \Omega_z, \quad 2 \leq n \leq \infty, \quad (15)$$

where the *tiles*  $\{T_\alpha, T'_\alpha\}$  are open Jordan domains, such that:

- i) The union of their closures  $\cup_\alpha (\overline{T_\alpha} \cup \overline{T'_\alpha})$  is  $\Omega_z \cup \partial_I \Omega_z$ .
- ii) The boundary of the closure of each tile  $\partial \overline{T_\alpha}$  (resp.  $\partial \overline{T'_\alpha}$ ) has  $\rho$  vertices and  $\rho$  edges, where  $2 \leq \rho \leq q$  and  $\rho$  depends on the particular tile.
- iii) If the intersection of the closures of any two tiles is non–empty, then it consists of a finite number of simple paths (edges) and their extreme points (vertices).

2) If all the tiles  $\{T_\alpha\}$  (resp.  $\{T'_\alpha\}$ ) have the same number of vertices and edges, we shall say that the tessellation is *homogeneous*.

Note that, if  $n < \infty$ , then a tessellation  $\mathcal{T}$  has  $n$  blue tiles and  $n$  grey tiles; this is called the *global balance condition* in [2], see §8 for further discussion. In the case of  $n = \infty$ , we shall say that the tessellation  $\mathcal{T}$  satisfies the *global balance condition* if the cardinality of the blue and gray tiles are equal. By looking at the boundaries of the tiles, say  $\partial \overline{T_\alpha}, \partial \overline{T'_\alpha}$ , a tessellation  $\mathcal{T}$  determines an underlying graph  $\Gamma$ .

**Definition 5.2.** A *t–graph*  $\Gamma$  is an oriented connected graph embedded in  $(\Omega_z \cup \partial_I \Omega_z)$ , with vertices  $V(\Gamma)$  of infinite or even valence greater than or equal to 4 and edges  $E(\Gamma)$ , such that:

i)

$$\begin{aligned} \mathcal{T}(\Gamma) &\doteq (\Omega_z \cup \partial_I \Omega_z) \setminus \Gamma \\ &= \underbrace{T_1 \cup \dots \cup T_\alpha \cup \dots \cup T'_1 \cup \dots \cup T'_\alpha \cup \dots}_{n \text{ blue tiles}} \subset \Omega_z \cup \partial_I \Omega_z, \quad 2 \leq n \leq \infty, \end{aligned} \quad (16)$$

is a tessellation, as in Definition 5.1.

- ii) Each blue tile  $T_\alpha$  is on the left side of the oriented edges of  $\Gamma$ .
- iii) If there are vertices  $V(\Gamma)$  with infinite valence, they are on the ideal boundary  $\{\infty_1, \dots, \infty_p\}$  or  $\partial_I \Delta_z$ . Moreover, there are no finite valence vertices on the ideal boundary.

With the above in mind, a tessellation  $\mathcal{T}$  and a *t–graph*  $\Gamma$  are essentially equivalent objects, where the alternating colouring in Equation (15) corresponds to the orientation of the edges in Definition 5.2. In simple words, a *t–graph* must be understood as the simplest oriented graph describing a tessellation.

The tessellations arising from complex analytic functions are homogeneous and require a more accurate notion, as follows.

**Definition 5.3.** 1) An *A–map*  $\widehat{\Gamma}_q$  is an oriented, connected graph embedded in  $\Omega_z \cup \partial_I \Omega_z$ , with vertices  $V(\widehat{\Gamma}_q)$  of infinite or even valence greater than or equal to 2 and edges  $E(\widehat{\Gamma}_q)$ , such that:

<sup>10</sup>Regarding the vertices of infinite valence.

- i) The subset of vertices of valence greater than or equal to 4 is non empty.
- ii) If we forget all the vertices of valence 2 of  $\widehat{\Gamma}_q$ , then we obtain a  $t$ -graph  $\Gamma$  such that:

$$\mathcal{T}(\widehat{\Gamma}_q) \doteq \mathcal{T}(\Gamma) \quad (17)$$

is, set theoretically, a tessellation as in Definition 5.1.

- 2) The boundary  $\partial\overline{T}_\alpha$  (resp.  $\partial\overline{T}'_\alpha$ ) of each tile consists of exactly  $q$  vertices and  $q$  edges of  $\widehat{\Gamma}_q$ , i.e. the tessellation  $\mathcal{T}(\widehat{\Gamma}_q)$  is homogeneous.
- 3) We shall say that  $\Gamma$  and  $\widehat{\Gamma}_q$ , as in (ii) above, are *compatible*.

The *forgetting vertices operation* in part (ii) above is as follows. We consider a vertex, say  $z_1 = 0$  of valence 2 in  $\widehat{\Gamma}_q$  and its two adjacent edges, say  $(-1, 0)$  and  $(0, 1)$ , thus we have  $(-1, 0) \cup \{0\} \cup (0, 1)$ . The operation of forgetting the vertex 0 replaces the above by a unique edge  $(-1, 1)$ .

**Example 5.1.** In Figure 1 we show three tessellations corresponding to  $t$ -graphs  $\Gamma$  that do not represent Speiser functions on  $\widehat{\mathbb{C}}_z$ . For Figure 1.a this follows by observing that it only has one branch point. For Figures 1.b–c this will be shown in §8.

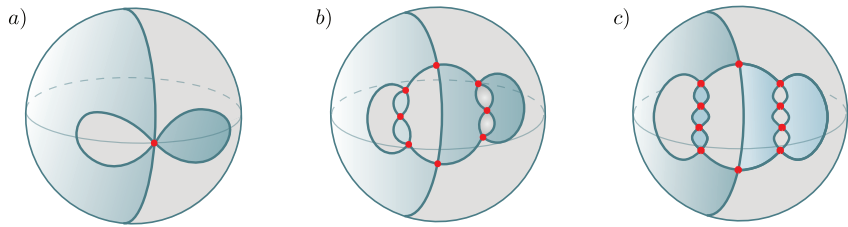


Figure 1: Examples of  $t$ -graphs  $\Gamma$ , whose corresponding tessellations  $\mathcal{T}(\Gamma)$  do not represent Speiser functions.

**Example 5.2.** Consider the non generic rational function

$$R(z) = \frac{z(z^2 - 1)(z^2 - 4)}{(z - 3)}$$

of degree 5. It has 6 critical points (5 simple ones located on the plane and an multiplicity 4 critical point at  $\infty \in \widehat{\mathbb{C}}_z$ ), and 6 critical values  $SV_R = \{w_1, w_2, w_3, w_4, w_5, w_6 = \infty\}$  lying on  $\gamma = \mathbb{R} \cup \{\infty\}$ . The inverse image of  $\gamma$  under  $R(z)$ , namely  $\Gamma = R^{-1}(\mathbb{R} \cup \{\infty\})$  is a  $t$ -graph with tessellation  $\mathcal{T}(\Gamma)$  as in Figure 2.a–b. Figure 2.c shows an  $A$ -map  $\widehat{\Gamma}_6$ , constructed by edge subdivision of  $\Gamma$  (hence they are compatible), and its corresponding homogeneous tessellation  $\mathcal{T}(\widehat{\Gamma}_6) = \widehat{\mathbb{C}}_z \setminus \widehat{\Gamma}_6$  whose tiles are 6-gons with two types of vertices: red vertices of valence greater than or equal to 4 corresponding to the critical points of  $R(z)$ , and green vertices of valence 2 corresponding to the cocritical points of  $R(z)$ . All tiles are 6-gons having labelled vertices with cyclic order  $\mathcal{W}_6 = [w_1, \dots, w_6]$ .

**Example 5.3.** In Figure 18.a we observe a tessellation  $\mathcal{T}(\widehat{\Gamma}_4)$  corresponding to the Speiser function of index 4  $w(z) = \sin(z) \exp(\sin(z))$ .

The  $t$ -graph  $\Gamma$  consists of: the black edges, an infinite number of red vertices of valence 4 or 8 (corresponding to the real critical points of  $w(z)$  with critical values  $e$  and  $-e^{-1}$ ), and an infinite number of vertices “at infinity” of infinite valence (ideal points  $\{\infty_1, \infty_2, \dots, \infty_p, \dots\}$  in the non-Hausdorff compactification  $\mathbb{C}_z \cup \{\infty_1, \infty_2, \dots, \infty_p, \dots\}$  corresponding to the logarithmic singularities of  $w^{-1}(z)$  with asymptotic values 0 and  $\infty$ ). A compatible  $A$ -map is obtained by edge subdivision consisting of adding an infinite number of green vertices of valence 2 at the cosingular points (with cosingular values 0,  $e$  and  $-e^{-1}$ ). See Example 10.5 for further details.

**Definition 5.4.**

- 1) Consider  $q \geq 2$  distinct values  $\{w_\ell\}_{\ell=1}^q \subset \widehat{\mathbb{C}}_w$ , and assign them a *cyclic order*, say  $\mathcal{W}_q = [w_1, \dots, w_j, \dots, w_q]$ ;

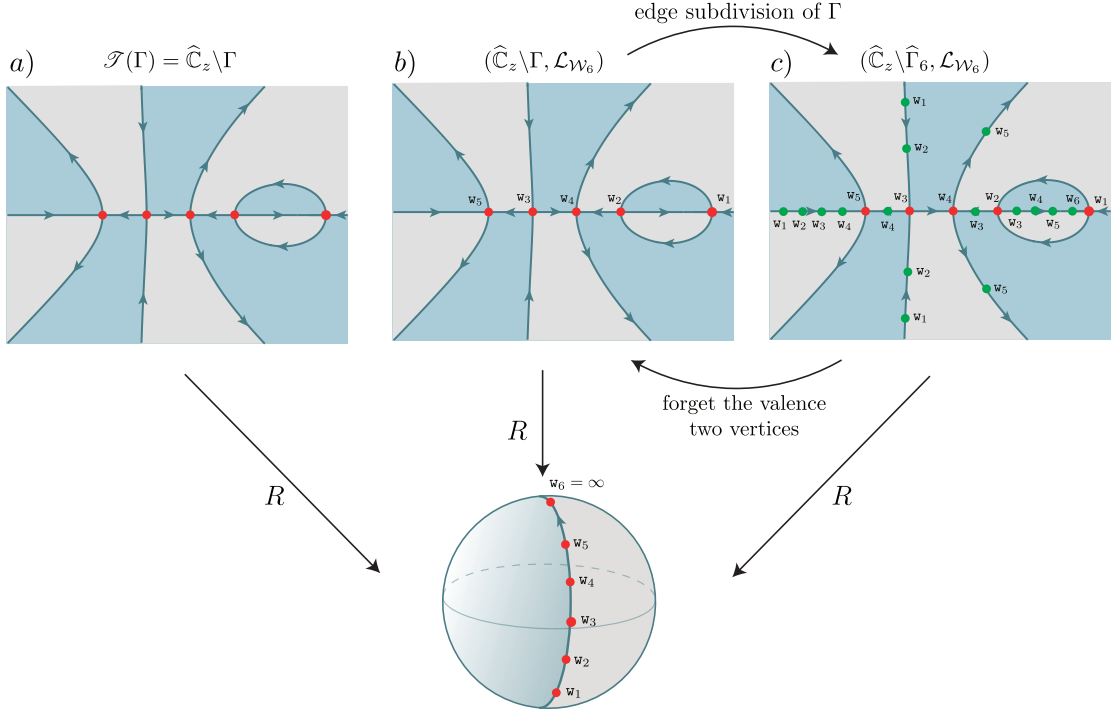


Figure 2: Affine view of the tessellation of the non generic rational function  $R(z) = z(z^2 - 1)(z^2 - 4)/(z - 3)$  of degree 5. It has 6 critical points, one of them being  $\infty \in \widehat{\mathbb{C}}_z$  and 6 critical values  $SP_R = \{w_1, w_2, w_3, w_4, w_5, w_6 = \infty\}$  lying on  $\gamma = \mathbb{R} \cup \{\infty\}$ . a) The t-graph  $\Gamma = R^{-1}(\mathbb{R} \cup \{\infty\})$  and its non homogeneous tessellation  $\mathcal{J}(\Gamma)$ . b) The t-graph  $\Gamma$  with consistent 6-labelling  $\mathcal{J}_{W_6} : V(\Gamma) \rightarrow W_6$ , where  $\mathcal{J}_{W_6}(\infty) = w_6$ . c) The A-map  $\widehat{\Gamma} = R^*\gamma$ , its homogeneous tessellation  $\mathcal{J}(\widehat{\Gamma}_6)$ , and its consistent 6-labelling  $\mathcal{J}_{W_6}$ ; each tile is a 6-gon, with vertices at the (red) critical points  $SP_R$ , the point  $\infty \in \widehat{\mathbb{C}}_z$  (which has label  $w_6$ ), and the (green) cocritical points  $CS_R$ . This figure appears as figure 1 of [9] with slightly different notation.

further, consider a representative  $\gamma$  of the isotopy class of Jordan paths relative to the  $q$  distinct values traversed in the order given above. Thus

$$\gamma \subset \widehat{\mathbb{C}}_w \text{ runs through } W_q \text{ (in the chosen order).}$$

The isotopy class  $[\gamma]$  realizes the above *cyclic order*  $\mathcal{L}_\gamma$  for the  $q$  distinct values.

2) The path  $\gamma$  determines a *trivial tessellation* of the sphere

$$\mathcal{J}(\gamma) = \widehat{\mathbb{C}}_w \setminus \gamma = T \cup T'$$

with two tiles (which are topological  $q$ -gons), the *blue tile*  $T$  is on the left side of  $\gamma$ , the *grey tile*  $T'$  is on the right side of  $\gamma$ .

**Remark 5.5** (Cyclic order). By definition, the cyclic order  $\mathcal{L}_\gamma$  and the cyclic order of the  $q$  distinct values

$$W_q = [w_1, \dots, w_j, \dots, w_q]$$

are to be thought of as equivalent.

**Remark 5.6** (Graph and geodesic structures on  $\gamma$ ). 1. As a graph,  $\gamma$  is a cyclic graph with  $q$  ordered vertices, namely  $[w_1, \dots, w_j, \dots, w_q] \subset \widehat{\mathbb{C}}_w$ , and the respective segments  $\{\overline{w_j w_{j+1}}\} \subset \gamma$  as edges.

2. Moreover, when it is convenient, one may choose  $\gamma$  as a polygonal with  $q$  geodesic segments

$$\overline{w_1 w_2} \cup \dots \cup \overline{w_{q-1} w_q} \cup \overline{w_q w_1}.$$

The orientation of  $\widehat{\Gamma}_q$  is inherited by the cyclic order  $\mathcal{L}_\gamma$ , i.e. anticlockwise for the blue tiles  $T_a$  of the tessellation.

After Theorem 5.16, the name A-map for  $\widehat{\Gamma}_q$  must be understood as a coarse abbreviation of “complex analytic function”.

By condition (iii) of Definition 5.2,  $\Gamma$  or  $\widehat{\Gamma}_q$  are on  $\Omega_z = \widehat{\mathbb{C}}$  if and only if they do not have vertices of infinite valence.

**Definition 5.7.** A *consistent  $q$ -labelling*

$$\mathcal{L}_{W_q} : V(\Gamma) \longrightarrow W_q, \quad q \geq 2,$$

for a  $t$ -graph  $\Gamma$  satisfies the following conditions:

- i) For each blue tile  $T_\alpha$  of the tessellation  $\mathcal{T}(\Gamma)$ , if  $\{z_i\}$  are the vertices of its boundary  $\partial T_\alpha$ , ordered with cyclic anti-clockwise sense, then the labels (values)  $\{\mathcal{L}_{W_q}(z_i)\} \subset W_q$  appear exactly once and with the same cyclic order provided by  $\mathcal{L}_\gamma$ .
- ii) Each label (value)  $w_j \in W_q$  appears under  $\mathcal{L}_{W_q}$  for at least one vertex  $z_i \in V(\Gamma)$  of  $\Gamma$ , which by definition have valence greater than or equal to 4.

**Remark 5.8** (Consistent  $q$ -labelling for  $A$ -maps). 1. The notion of consistent  $q$ -labelling for a  $t$ -graph  $\Gamma$  extends to any compatible  $A$ -map  $\widehat{\Gamma}_q$ , with a notable distinction:

- all the labels of  $W_q$  appear on the vertices of each blue tile  $T_\alpha$ , since all the tiles of  $\mathcal{T}(\widehat{\Gamma}_q)$  are  $q$ -gons.
- 2. On the other hand, for a  $t$ -graph  $\Gamma$  some labels of  $W_q$  are usually hidden in the boundary of each blue tile, since the tiles of the tessellation  $\mathcal{T}(\Gamma)$  can be  $\rho$ -gons, for  $2 \leq \rho \leq q$ , see example 2 and figure 1 of [9]. By abuse of notation, we use the notion of consistent  $q$ -labelling for  $t$ -graphs and  $A$ -maps.

A precise statement for the above remark is as follows.

**Lemma 5.9** (Consistent  $q$ -labellings for  $\Gamma$  and  $\widehat{\Gamma}_q$ ). *Let  $\Gamma$  be a  $t$ -graph and  $\widehat{\Gamma}_q$  an  $A$ -map that are compatible ( $\Gamma$  can be obtained from  $\widehat{\Gamma}_q$  by forgetting vertices of valence 2).*

- 1. *If  $\Gamma$  supports a consistent  $q$ -labelling  $\mathcal{L}_{W_q}$ , then  $\mathcal{L}_{W_q}$  extends to a consistent  $q$ -labelling on  $\widehat{\Gamma}_q$ .*
- 2. *If  $\widehat{\Gamma}_q$  supports a consistent  $q$ -labelling  $\mathcal{L}_{W_q}$ , then  $\mathcal{L}_{W_q}$  restricts to a consistent  $q$ -labelling on  $\Gamma$ .*

*Proof.* Statement 1 follows by edge subdivision that adds valence two vertices to  $\Gamma$  to obtain  $\widehat{\Gamma}_q$ . Statement 2, the converse, is also true by the forgetting vertices of valence 2 operation.  $\square$

Note that a given  $t$ -graph  $\Gamma$  can support several consistent  $q$ -labellings:

- Figure 2.a shows a  $t$ -graph  $\Gamma$  that supports the consistent 6-labelling shown in Figure 2.b. The consistent 6-labelling of a compatible  $A$ -map  $\widehat{\Gamma}_6$  is shown in Figure 2.c.
- Figure 2.a of [9], shows a consistent 4-labelling for another  $A$ -map obtained from the same  $t$ -graph  $\Gamma$  of Figure 2.a. Figures 2.b and 2.c of [9] show two different consistent 5-labellings for two different  $A$ -maps, whose subjacent  $t$ -graphs are also the same  $\Gamma$ .

The above shows that, for a given  $t$ -graph, there might be several different consistent  $q$ -labellings for fixed  $q$  and for different  $q$ 's.

**Definition 5.10.** A *Speiser  $q$ -tessellation* is a pair  $(\mathcal{T}(\widehat{\Gamma}_q), \mathcal{L}_{W_q})$  where

- i)  $\mathcal{T}(\widehat{\Gamma}_q)$  is a tessellation on  $\Omega_z$ , arising from an  $A$ -map  $\widehat{\Gamma}_q$  as in Definition 5.3, and
- ii)  $\mathcal{L}_{W_q}$  is a consistent  $q$ -labelling of  $\widehat{\Gamma}_q$ .

### 5.1. Schwarz–Klein–Speiser’s algorithm

Let  $w(z) : \Omega_z \longrightarrow \widehat{\mathbb{C}}_w$  be a Speiser function. Recall that  $\Omega_z$  is either  $\widehat{\mathbb{C}}_z$ ,  $\mathbb{C}_z$ , or  $\Delta_z$ .

**Step 1.** Choose a cyclic order for the  $q$  singular values of  $w(z)$

$$W_q = [w_1, \dots, w_j, \dots, w_q] \subset \widehat{\mathbb{C}}_w,$$

and consider a Jordan path  $\gamma$  realizing the cyclic order  $\mathcal{L}_\gamma$  of the singular values, as in Definition 5.4.1.

**Step 2.** Compute the inverse image of  $\gamma$ ,

$$w^{-1}(\gamma) \subset \Omega_z.$$

and complete it to  $\Gamma \subset (\Omega_z \cup \partial_I \Omega_z)$  by adding the ideal points (logarithmic singularities, see (7)),  $\{z_\sigma\} \subset \partial_I \Omega_z$ . Note that  $\partial_I \Omega_z$  can be  $\emptyset$ ,  $\{\infty_1, \dots, \infty_p\}$  or a subset of  $\{|z| = 1\}$ , according to whether the Riemann surface  $\mathcal{R}_{w(z)}$  has elliptic, parabolic or hyperbolic conformal type, respectively.

In graph theory, the pullback graph

$$\widehat{\Gamma}_q = w(z)^* \gamma \subset (\Omega_z \cup \partial_I \Omega_z)$$

is well defined. It has the singular points  $\mathcal{SP}_w$  and the cosingular points  $\mathcal{CS}_w$  of  $w(z)$  as vertices  $V(\widehat{\Gamma}_q)$ , and the respective segments in  $\widehat{\Gamma}_q$  as edges. Moreover, the logarithmic singularities are vertices located in  $\partial_I \Omega_z$  and with infinite valence.

Set theoretically  $\Gamma = \widehat{\Gamma}_q$ , however they are isomorphic as graphs if and only the cosingular point set  $\mathcal{CS}_w$  of  $w(z)$  is empty.

**Step 3.** The tessellation determined by  $w(z)$  and  $\gamma$  is

$$(\Omega_z \cup \partial_I \Omega_z) \setminus \widehat{\Gamma}_q = \underbrace{T_1 \cup \dots \cup T_\alpha \dots}_{n \text{ blue tiles}} \cup \underbrace{T'_1 \cup \dots \cup T'_{\beta} \dots}_{n \text{ grey tiles}}, \quad 2 \leq n \leq \infty.$$

**Step 4.** The cosingular points  $\mathcal{CS}_w$  play a crucial role on the boundary of the tiles; they are vertices of  $\widehat{\Gamma}_q$  of valence 2. In fact, the tiles of the tessellation are also topological  $q$ -gons. For each tile  $T_\alpha$ , the pullback of the cyclic order  $\mathcal{L}_\gamma$

$$\begin{array}{ccccccc} w^{-1}(w_1) & \dots & w^{-1}(w_j) & \dots & w^{-1}(w_q) & \in \partial \overline{T_\alpha} & \subset \mathcal{SP}_w \cup \mathcal{CS}_w \\ \downarrow & & \downarrow & & \downarrow & & \\ w_1 & \dots & w_j & \dots & w_q & & \in \mathcal{W}_q, \end{array} \quad (18)$$

determines a consistent<sup>11</sup>  $q$ -labelling,  $w(z)^* \mathcal{L}_\gamma$ , for  $\widehat{\Gamma}_q$ . We have constructed the analytic Speiser  $q$ -tessellation

$$(\mathcal{T}_\gamma(w(z)), w(z)^* \mathcal{L}_\gamma) = \left( \underbrace{(\Omega_z \cup \partial_I \Omega_z) \setminus w(z)^* \gamma}_{\text{tessellation}}, \underbrace{w(z)^* \mathcal{L}_\gamma}_{\substack{\text{consistent} \\ q\text{-labelling}}} \right), \quad (19)$$

that is the output of the algorithm.

**Example 5.4** (Speiser  $q$ -tessellations for some functions). On  $\widehat{\mathbb{C}}_z$ , for Speiser  $q$ -tessellations of rational functions, see [9], figures 1, 2, 5, and 6. Examples of consistent  $q$ -labellings are in [8], figures 4, 6. Obviously, Speiser  $q$ -tessellations are natural for meromorphic functions on compact Riemann surfaces of genus  $g \geq 1$ , see [9] figure 7.

On  $\mathbb{C}_z$ , for Speiser  $q$ -tessellations arising from transcendental Speiser functions  $w(z)$  (with an essential singularity at  $\infty \in \widehat{\mathbb{C}}_z$ ), see Figures 12.a, 14.a, 15.a, 16.a, 17.a, and 18.a.

**Example 5.5** (Not all labelled A-maps are consistent  $q$ -labelled A-maps). We provide two examples of this issue.

1. The first one is for a finite A-map and is based upon figure 10 of [2], which we have reproduced as Figure 3 to make things easier for the reader. The figure depicts an A-map with 4 tiles of each color, where each tile is a 6-gon, and a labelling with labels  $\mathcal{W}_6 = [1, 2, 3, 4, 5, 6]$ . However, all the vertices labelled 5 have valence 2, thus,

- the labelling is not a consistent 6-labelling,
- the vertices labelled 5 are fake cocritical points, equivalently, 5 is a fake critical value.

However, by forgetting the vertices labelled 5, we obtain another A-map, presumably corresponding to a rational function of degree 4, whose tiles are 5-gons, in fact a consistent 5-labelling exists, see Example 8.1, case  $q = 5$ , particularly Figure 6.b.

2. The second example is for an infinite A-map, shown in Figure 4.f; in this case the A-map depicted has a labelling in  $\mathcal{W}_4 = [1, 2, 3, 4]$ . Once again, there is a label (in this case 4) that does not appear as a vertex of valence greater than or equal to 4, thus

- the labelling is not a consistent 4-labelling,
- the vertices labelled 4 are fake cosingular points, equivalently, 4 is a fake singular value.

However, by forgetting the vertices labelled 4, we obtain another A-map with  $q = 3$ , that is tiles which are 3-gons and a consistent 3-labelling; Figure 4.d shows the dual graph<sup>12</sup>  $\mathcal{S}_3$  of the new A-map.

For a more general discussion and further examples see §8.

<sup>11</sup>Since  $\{w_j\}$  is the set of singular values of  $w(z)$ , condition (ii) of Definition 5.7 is trivially satisfied by  $w(z)^* \mathcal{L}_\gamma$ .

<sup>12</sup>A Speiser graph of index 3, as will be seen in §6.

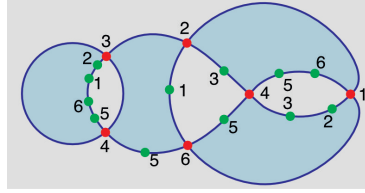


Figure 3: A-map with 4 tiles of each color, where each tile is a 6-gon, and a non consistent 6-labelling with labels  $W_6 = [1, 2, 3, 4, 5, 6]$ ; label '5' is only assigned to vertices of valence 2. This is figure 10 of [2] and is attributed to W. P. Thurston.

**Remark 5.11** (Properties of Speiser  $q$ -tessellations). 1. The conformal type of  $\mathcal{R}_{w(z)}$  determines the ambient space  $\Omega_z \cup \partial_I \Omega_z$  of the oriented graph  $\widehat{\Gamma}_q$  in Definition 5.3, namely  $\widehat{\mathbb{C}}_z, \mathbb{C}_z \cup \{\infty_1, \dots, \infty_p\}$  or  $\Delta_z \cup \partial_I \Delta_z$ . 2. The tiles of the Speiser  $q$ -tessellation (19) are  $q$ -gons; blue and grey tiles corresponding to the inverse image under  $w^{-1}(z)$  of the blue and grey tiles  $T, T'$  in Step 3, respectively. 3. Considering the graph  $\widehat{\Gamma}_q = w(z)^* \gamma$ , the vertices of

- valence 2 are cosingular points of  $w(z)$  in  $\Omega_z$ ,
- finite valence greater than or equal to 4 are algebraic singularities of  $w^{-1}(z)$  (critical points of  $w(z)$ ) in  $\Omega_z$ , and
- infinite valence are logarithmic singularities of  $w^{-1}(z)$  in  $\partial_I \Omega_z$ .

We provide some features for the simplest families of Speiser functions.

**Remark 5.12** (Tessellations for rational functions). Let  $R(z)$  be a rational function of degree  $n \geq 2$ , due to Remark 2.1, we have  $\Omega_z = \widehat{\mathbb{C}}_z$ . The set of asymptotic values of  $R(z)$  is empty and the set of singular values consists exclusively of critical values. The finite number of critical points is  $2 \leq r \leq 2n - 2$ , the cosingular points are called cocritical points. Obviously,  $\widehat{\Gamma}_q \subset \widehat{\mathbb{C}}_z$  is a finite graph<sup>13</sup>, with vertices of valence 2 at the cocritical points of  $R(z)$ , and even valence greater than or equal to 4 at the critical points of  $R(z)$ .

Furthermore, if the distinct  $q$  critical values of  $R(z)$  lie in  $\mathbb{R}$ , the computation of the topological tessellation is readily available. In fact,  $\mathcal{T}_\gamma(R(z)) = \widehat{\mathbb{C}}_z \setminus R^{-1}(\mathbb{R} \cup \{\infty\})$ , where  $R^{-1}(\mathbb{R} \cup \{\infty\})$  is a real algebraic curve.

**Remark 5.13** (Tessellations for  $N$ -functions). Let  $w(z) : \mathbb{C}_z \rightarrow \widehat{\mathbb{C}}_w$  be an  $N$ -function. The set of critical values is empty and the set of singular values consists exclusively of asymptotic values:

$$\mathcal{AV}_w = \{(a_1, \mu_1), (a_2, \mu_2), \dots, (a_q, \mu_q)\}.$$

Moreover, the cosingular points are called coasymptotic points, and they can be defined by

$$\{w^{-1}(a_j)\}_{j=1}^q \cap \Omega_z.$$

In this case  $\widehat{\Gamma}_q$  is an infinite graph with vertices of valence 2 at the coasymptotic points of  $w(z)$ .

Furthermore, as was shown by R. Nevanlinna [13] §8, [6] §XI.3.5, the fact that  $w(z)$  satisfies the Schwarzian differential equation (11), implies that  $\Omega_z = \mathbb{C}_z$ , and that the set of logarithmic singularities is finite, *i.e.*  $p < \infty$ . Thus, the  $p$  vertices of infinite valence  $\{\infty_1, \dots, \infty_p\}$  of  $\widehat{\Gamma}_q$ , are the logarithmic singularities of  $w(z)$ . The compactification  $\mathbb{C}_z \cup \{\infty_1, \dots, \infty_p\}$  is non Hausdorff.

Example 9.1.c illustrates the simplest case of the Speiser  $q$ -tessellations for an  $N$ -function. Additionally, two non-trivial cases of  $N$ -functions when  $q = 3$  are in Examples 10.1.c and 10.2.c. Examples 10.3.c, 10.4.c, and 10.5.c show  $q$ -tessellations for Speiser functions that are not  $N$ -functions, the first for  $q = 3$  and the last two for  $q = 4$ .

**Remark 5.14** (Bounds on  $q$  for a consistent  $q$ -labelling of a  $t$ -graph, depending on its tessellation). Given a  $t$ -graph  $\Gamma$ , there are natural upper and lower bounds on the positive integer  $q$  of a consistent  $q$ -labelling  $\mathcal{L}_{W_q}$  that can be assigned to  $\Gamma$ . Recall from Definition 5.1.ii that for each tile  $T_\alpha$ , its boundary  $\partial T_\alpha$  consists of  $2 \leq \rho_\alpha \leq q$  vertices, thus taking the largest  $\rho_\alpha$  in  $\Gamma$  provides a lower bound for  $q$ . On the other hand, from Definition 5.7.ii it follows that  $q$

<sup>13</sup>Thus condition (iii) of Definition 5.2 is satisfied.

is bounded above by the number of vertices of valence greater than or equal to 4. Summarizing,

$$q_{\min} \doteq \max \# \left\{ \begin{array}{l} \text{vertices on } \partial \overline{T}_\alpha, \\ \text{for } T_\alpha \in \mathcal{T}(\Gamma) \end{array} \right\} \leq q \leq q_{\max} \doteq \# \left\{ \begin{array}{l} \text{vertices of } \Gamma \text{ with} \\ \text{valence} \geq 4 \end{array} \right\}. \quad (20)$$

Note that  $q_{\max}$  can be infinite.

The following is a surprising but useful result.

**Lemma 5.15.** *An A-map  $\widehat{\Gamma}_q$  supports at least one consistent  $q_o$ -labelling  $\mathcal{L}_{W_{q_o}}$ , for  $2 \leq q_{\min} \leq q_o \leq q \leq q_{\max}$ .*

*Proof.* Given the A-map  $\widehat{\Gamma}_q$ , let  $\Gamma$  be the t-graph, alluded to in Definition 5.3.ii (in other words  $\Gamma$  and  $\widehat{\Gamma}_q$  are compatible). Note that  $q_{\min} \leq q \leq q_{\max}$  as in the above Remark. The existence of a consistent  $q$ -labelling is as follows:

- 1) Choose  $q_o = q$ ,
- 2) assign the labels  $W_{q_o}$  to the  $q_o$  vertices of any blue tile  $T_\alpha$  of  $\widehat{\Gamma}_q$ , in an anticlockwise order,
- 3) propagate the labelling to all the neighbor grey tiles, this can be done since the tessellation  $\mathcal{T}(\widehat{\Gamma}_q)$  is homogeneous, i.e. its tiles are topological  $q_o$ -gons,
- 4) continue as above to all the tiles of  $\mathcal{T}(\widehat{\Gamma}_{q_o})$ , using the fact that  $\Omega_z$  is simply connected.

This provides a labelling

$$\mathcal{L}_{W_{q_o}} : V(\widehat{\Gamma}_{q_o}) \longrightarrow W_{q_o},$$

to  $\widehat{\Gamma}_{q_o}$ . Clearly,  $\mathcal{L}_{W_{q_o}}$  satisfies condition (i) of a consistent  $q_o$ -labelling, see Definition 5.7.

If the choice of  $q_o$  satisfies condition (ii) then we are done.

Otherwise, there is a label (value), say  $w_{j_o}$ , that does not appear under  $\mathcal{L}_{W_{q_o}}$  for a vertex of  $\widehat{\Gamma}_{q_o}$  of valence greater than or equal to 4. We can erase this label from the cyclic order  $W_{q_o}$ , obtaining a new cyclic order with  $q_o - 1$  distinct values. Now, go back to (2) with a new  $q_o$  being one less than the previous one and repeat the process. Since the original A-map  $\widehat{\Gamma}_q$  has a non empty subset of vertices of valence greater than or equal to 4, this process eventually stops at a  $q_o \geq q_{\min}$ .  $\square$

The reader is invited to keep in mind the above result when considering Remark 6.7 (an interpretation of the consistent  $q$ -labeling as a minimality condition).

**Theorem 5.16** (From Speiser functions to tessellations and back).

Let  $\Omega_z$  be a simply connected Riemann surface.

- 1) A Speiser function  $w(z) : \Omega_z \longrightarrow \widehat{\mathbb{C}}_w$  of index  $2 \leq q < \infty$ , provided with a cyclic order  $W_q$  and a path  $\gamma$  realizing it, determine a homogeneous tessellation

$$\begin{aligned} \mathcal{T}_\gamma(w(z)) &= (\Omega_z \cup \partial_I \Omega_z) \setminus \Gamma = \begin{cases} \widehat{\mathbb{C}}_z \setminus \Gamma \\ (\mathbb{C}_z \cup \{\infty_1, \dots, \infty_p\}) \setminus \Gamma \\ (\Delta \cup \partial_I \Delta) \setminus \Gamma \end{cases} \\ &= \underbrace{T_1 \cup \dots \cup T_\alpha \cup \dots}_{n \text{ blue tiles}} \cup \underbrace{T'_1 \cup \dots \cup T'_\alpha \cup \dots}_{n \text{ grey tiles}} \subset \Omega_z \cup \partial_I \Omega_z, \end{aligned}$$

whose tiles are topological  $q$ -gons with alternating colors, and a consistent  $q$ -labelling  $w(z)^* \mathcal{L}_\gamma$ .

- 2) Let  $\mathcal{T}$  be a possibly non homogeneous tessellation of  $\Omega_z$ . Assume in addition that  $\mathcal{T}$  is provided with a consistent  $q$ -labelling  $\mathcal{L}_{W_q}$ . Then, they determine a Riemann surface  $\Omega_z$ , a non unique Speiser function

$$w(z) : \Omega_z \longrightarrow \widehat{\mathbb{C}}_w,$$

and a Jordan path  $\gamma$  satisfying that the tessellation

$$(\mathcal{T}_\gamma(w(z)), w(z)^* \mathcal{L}_\gamma) \quad \text{is} \quad (\mathcal{T}, \mathcal{L}_{W_q}),$$

up to orientation preserving homeomorphism of  $\Omega_z$ .

**Remark 5.17.** Note that in statement (2), the fact that the consistent  $q$ -labelling  $\mathcal{L}_{W_q}$  is provided to  $\mathcal{T}$ , ensures that the choice and ordering of the values  $W_q$  are an essential part of the hypothesis.

Clearly, the number of tiles  $2n$  of  $\mathcal{T}$  is finite if and only if  $w(z)$  is rational function of degree  $n$  on  $\widehat{\mathbb{C}}_z$ .

*Proof.* Statement (1) follows directly from the Schwarz–Klein–Speiser’s algorithm.

For statement (2), we proceed with the following steps:

Step 1. Recall that the tessellation  $\mathcal{T}$  is equivalent to a  $\mathbf{t}$ –graph  $\Gamma \subset \Omega_z \cup \partial_I \Omega_z$ , thus in fact we have  $(\Gamma, \mathcal{L}_{W_q})$ .

Step 2. By using the consistent  $q$ –labelling  $\mathcal{L}_{W_q}$  and edge subdivision operation for  $\Gamma$ , we get an associated  $\mathbf{A}$ –map  $\widehat{\Gamma}_q \subset \Omega_z \cup \partial_I \Omega_z$  with a consistent  $q$ –labelling

$$\mathcal{L}_{W_q} : V(\widehat{\Gamma}_q) \longrightarrow W_q,$$

as follows.

*Edge subdivision operation.* Let  $\overline{z_\ell z_\sigma}$  be an edge of  $\Gamma$  with labels, say  $\mathcal{L}_{W_q}(z_\ell) = w_h$  and  $\mathcal{L}_{W_q}(z_\sigma) = w_j$ .

If  $j - h = (z_\ell) = 1 \pmod{q}$ , then  $\overline{z_\ell z_\sigma}$  is an edge of  $\widehat{\Gamma}_q$ .

If  $j - h = v + 1 \geq 2 \pmod{q}$ , then we consider  $v$  new vertices,  $\zeta_1, \dots, \zeta_v$ , in the original edge  $\overline{z_\ell z_\sigma}$ , which is replaced by  $v + 1$  new edges

$$\overline{z_\ell \zeta_1}, \overline{\zeta_1 \zeta_2}, \dots, \overline{\zeta_v z_\sigma}$$

of  $\widehat{\Gamma}_q$ . Moreover, the labels of these new vertices of valence 2 of  $\widehat{\Gamma}_q$  are

$$\mathcal{L}_{W_q}(z_\ell) = w_h, \mathcal{L}_{W_q}(\zeta_1) = w_{h+1}, \dots, \mathcal{L}_{W_q}(\zeta_v) = w_{h+v}, \mathcal{L}_{W_q}(z_\sigma) = w_j;$$

with arithmetic mod  $q$  in the subindices.

Step 3. Since  $\widehat{\Gamma}_q$  is homogeneous, we can recognize that  $\mathcal{T}(\widehat{\Gamma}_q)$  inherits a natural conformal structure from the glueing of the contiguous tiles  $T_\alpha$  and  $T'_\alpha$  according to the consistent  $q$ –labelling  $\mathcal{L}_{W_q}$ . In fact, we recognize that there is a Speiser Riemann surface  $\mathcal{R}(\widehat{\Gamma}_q, \mathcal{L}_{W_q}) \subset \Omega_z \times \widehat{\mathbb{C}}_w$ , with a tessellation as above, that projects via  $\pi_1$ , see (5), to  $\mathcal{T}(\widehat{\Gamma}_q)$ .

Step 4. Finally, the Speiser Riemann surface  $\mathcal{R}(\widehat{\Gamma}_q, \mathcal{L}_{W_q})$  provides the Speiser function  $w(z)$ .

The non–uniqueness of the Speiser function  $w(z)$  arises from the following.

**Definition 5.18.** Let  $Stab(W_q)$  be the isotropy group of  $W_q$ , that is the subgroup of  $Aut(\widehat{\mathbb{C}}_w)$  that leaves invariant the set  $\{w_j\}_{j=1}^q$  and also preserves the chosen cyclic order on them.

**Lemma 5.19** (Non uniqueness of Speiser functions arising from tessellations). *Let  $w(z)$  be a Speiser function provided with a cyclic order  $W_q$  for its  $q$  singular values. Consider the action*

$$\begin{aligned} Aut(\Omega_z) \times Stab(W_q) \times (\Omega_z \times \widehat{\mathbb{C}}_w) &\longrightarrow \Omega_z \times \widehat{\mathbb{C}}_w \\ (g, h, z, w) &\longmapsto (g(z), h(w)). \end{aligned}$$

Each non–trivial element in  $Aut(\Omega_z) \times Stab(W_q)$  provides a different function with the same  $W_q$ .

- i) Since  $Aut(\Omega_z)$  is a Lie group, it gives rise to an infinite number of functions.
- ii) For the group  $Stab(W_q)$  we have the following (up to conjugation in  $Aut(\widehat{\mathbb{C}}_w)$ ) cases.
  - If  $q = 2$  and  $Stab(W_q) \neq Id$ , then  $Stab(W_q) \cong \mathbb{C}^*$  are the homotheties.
  - If  $q \geq 3$  and  $Stab(W_q) \neq Id$ , then  $Stab(W_q)$  is one of the finite subgroups of  $PSL(2, \mathbb{C})$ .

*Proof of Lemma.* The action of  $Aut(\Omega_z) \times Stab(W_q)$  extends to functions as

$$(g, h, w(z)) \mapsto h(w(g(z))).$$

Note that the cyclic order of the  $q$  singular values  $W_q$ , may have non–trivial isotropy

$$Id \neq Stab(W_q) \subset Aut(\widehat{\mathbb{C}}_w).$$

The finite subgroups of  $PSL(2, \mathbb{C})$  are: the rotations  $\mathbb{Z}_n$  for  $n \geq 2$ , the dihedral group  $\mathbb{D}_n$  for  $n \geq 2$  (generated by the rotations, and the inversion  $w \mapsto 1/w$ ), and the groups  $H_{p,q,r}$  with  $p, q, r \geq 2$ , associated to the symmetries of the regular polyhedra inscribed in  $\widehat{\mathbb{C}}_w$ . See [29] for more details.  $\square$

**Example 5.6.** 1. A simple family is  $\{h(\sin(g(z))) \mid g \in Aut(\widehat{\mathbb{C}}_z), h \in Stab([-1, 1, \infty])\}$ . Obviously  $\cos(z)$  is an element of it.  
2. Let  $G \subset Aut(\widehat{\mathbb{C}}_z)$  be a finite group. For the classical rational  $G$ –invariant functions  $R(z)$  the Lemma applies, giving origin to different explicit expressions for  $R(z)$  in the literature. Compare with [3] and [30].

Theorem 5.16 is proved.  $\square$

## 6. Speiser graphs

Recalling Equation (19), Speiser  $q$ -tessellations  $((\Omega_z \cup \partial_I \Omega_z) \setminus w(z)^* \gamma, w(z)^* \mathcal{L}_\gamma)$  arising from Speiser functions  $w(z)$ , as in Theorem 5.16.1, are very concrete objects. The dual graph  $\mathfrak{S}_{w(z)}$  of the A-map  $\widehat{\Gamma}_q = w(z)^* \gamma$  is the Speiser graph of index  $q$ , of  $w(z)$ . Here, we develop Speiser graphs in an ad hoc axiomatic way. As departure point, our Speiser graphs are embedded in  $\mathbb{S}^2$  or  $B(0, 1)$ ; because of the uniformization theorem this will be enough to completely specify the conformal type of the domain of the associated Speiser functions.

The original concept is in [5]. We roughly follow [6], [10] p. 355, and [31] p. 54. Once again, we make some precisions that we consider improve the presentation and our understanding.

**Definition 6.1** ([10] p. 355). A *Speiser graph of index  $q \geq 2$*  (or *line complex of index  $q$* ),

$$\mathfrak{S}_q = \left( V(\mathfrak{S}_q) = \underbrace{\{\times_\alpha, \circ_\beta\}}_{\text{vertices}}, E(\mathfrak{S}_q) = \underbrace{\{\overbrace{\times_\alpha \circ_\beta}\}}_{\text{edges}} \right),$$

is a connected, locally finite<sup>14</sup>, multigraph satisfying the following:

- i) The graph  $\mathfrak{S}_q$  is properly embedded in  $\mathbb{S}^2$  when it is finite, or in  $B(0, 1)$  when it is infinite.
- ii) The set of vertices  $V(\mathfrak{S}_q)$  is a finite or countable set.
- iii) The graph  $\mathfrak{S}_q$  is bipartite, with vertices in  $\{\times, \circ\}$ .
- iv) Every vertex has valence  $q$ .

Note that a Speiser graph of index  $q$  is the dual of an A-map  $\widehat{\Gamma}_q$ . Of course, the dual of a  $t$ -graph  $\Gamma$  also exists.

**Definition 6.2.** A *pre-Speiser graph*  $\mathfrak{S}$  is a graph satisfying Definition 6.1, with (iv) replaced by:

iv') each vertex has a valence  $2 \leq \rho \leq q$ ; the valence of each vertex is allowed to differ.

**Remark 6.3** (Regular graph / homogeneous tessellation). If a graph satisfies condition (iv) of Definition 6.1, it is said to be  *$q$ -regular*, or just *regular*.

1. Through duality, the fact that the Speiser graph  $\mathfrak{S}_q$  of index  $q$  is regular is equivalent to the fact that the tessellation  $\mathcal{T}(\widehat{\Gamma}_q)$  is homogeneous, recall Definition 5.1.2.
2. A priori, pre-Speiser graphs  $\mathfrak{S}$  are not regular, similarly the tessellations  $\mathcal{T}(\Gamma)$  arising from a  $t$ -graph  $\Gamma$  are usually not homogeneous.

The concept of consistent  $q$ -labelling  $\mathcal{L}_{W_q}$ , for  $t$ -graphs  $\Gamma$  and A-maps  $\widehat{\Gamma}_q$ , has its corresponding dual for pre-Speiser graphs  $\mathfrak{S}$  and Speiser graphs  $\mathfrak{S}_q$  of index  $q$ . We shall convene on using the same name and symbol  $\mathcal{L}_{W_q}$  when applied to  $\mathfrak{S}$  or  $\mathfrak{S}_q$ .

**Definition 6.4.** Given a cyclic order  $W_q$ , a *consistent  $q$ -labelling*

$$\mathcal{L}_{W_q} : E(\mathfrak{S}) \longrightarrow W_q, \quad q \geq 2,$$

for a pre-Speiser graph  $\mathfrak{S}$  (Speiser graph  $\mathfrak{S}_q$  of index  $q$ ) satisfies the following conditions:

- i) The edges have labels in  $W_q = [w_1, \dots, w_q]$ , with no label repeated around each vertex, the ordering of the edges around a vertex is according to their labels, cyclic clockwise for a  $\times$ -vertex, cyclic anticlockwise for a  $\circ$ -vertex.
- ii) For  $w_j \in W_q$ , a  $w_j$ -face of  $\mathfrak{S}$  is a component of  $\mathbb{S}^2 \setminus \mathfrak{S}$  (when  $V(\mathfrak{S})$  is finite), or of  $B(0, 1) \setminus \mathfrak{S}$  (when  $V(\mathfrak{S})$  is infinite), with alternating edges labeled  $w_{j-1}$  and  $w_j$ . We require that, for each  $w_j \in W_q$ , there is at least one  $w_j$ -face of  $\mathfrak{S}$  that is not a digon.

The same applies to a Speiser graph  $\mathfrak{S}_q$  of index  $q$ .

**Definition 6.5.** An *analytic Speiser graph of index  $q$*  is a pair

$$(\mathfrak{S}_q, \mathcal{L}_{W_q}),$$

where  $\mathfrak{S}_q$  is a Speiser graph of index  $q$  and  $\mathcal{L}_{W_q}$  is a consistent  $q$ -labelling.

<sup>14</sup>“Locally finite” means every vertex has finite valence and each compact subset of  $\mathbb{S}^2$  or  $B(0, 1)$  meets only finitely many edges.

**Remark 6.6** (On the notation for the labels). As is usual in the literature, unless explicitly stated, we shall consider the labels to be  $\mathcal{W}_q = [1, \dots, q] \subset \widehat{\mathbb{C}}_w$  to make the discussion simpler. In general,

$$\mathcal{W}_q = [w_1, \dots, w_q] \doteq [1, \dots, q] \subset \widehat{\mathbb{C}}_w,$$

according to Definition 5.4.1.

**Remark 6.7** (Requirement (ii) of  $\mathcal{L}_{W_q}$  is a *minimality condition*). Suppose a labelling for a Speiser graph  $\mathfrak{S}_q$  fails to satisfy (ii) for exactly one label, say  $w_{j_0} \in \mathcal{W}_q$ . Then all  $w_{j_0}$ -faces are digons. Forgetting<sup>15</sup> the edges labelled  $w_{j_0}$ , also forgets the  $w_{j_0}$ -face, and the resulting graph satisfies all the requirements of a Speiser graph of index  $q - 1$ .

In other words, when considering analytic Speiser graphs and relaxing the labelling so that it only satisfies (i) but not (ii), then several such Speiser graphs of different indices  $q$  give origin to the same function  $w(z)$ .

For instance, Figure 4.e is a graph, with  $q = 4$ , with a labelling satisfying the requirements of Definition 6.4 except for condition (ii); Figure 4.d is a graph, with  $q = 3$ , satisfying all the requirements: both represent the same function. Furthermore, by replacing each digon labelled 4 in Figure 4.e with two digons labelled 4 and 5, we obtain another graph, with  $q = 5$ , that satisfies Definition 6.4 except for condition (ii). Clearly this can be continued to an arbitrary  $q > 3$ . Compare with [10] p. 355, where the minimality condition is not included.

An alternate description of condition (ii) of Definition 6.4, appears in [31] p. 54 in terms of the monodromy:

ii') For any  $j \in \mathbb{Z}_q$ , define a map  $\nu_j$  from  $V(\mathfrak{S}_q)$  to itself as follows  $\nu_j(v)$  is the vertex adjacent to  $v$  with respect to the edge  $j$ . The composition  $\Sigma_j(v) \doteq \nu_j \circ \nu_{j-1}(v)$  of two maps is a permutation of the vertices  $\circ$  and  $\times$ . Require that for each  $j \in \mathbb{Z}_q$ ,  $\Sigma_j(v) \neq v$  for some  $v \in V(\mathfrak{S}_q)$ , i.e. none of the maps  $\Sigma_j$  are the identity.

**Remark 6.8.** 1. An analytic Speiser graph  $(\mathfrak{S}_q, \mathcal{L}_{W_q})$  naturally induces a cell decomposition  
 $\mathbb{S}^2 \setminus \mathfrak{S}_q$  or  $B(0, 1) \setminus \mathfrak{S}_q$ ,

depending on whether  $\mathfrak{S}_q$  is finite or infinite, respectively.

- The cells of dimension 0 correspond to  $V(\mathfrak{S}_q)$ .
- The cells of dimension 1 correspond to the edges  $E(\mathfrak{S}_q)$ .
- The cells of dimension 2 are the connected components of the decomposition of  $\mathbb{S}^2 \setminus \mathfrak{S}_q$  or  $B(0, 1) \setminus \mathfrak{S}_q$ , which are called *faces*.

2. The faces inherit the cyclic order of the edges; the faces have cyclic clockwise order, around each  $\times$ -vertex, and the cyclic anticlockwise order around each  $\circ$ -vertex. Thus, the order of the faces coincides with the order of the edges. As matter of record:

*labelling edges of  $\mathfrak{S}_q$  or labelling faces of the cell decomposition is equivalent.*

3. It is easy to see that when we go around the boundary of a face, the edges have labels  $w_{j-1}$  and  $w_j$  (for some  $w_j \in \mathcal{W}_q$ ) and the labels alternate, i.e. each face is a  $w_j$ -face for some label  $w_j \in \mathcal{W}_q$ .

4. Each face is bounded by either

- an finite even set of edges, a *bounded face* (*algebraic elementary region* according to [10]), or
- by an infinite set of edges, an *unbounded face* (*logarithmic elementary region* according to [10]).

5. Several edges with consecutive labels, having common vertices  $\circ$  and  $\times$ , form a so-called *edge bundle*. Clearly, two edges belonging to the same edge bundle and having labels  $j - 1$  and  $j$  form a boundary of a face, which is a digon. In graph theory language, a multigraph admits edge bundles, thus our Speiser graphs of index  $q$  are (generically) multigraphs.

6. If a face is not a digon, its label will be written inside it. Because of condition (ii) of Definition 6.4, it is not necessary to write labels inside digons.

**Example 6.1** (Speiser graphs of index  $q$  for some functions). For Speiser graphs of index  $q$  arising from transcendental Speiser functions  $w(z)$  on  $\mathbb{C}_z$ , with an essential singularity at  $\infty \in \widehat{\mathbb{C}}_z$ , see [10] ch. 4 and our Figures 12.c, 14.c, 15.c, 16.b, 17.b, 18.b.

### 6.1. Duality: Tessellations and Speiser graphs

The duality between the A-maps  $\widehat{\Gamma}_q$  and Speiser graphs  $\mathfrak{S}_q$  of index  $q$  provides the following bijections.

---

<sup>15</sup>The forgetting edge operation for  $\mathfrak{S}_q$  is the analogue of the forgetting vertex operation for the corresponding A-map  $\widehat{\Gamma}_q$ .

**Proposition 6.9** (Bijection between Speiser tessellations and analytic Speiser graphs). *Let  $\mathcal{W}_q$  be fixed (that is the set of  $q$  distinct values  $\{w_j\}_{j=1}^q$  and the cyclic order on them are fixed).*

1) *There is a bijection between Speiser  $q$ -tessellations and analytic Speiser graphs of index  $q$ ,*

$$(\mathcal{T}(\widehat{\Gamma}_q), \mathcal{L}_{W_q}) \longleftrightarrow (\mathfrak{S}_q, \mathcal{L}_{W_q}).$$

2) *The above bijection extends to a bijection that includes the action of  $\text{Aut}(\Omega_z) \times \text{Stab}(\mathcal{W}_q)$ , i.e.*

$$\text{Aut}(\Omega_z) \times \text{Stab}(\mathcal{W}_q) \times ((\Omega_z \cup \partial_I \Omega_z) \setminus \widehat{\Gamma}_q, \mathcal{L}_{W_q}) \longleftrightarrow \text{Aut}(\Omega_z) \times \text{Stab}(\mathcal{W}_q) \times (\mathfrak{S}_q, \mathcal{L}_{W_q}).$$

*Proof.* Because of the duality between the A-maps  $\widehat{\Gamma}_q$  and the Speiser graphs  $\mathfrak{S}_q$  of index  $q$ , the bijection should follow immediately.

However, since

$$\mathcal{T}(\widehat{\Gamma}_q) = (\Omega_z \cup \partial_I \Omega_z) \setminus \widehat{\Gamma}_q,$$

care must be taken with the ideal boundary.

*Finite  $\widehat{\Gamma}_q$  case.* Note that  $\widehat{\Gamma}_q \subset \widehat{\mathbb{C}}_z$ . Since the ideal boundary is empty,  $\partial_I \Omega_z = \emptyset$ , the cell decomposition  $\widehat{\mathbb{C}}_z \setminus \widehat{\Gamma}_q$ , is the dual of  $\widehat{\mathbb{C}}_z \setminus \mathfrak{S}_q$ .

*Infinite  $\widehat{\Gamma}_q$  case.* Recalling condition (iii) of Definition 5.2, it follows that the ambient space for  $\widehat{\Gamma}_q$  is either  $\mathbb{C}_z \cup \{\infty_1, \dots, \infty_p\}$  or  $\Delta_z \cup \partial_I \Delta_z$ . Let  $\widehat{\Gamma}_0 = \widehat{\Gamma}_q \setminus V_\infty$ , where  $V_\infty$  denotes the vertices with infinite valence of  $V(\widehat{\Gamma}_q)$ . Considering the cell decomposition  $\mathbb{C}_z \setminus \widehat{\Gamma}_0$  or  $\Delta_z \setminus \widehat{\Gamma}_0$ , note that within the  $C^1$ -category  $\mathbb{C}_z \cong \Delta_z \cong B(0, 1)$ , hence the cell decomposition is  $B(0, 1) \setminus \widehat{\Gamma}_0$ . Its dual, is  $B(0, 1) \setminus \mathfrak{S}_q$ .

This finishes the proof of statement 1.

For statement 2, note that the action commutes with the duality.  $\square$

Speiser graphs have been used extensively in various contexts, one of the most common is for studying Speiser functions  $w(z)$  from a combinatorial perspective. From Theorem 5.16 and the above bijection we immediately obtain.

**Corollary 6.10** (An analytic Speiser graph determines a family of Speiser functions). *An analytic Speiser graph  $(\mathfrak{S}_q, \mathcal{L}_{W_q})$  of index  $q$ , determines a non unique Speiser function  $w(z)$  provided with  $q$  distinct singular values  $\mathcal{W}_q$ .*  $\square$

In fact, because of the complete duality/bijection given by Proposition 6.9, once a consistent  $q$ -labelling is chosen, working with either of the following pairs is the same

$$\underbrace{(\widehat{\Gamma}_q, \mathcal{L}_{W_q})}_{\text{A-map \& consistent } q\text{-labelling}} \longleftrightarrow \underbrace{(\mathcal{T}_\gamma(w(z)), w(z)^* \mathcal{L}_\gamma)}_{\text{Tessellation arising from Speiser function } w(z)} \longleftrightarrow \underbrace{(\mathfrak{S}_q, \mathcal{L}_{W_q})}_{\text{analytic Speiser graph \& consistent } q\text{-labelling}}.$$

**Proposition 6.11** (The faces of  $(\mathfrak{S}_q, \mathcal{L}_{W_q})$  and their relation to singularities of the inverse  $w^{-1}(z)$ ). *The cell decomposition provides the following relationships.*

- 1) *If a  $w_j$ -face is a digon, then the corresponding point  $\zeta_t \in \Omega_z$  (a vertex of valence 2 of the A-map  $\widehat{\Gamma}_q$ ) is an ordinary point, equivalently a cosingular point with cosingular value  $w(\zeta_t) = w_j$ .*
- 2) *If a  $w_j$ -face is a  $2m$ -gon, for  $2 \leq m < \infty$ , then the corresponding point  $z_t \in \Omega_z$  (a vertex of finite even valence greater than or equal to 4 of the A-map  $\widehat{\Gamma}_q$ ) is an algebraic singularity of the inverse  $w^{-1}(z)$ , with critical value  $w(z_t) = w_j$ . Moreover,  $m_t$  is the ramification index of  $z_t$ , equivalently the multiplicity of the critical point  $z_t$ .*
- 3) *If a  $w_j$ -face is unbounded (an  $\infty$ -gon), then it corresponds to a logarithmic singularity of  $w^{-1}(z)$  over the asymptotic value  $a_j \doteq w_j$ .*

*Proof.* Follows from Definition 6.5 and Remark 6.8.4.  $\square$

**Remark 6.12** (Recognizing conformal type of  $(B(0, 1), J)$  directly from the infinite Speiser graphs  $\mathfrak{S}_q$ ). It is clear that the Riemann surface  $\mathcal{R}_{w(z)}$  associated to a finite Speiser graph  $\mathfrak{S}_q$  has parabolic type. The recognition of the conformal type of  $\mathcal{R}_{w(z)}$  can be done in several different ways: all of which are equivalent on any infinite, finitely-ended, locally finite planar graph, in particular on the Speiser graph of a Speiser function  $w(z)$ .

1. Random-walk criterion; see [32], [33], [34].
2. Resistance (Nash–Williams) criterion; see [35], [36].

3. Modulus (extremal length) criterion; see [37], [38], [39].
4. Circle-packing criterion; see [40], [41].
5. Isoperimetric or Cheeger Constant  $h(\mathfrak{S}_q)$  criterion; see [42].

Recalling Remark 5.14 and using duality, we have the following bounds, in terms of the pre-Speiser graph  $\mathfrak{S}$ , for  $q$  to be a consistent  $q$ -labeling of  $\mathfrak{S}$ .

$$q_{\min} \doteq \max \left\{ \begin{array}{l} \text{valence of the} \\ \text{vertices of } \mathfrak{S} \end{array} \right\} \leq q \leq q_{\max} \doteq \# \left\{ \begin{array}{l} \text{faces of } \mathfrak{S}, \\ \text{that are not digons} \end{array} \right\}. \quad (21)$$

Once again, note that  $q_{\max}$  can be infinite.

**Lemma 6.13.** *A Speiser graph  $\mathfrak{S}_q$  of index  $q$  supports at least one consistent  $q_0$ -labelling  $\mathcal{L}_{W_{q_0}}$ , for  $2 \leq q_{\min} \leq q_0 \leq q \leq q_{\max}$ .*

*Proof.* Follows directly from duality and Lemma 5.15.  $\square$

**Remark 6.14** (Non uniqueness of the functions).

1. Let us consider in more detail the case when  $\text{Stab}(\mathcal{W}_q) \neq \text{Id}$ .

For  $q = 2$ . The subcase of two algebraic singularities of  $w^{-1}(z)$  leads to  $w(z) = \lambda(z - a)^n / (z - b)^n$ , for  $n \geq 2$ ,  $a \neq b$ . The subcase of two logarithmic singularities of  $w^{-1}(z)$ , leads to

$$w(z) = \mathcal{E}(z) = e^z \text{ and } w(z) = \mathcal{Th}(z) = \tanh(z),$$

which will give rise to “elementary blocks” as in Definition 9.6. See also Example 9.1.

For  $q = 3$ . Up to  $\text{Aut}(\mathbb{C}_w)$  the choice of the singular values is  $\{0, 1, \infty\}$ , that is  $w(z)$  is an algebraic or transcendental Belyi’s function. The theory of dessins d’ enfants applies for  $w(z)^* \gamma$  in this case, see [11].

2. E. Drape [43], and C. Blanc [44] studied the classification of the Speiser graphs associated to  $N$ -functions with only one branch point over each asymptotic value, later W. Lotz [45], in his thesis, dropped the assumption of only one branch point over each asymptotic value.

3. Given a pair (A-map, consistent  $q$ -labelling), say  $(\widehat{\Gamma}, \mathcal{L}_{W_q})$ , note that choosing any representative  $\gamma$  of the isotopy class of simple closed paths relative to the  $q$  distinct values  $\{w_1, \dots, w_q\}$  does not change the cyclic order  $\mathcal{L}_\gamma = \mathcal{W}_q$  and thus does not change the consistent  $q$ -labelling  $\mathcal{L}_{W_q}$ . However, by relaxing the condition of isotopy relative to the  $q$  distinct values  $\{w_1, \dots, w_q\}$ , that is by choosing  $\widetilde{\gamma} \notin [\gamma]$  but still requiring that  $\widetilde{\gamma}$  visit the  $q$  distinct values, the cyclic order  $\mathcal{L}_{\widetilde{\gamma}} \neq \mathcal{L}_\gamma$  changes. Thus the corresponding consistent  $q$ -labelling also changes, say to  $\mathcal{L}_{\widetilde{W}_q}$ , and the new pair  $(\widehat{\Gamma}, \mathcal{L}_{\widetilde{W}_q}) \neq (\widehat{\Gamma}, \mathcal{L}_{W_q})$ . Compare with [46], [47], [48].

We provide some features for the simplest families of Speiser functions.

**Remark 6.15** (Speiser graphs for rational functions). Let  $(\mathfrak{S}_{w(z)}, \mathcal{L}_{W_q})$  be the analytic Speiser graph of a rational function  $w(z) = R(z)$  of degree  $n \geq 2$ . The dual of  $\mathfrak{S}_{w(z)}$  is an A-map  $\widehat{\Gamma}_q$  embedded in  $\widehat{\mathbb{C}}_z$ . In particular, there are no unbounded faces of  $\widehat{\mathbb{C}}_z \setminus \mathfrak{S}_{w(z)}$ . Furthermore, for each  $w_j \in \mathcal{W}_q$ , at least one  $w_j$ -face is a  $2m$ -gon for some  $m \geq 2$  (where  $m$  is the multiplicity of the corresponding critical point, see Definition 3.5). In simple words, each label  $w_j$  comes from a critical point of  $w(z)$ , i.e. the labels are exactly the critical values.

In the case of polynomials of degree  $r \geq 2$ , once again  $\mathfrak{S}_{w(z)}$  is finite and embedded in  $\widehat{\mathbb{C}}_z$ . Furthermore, the  $w_j$ -face containing  $\infty \in \widehat{\mathbb{C}}_z$  has  $2r$  edges, and in fact  $w_j = \infty \in \widehat{\mathbb{C}}_w$ .

## 6.2. Speiser graphs for $N$ -functions

From Proposition 6.11 and the definition of  $N$ -function, it follows immediately that an analytic Speiser graph of index  $q$   $(\mathfrak{S}_{w(z)}, \mathcal{L}_{W_q})$  for an  $N$ -function  $w(z) : \Omega_z \rightarrow \widehat{\mathbb{C}}_w$ , requires that:

- i) its conformal type is parabolic, so  $\Omega_z = \mathbb{C}_z$ ,
- ii) the only bounded faces of  $\mathfrak{S}_{w(z)}$  are digons,
- iii) the labels  $\mathcal{W}_q$  are exactly the asymptotic values of  $w(z)$ ,
- iv) there are  $2 \leq p < \infty$  unbounded faces of  $\mathfrak{S}_{w(z)}$ : for  $\iota = 1, \dots, p$ , the unbounded face with label  $w_{j(\iota)} = a_{j(\iota)} \in \mathcal{W}_q$  corresponds to the class of asymptotic paths  $[\alpha_{j(\iota)}]$  associated to the asymptotic value  $a_{j(\iota)}$  (recall (10) for notation),

v)  $\mathfrak{S}_{w(z)}$  has  $p$  “logarithmic ends” and no other ends.

**Remark 6.16** (Historical origin and remarks on logarithmic ends). In the literature, the structure appearing in (v) above can be found with different names and also for different objects: the term “logarithmic end” appears in [6] p. 292 (who attributes it to A. Speiser), also [10] p. 379–380 uses it for the combinatorial and analytic objects. The terms “logarithmic tower”, “helicoid”, “half–logarithmic spiral” appear in [20] p. 152, 194, and [18] p. 23, once again for the combinatorial and analytic objects. The term “logarithmic staircase” is used in [49] p. 362 for the analytic object. We shall use the term “logarithmic end” for the combinatorial objects, and “logarithmic tower” for the analytic objects (see Definition 9.8 and Remark 9.11).

To make a precise definition in the combinatorial case, we shall need the following.

**Definition 6.17.** Let  $v \in V(\mathfrak{S}_q)$  be a vertex of a Speiser graph  $\mathfrak{S}_q$ , and  $S \subset V(\mathfrak{S}_q)$  be a subset of vertices a Speiser graph  $\mathfrak{S}_q$ .

1. An *open neighborhood*  $N(v)$  of the vertex  $v$  consists of vertices directly adjacent to  $v$  by an edge of  $\mathfrak{S}_q$ .
2. The *open neighborhood complex* of  $S$ , denoted<sup>16</sup> by  $N^o(S)$ , is the union of the open neighborhoods of each vertex in  $S$ , that is

$$N^o(S) = \bigcup_{v \in S} N(v).$$

3. The *open neighborhood* of the set  $S$ , denoted,  $N(S)$  is  $N^o(S) \setminus S$ .

**Example 6.2.** Note that  $N^o(S)$  may or may not contain  $S$ . For instance  $v \notin N(v)$ , since there are no loops in  $\mathfrak{S}_q$ ; that is why  $N(v)$  is called an *open* neighborhood. However, if the subgraph  $\mathfrak{S}_q[S]$  spanned by  $S$  is connected and contains more than one vertex, then  $S \subset N^o(S)$ . As is usual in graph theory, saying “the neighborhood of  $S$ ” should be understood as “the open neighborhood of  $S$ ”.

**Definition 6.18.** 1. A *logarithmic end*  $\mathcal{T}$ , of a Speiser graph  $\mathfrak{S}_q$  of index  $q \geq 3$ , is a subset  $\mathcal{T} \subset \mathfrak{S}_q$  such that:

- i) It has an infinite number of ordered vertices  $v_{2\tau-1}, v_{2\tau} \in \{\times, \circ\}$  with  $\tau \in \mathbb{N}$ .
- ii) All even vertices  $v_{2\tau}$  are of the same type ( $\times$  or  $\circ$ ), and all odd vertices  $v_{2\tau-1}$  are of the other type.
- iii) There are  $1 \leq \rho_1 < q$  edges connecting  $v_{2\tau-1}$  to  $v_{2\tau}$  and  $1 \leq \rho_2 < q$  edges connecting  $v_{2\tau}$  to  $v_{2\tau+1}$ , where  $q = \rho_1 + \rho_2$ . In other words,  $\mathcal{T}$  is formed by a sequence of edge bundles with alternating number of edges  $\rho_1$  and  $\rho_2$ .
- iv) The open neighborhood  $N(\mathcal{T})$  consists of only one vertex.
- v)  $\mathcal{T}$  is maximal in  $\mathfrak{S}_q$ , that is; if given any  $\mathcal{T}'$  satisfying (i)–(iv) such that  $\mathcal{T} \subset \mathcal{T}'$ , then  $\mathcal{T} = \mathcal{T}'$ .

2. The *nucleus*<sup>17</sup>  $\mathfrak{N}_{\mathfrak{S}}$ , of a Speiser graph  $\mathfrak{S}_q$  of index  $q$ , is the subset obtained as the complement of the logarithmic ends in  $\mathfrak{S}_q$ .

**Remark 6.19.** 1. Note that logarithmic ends  $\mathcal{T}$  of a Speiser graph  $\mathfrak{S}_q$  are not Speiser graphs in themselves. In fact, they are pre–Speiser graphs because the first vertex  $v_1$  of each logarithmic end of  $\mathfrak{S}_q$  has valence  $\rho_1 < q$ , instead of the required  $q$ . On the other hand, the nucleus  $\mathfrak{N}_{\mathfrak{S}}$  of  $\mathfrak{S}_q$  has “loose edges” (i.e. homeomorphic to  $[0, 1]$ , see Figure 4) where the logarithmic ends used to be attached to, so it is not even a pre–Speiser graph.

2. Condition (iv) of Definition 6.18.1 is a condition that allows for the nucleus to be well defined and unique.

3. Logarithmic ends, and hence the nucleus, are defined for arbitrary Speiser graphs, not only for those associated to  $N$ –functions. See for instance, Figures 4, 14–19, where the nucleus is colored red and the logarithmic ends are black.

**Example 6.3** (Speiser graphs following Nevanlinna brothers). In Figure 4, we illustrate four Speiser graphs  $(\mathfrak{S}_q, \mathcal{L}_{W_q})$  of index  $q = 3, 4$ . The cyclic order for the labels of the faces of  $\mathfrak{S}_q$  is  $W_q = [1, \dots, q]$ ; in accordance to Remark 6.6. Usually, the labelling is not shown on digons of the Speiser graph, however throughout Figure 4 they are shown for pedagogical reasons. The corresponding nucleus are red.

Figure 4.a–c are Speiser graphs with  $p = q = 4$  and nuclei consisting of 1, 2, and 3 vertices respectively. Clearly, there are Speiser graphs with  $p = q = 4$  and any number  $n \in \mathbb{N}$  of vertices in the nucleus.

<sup>16</sup>As far as we know, there is no commonly used notation for the union of the open neighborhoods the vertices of the set  $S$ .

<sup>17</sup>This concept appears as “nucleus” in [6] p. 299, and “soul” in [20] p. 196 and [18] p. 56.

Figure 4.a. and 4.c appear in [6] p.298, whereas, Figure 4.d. appears in [6] p.300 as the corresponding Speiser 3-tessellation.

Figure 4.e is an example of a planar graph that does not satisfy the minimality condition (ii) of Definition 6.4, hence is not a Speiser graph of index 4. However, by forgetting the edges/faces labelled 4, it reduces to  $\mathfrak{S}_3$  the Speiser graph of index 3 shown in Figure 4.d.

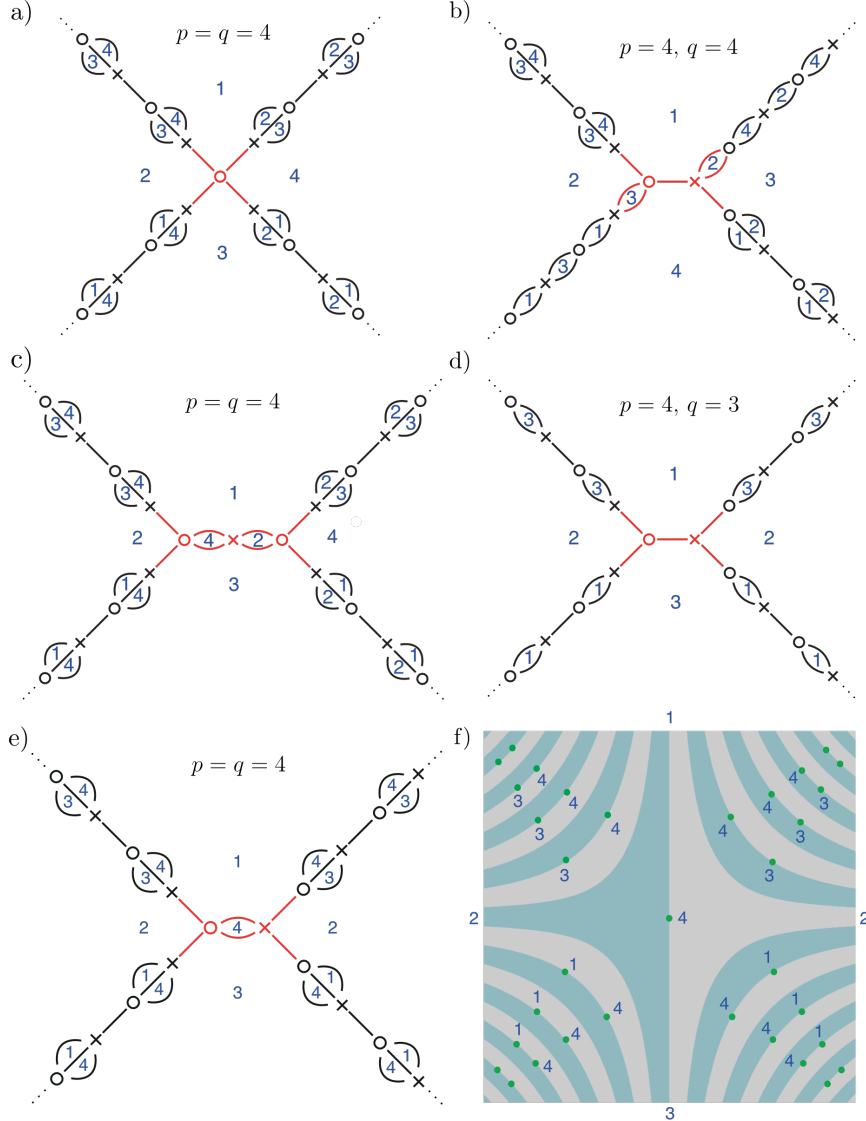


Figure 4: Analytic Speiser graphs of index  $q$  that represent  $N$ -functions  $w(z)$ ; (a)–(c) with  $p = q = 4$ , (d) with  $p = 4, q = 3$ . The nuclei are colored red and the  $p$  logarithmic ends are colored black. (e) is a labelled Speiser graph that does not have a consistent 4-labelling, since every 4-face is a digon. (f) The tessellation corresponding to the Speiser graph of (e), does not have a consistent 4-labelling since the label ‘4’ only appears on vertices of valence 2. The labels follow the convention of Remark 6.6.

**Lemma 6.20** (Nevanlinna [6] ch. XI, §12–13). *Let  $(\mathfrak{S}_q, \mathcal{L}_{W_q})$  be an analytic Speiser graph of index  $q$ , with  $p$  logarithmic ends and whose bounded faces are digons.*

1) *For each fixed  $p = 2, 3$ , there exist only one Speiser graph  $\mathfrak{S}_q$  of index  $q$ .*

2) For each  $p \geq 4$ , there exist infinitely many Speiser graphs.

The above Speiser graphs  $\mathfrak{S}_q$ , characterize families of  $N$ -functions  $\{w(z)\}$ , as we will see in Corollary 7.2.3.

*Proof.* First note that if  $p = 2, 3$ , then the index  $q = p$ .

Case  $p = 2$ , is in Figure 12.c, the vertices have valence 2, it is infinite in both directions. It corresponds to the exponential function (up to post–composition with a Möbius transformation), see [50] § 6.16.

Case  $p = 3$  is in Figure 14.c.

For assertion (2), we consider  $p = 4$ : the existence of an infinite number of Speiser graphs of index 4, follows from Figure 4.a–c by noting that the nuclei can contain an arbitrary number of vertices.  $\square$

**Remark 6.21** (On the multiplicity of asymptotic values). Note that for the Speiser graph of an  $N$ -function, if some asymptotic values have multiplicity  $\geq 1$ , then necessarily the number of logarithmic ends, namely  $p$ , is strictly greater than the index  $q$ . This can be observed for instance in Figure 4.d.

For more examples of Speiser graphs of index  $q$ , the reader is invited to consult Example 9.1.d for the simplest case of an  $N$ -function, Examples 10.1.d and 10.2.d for two non–trivial cases of  $N$ -functions when  $q = 3$ ; Examples 10.3.d, 10.4.d, and 10.5.d show Speiser graphs of index  $q$  for Speiser functions that are not  $N$ -functions, the first for  $q = 3$  and the last two for  $q = 4$ ; Example 10.6 shows a Speiser graph of index  $q = 4$  with one logarithmic end, an infinite number of unbounded faces and an infinite number of bounded 4–gons.

**Example 6.4** (There are “ends” of a Speiser graph  $\mathfrak{S}_q$  of index  $q$ , which are not logarithmic ends). Consider  $w(z) = \sin(z^2)$ , it is a Speiser function with  $\mathcal{SV}_w = \{-1, 1, \infty\}$ . It has an infinite number of algebraic singularities and 4 logarithmic singularities. However, its Speiser graph of index 3 has no logarithmic ends; the unbounded faces are separated by an infinite collection of 4–gons and digons, see figure 14 in [10] p. 360.

Moreover, it is easy to see that between two contiguous “ends” there must be an unbounded face of  $\mathfrak{S}_q$ . This in turn implies that there are the same number of “ends” as unbounded faces.

## 7. A complete correspondence

**Theorem 7.1.** Let  $\Omega_z$  be a simply connected Riemann surface, and let  $q \geq 2$ . There exists a one to one correspondence between:

1) Speiser functions

$$w(z) : \Omega_z \longrightarrow \widehat{\mathbb{C}}_w,$$

provided with a cyclic order  $\mathcal{W}_q$  for its  $q$  singular values.

2) Speiser Riemann surfaces

$$\mathcal{R}_{w(z)} \subset \Omega_z \times \widehat{\mathbb{C}}_w,$$

provided with a cyclic order  $\mathcal{W}_q$  for its  $q$  singular values.

3) Speiser  $q$ –tessellations

$$\left( \underbrace{(\Omega_z \cup \partial_I \Omega_z) \setminus w(z)^* \gamma}_{\text{tessellation}}, \underbrace{w(z)^* \mathcal{L}_\gamma}_{\substack{\text{consistent} \\ q\text{–labelling}}} \right).$$

4) Analytic Speiser graphs of index  $q$

$$\left( \underbrace{\mathfrak{S}_{w(z)}}_{\substack{\text{Speiser} \\ \text{graph}}}, \underbrace{w(z)^* \mathcal{L}_\gamma}_{\substack{\text{consistent} \\ q\text{–labelling}}} \right).$$

*Proof.* The proof of Theorem 7.1 proceeds as in rows two and three of Diagram 1 in the Introduction.

(1)  $\iff$  (2) is Definition 3.1.2 (classical).

(1)  $\implies$  (3) is Theorem 5.16.1 (Schwarz–Klein–Speiser’s algorithm)

(3)  $\implies$  (1) is Theorem 5.16.2 (lifting the tessellation  $(\mathcal{T}, \mathcal{L}_{\mathcal{W}_q})$  to  $\mathcal{R}_{w(z)}$  followed by (1)  $\iff$  (2)).

(3)  $\iff$  (4) is given by Proposition 6.9 (duality of the  $A$ –map and the analytic Speiser graph).  $\square$

Table 1: Some relationships between the different objects, note that  $w_{j(\cdot)}, a_{j(\cdot)} \in \mathcal{W}_q \subset \widehat{\mathbb{C}}_w$ :

Speiser function $w(z)$	Speiser Riemann surface $\mathcal{R}_{w(z)}$	Speiser $q$ –tessellation $(\Omega_z \cup \partial_I \Omega_z) \setminus \widehat{\Gamma}_q$	Analytic Speiser graph $(\mathfrak{S}_q, \mathcal{L}_{\mathcal{W}_q})$ of index $q$
singular value $w_{j(\iota)} \in \widehat{\mathbb{C}}_w$	$(z_\iota, w_{j(\iota)}, m_\iota)$	vertex label for a vertex of $\widehat{\Gamma}_q$ with valence $\geq 4$	face label
critical point $z_\kappa \in \Omega_z$ of order $2 \leq m_\kappa < \infty$	finitely ramified branch point $(z_\kappa, w_{j(\kappa)}, m_\kappa)$	vertex of $\widehat{\Gamma}_q$ with valence $2m_\kappa$	bounded $w_{j(\kappa)}$ –region is a $2m_\kappa$ –gon
$z_\sigma = U_{a_\sigma} \in \partial_I \Omega_z$ a logarithmic singularity of $w^{-1}(z)$ over $a_{j(\sigma)} \in \widehat{\mathbb{C}}_w$	infinitely ramified branch point $(z_\sigma, a_{j(\sigma)}, \infty)$	vertex of $\widehat{\Gamma}_q$ with $\infty$ valence on $\partial_I \Omega_z \subset$ $\partial B(0, 1) \cong \partial \mathbb{R}^2$ ,	unbounded $a_{j(\sigma)}$ –region $\infty$ –sided polygon
cosingular point $z \in \Omega_z$	regular point $(z, w_j, 1)$	“hollow” vertex of $\widehat{\Gamma}_q$ with valence 2	digon

**Corollary 7.2** (Speiser graph characterization of rational functions and  $N$ –functions). *Consider an analytical Speiser graph  $(\mathfrak{S}_q, \mathcal{W}_q)$  of index  $q$  in  $\Omega_z$ . For each case (1)–(3), the following statements are equivalent.*

1.
  - i) The associated function  $w(z)$  is rational.
  - ii) The Speiser graph  $\mathfrak{S}_q$  of index  $q$  is finite.
  - iii) The Speiser graph  $\mathfrak{S}_q$  of index  $q$  is properly embedded in  $\mathbb{S}^2$ .
  - iv) Considering the cell decomposition  $\Omega_z \setminus \mathfrak{S}_q$ , the number of unbounded faces is zero and the number of bounded faces, that are not digons, is finite (equal to the number of critical points of the associated function  $w(z)$ ).
2.
  - i) The associated function  $w(z)$  is, up to Möbius transformation, a polynomial of degree  $n \geq 2$ .
  - ii) The Speiser graph  $\mathfrak{S}_q$  of index  $q$  is finite and, considering the cell decomposition  $\Omega_z \setminus \mathfrak{S}_q$ , there is an  $w_j$ –face which is a  $2n$ –gon,  $n \geq 2$ .
3.
  - i) The associated  $w(z)$  is an  $N$ –function.
  - ii) The Speiser graph  $\mathfrak{S}_q$  of index  $q$  is infinite and, considering the cell decomposition  $\Omega_z \setminus \mathfrak{S}_q$ , there are a finite number  $p \geq 2$  of unbounded faces (equal to the number of singular values of the associated function  $w(z)$ , counted with multiplicity), and all bounded faces are digons. Note that the index of the Speiser graph is  $q \leq p$ .

*Proof.* Both Theorem 7.1 and Proposition 6.11.2 play key roles in all statements.

Statement (1) now follows directly from Definition 6.1.i.

Statement (2), up to Möbius transformations: the label assigned to the  $w_j$ –face, that is a  $2n$ –gon, is the critical value  $w_j = \infty \in \mathcal{W}_q$  of the critical point  $\infty \in \widehat{\mathbb{C}}_z$ .

Statement (3) follows from the definition of  $N$ –function in §3.2. Note that the singular values are in fact asymptotic values.  $\square$

The analogous Speiser tessellation characterization of Speiser functions is left for the interested reader.

## 8. When does a pre–Speiser graph represent a Speiser function?

The original question *what is the shape of a rational function?*, was posed in 2010 by W. P. Thurston in MathOverflow [1]. This can be translated in terms of Speiser functions,  $\mathbf{t}$ –graphs and pre–Speiser graphs.

Question: *is it possible to characterize whether a  $\mathbf{t}$ –graph  $\Gamma$ , or equivalently a pre–Speiser graph  $\mathfrak{S}$ , represents a Speiser function?* (2)

As far as we known, the problem of characterizing when a  $t$ -graph  $\Gamma$  arises from a rational function was considered by Speiser [5]. In 2020, a report of the results of W.P. Thurston, S. Koch and T. Lei for generic rational functions  $R(z)$  appeared in [2], *generic* of degree  $n$  means that  $R(z)$  has  $2n - 2$  distinct critical values. The report provides negative examples and states conditions under which a planar tessellation arises from generic rational functions  $R(z)$  and suitable paths  $\gamma$ . In 2015, J. Tomasini [51] proved a characterization for rational functions in the general case, with a different presentation. A constructive method for  $t$ -graphs  $\Gamma$  originating from generic polynomials was studied in L. González-Cely *et al.* in [8]; they provide a different characterization by showing an explicit construction of a consistent  $q$ -labelling.

In §8.1 we explore the suitable values of  $q$  for a pre-Speiser graph. §8.2 provides the necessary and sufficient conditions for a pre-Speiser graph to be extendable to a Speiser graph of index  $q$ . These subsections consider pre-Speiser Graphs with an arbitrary number of faces. For the rational case; in §8.3 we review W.P. Thurston's *et al.* approach, and in §8.4 a comparison of Tomasini's method is considered.

### 8.1. Certain constraints on the extension of pre-Speiser graphs to Speiser graphs.

Recalling that a cyclic order  $\mathcal{W}_q$  is equivalent to the isotopy class  $[\gamma]$  of paths  $\gamma$  relative to the values  $\{w_\ell\}_{\ell=1}^q$ , we can now answer Question (2).

**Corollary 8.1** (What is the shape of a Speiser function?). A  $t$ -graph  $\Gamma$ , or equivalently a pre-Speiser graph  $\mathfrak{S}$ , supports a consistent  $q$ -labelling  $\mathcal{L}_{\mathcal{W}_q}$  if and only if there exist Speiser functions  $w(z)$  with cyclic orders  $\mathcal{W}_q$  on their singular values such that  $\mathcal{T}_\gamma(w(z)) = \mathcal{T}(\Gamma)$ .

*Proof.* Follows directly from Theorem 5.16, Lemma 5.19 and Remark 6.7.  $\square$

Note that the consistent  $q$ -labelling associated to the Speiser function with cyclic order  $\mathcal{W}_q$  is given by  $\mathcal{L}_{\mathcal{W}_q} = w(z)^* \mathcal{L}_\gamma$ .

From the theory developed up to this point, it is clear that Question (2) is equivalent to *finding necessary and sufficient conditions for when a  $t$ -graph  $\Gamma$  (or its dual the pre-Speiser graph  $\mathfrak{S}$ ) can be extended to at least one  $A$ -map  $\widehat{\Gamma}_q$  (or their duals Speiser graphs  $\mathfrak{S}_q$  of index  $q$ ).*

As Example 8.1 below shows, both a  $t$ -graph  $\Gamma$  and a pre-Speiser graph  $\mathfrak{S}$  can be extended to  $A$ -maps  $\widehat{\Gamma}_q$  and Speiser graphs  $\mathfrak{S}_q$  of index  $q$  for distinct values of  $q < \infty$ .

**Example 8.1** (Non uniqueness of the extended Speiser graph of index  $q$ ). Consider the planar tessellation  $\mathcal{T}(\Gamma)$ , with  $t$ -graph  $\Gamma$ , attributed to W.P. Thurston, that appears as figure 10 in [2], and that we reproduce here in Figure 5.a without labels. In Figure 5.b is the corresponding dual; the pre-Speiser graph  $\mathfrak{S}$ .

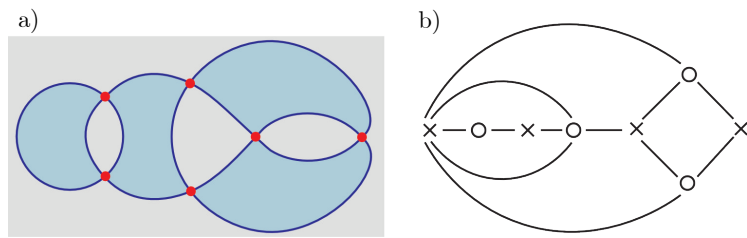


Figure 5: (a) Tessellation  $\mathcal{T}(\Gamma)$  of the sphere  $\mathbb{S}^2$ , its  $t$ -graph  $\Gamma$  has  $k$ -gons,  $k = 2, 3, 4, 5$ , as tiles. (b) The dual of (a) is a planar bipartite graph on  $\mathbb{S}^2$ , the pre-Speiser graph  $\mathfrak{S}_q$ , with vertices of valence  $k$ .

From Figure 5.a we see that, since the largest tiling is a 5-gon (equivalently in Figure 5.b the largest valence for a vertex is 5), then the minimum number of labels that are needed to specify the Speiser tessellation (equivalently the corresponding  $A$ -map  $\widehat{\Gamma}_q$  and Speiser graph  $\mathfrak{S}_q$ ) is  $q = 5$ . Moreover, since there are 6 vertices of the  $t$ -graph  $\Gamma$  of Figure 5.a (equivalently in Figure 5.b there are 6 faces on the pre-Speiser graph  $\mathfrak{S}_q$ ), then the maximum number of labels has to be  $q = 6$ . Thus there are two possibilities for  $q$ , namely 5 and 6.

Case  $q = 5$ . Consider Figure 6; in (a) labels  $\mathcal{W}_5 \doteq [1, 2, 3, 4, 6]$  are added to the 6 vertices of the  $t$ -graph  $\Gamma$  (thus necessarily at least one label is repeated); recall Remark 6.6. In (b), by edge subdivision, vertices of valence two are added so as to make each tile a 5-gon with a consistent 5-labelling  $\mathcal{L}_{\mathcal{W}_5}$  as in Definition 5.7; thus a Speiser 5-tessellation  $(\mathcal{T}(\widehat{\Gamma}_5), \mathcal{L}_5)$ . In (c) the corresponding Speiser graph  $\mathfrak{S}_5$  of index  $q = 5$  is shown. The corresponding rational function  $R(z)$ , obtained from the specific choice of  $\mathcal{W}_5$ , has simple critical points two of which lie over the same critical value  $w_4$ . Thus,  $R(z)$  is not a generic rational function.

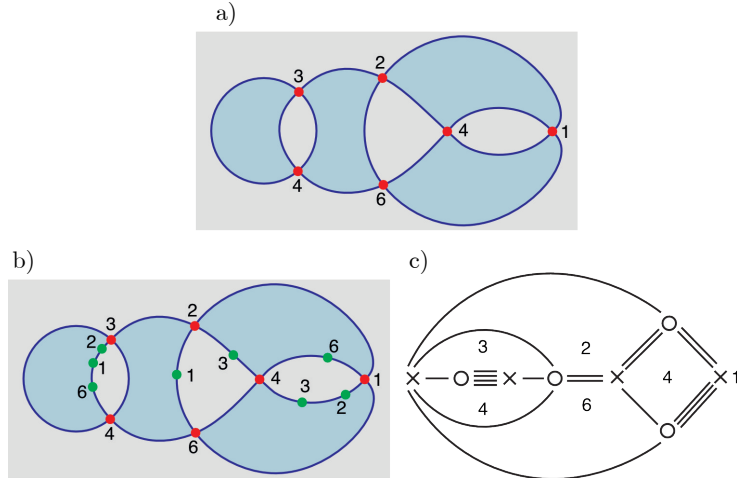


Figure 6: (a) Labelled  $t$ -graph with labels  $\mathcal{W}_5 \doteq [1, 2, 3, 4, 6]$ . (b) Vertices of valence 2 are added so as to have a consistent labelling  $\mathcal{L}_{\mathcal{W}_5}$ , thus obtaining a Speiser 5-tessellation. (c) The dual of (b), i.e. a Speiser graph of index 5. (b)–(c) represent a rational function  $R(z)$  with 6 simple critical points and 5 distinct critical values; the critical value of multiplicity two is the one corresponding to the label  $w_4 = 4$ . Thus,  $R(z)$  is not a generic rational function.

Case  $q = 6$ . Consider Figure 7; in (a) labels  $\mathcal{W}_6 \doteq [1, 2, 3, 4, 5, 6]$  are added to the 6 vertices of the  $t$ -graph  $\Gamma$ ; recall Remark 6.6. In (b), by edge subdivision, vertices of valence two are added so as to make each tile a 6-gon with a consistent 6-labelling  $\mathcal{L}_{\mathcal{W}_6}$  as in Definition 5.7; thus a Speiser 6-tessellation  $(\mathcal{T}(\widehat{\Gamma}_6), \mathcal{L}_6)$ . In (c) the corresponding Speiser graph  $(\mathfrak{S}_6, \mathcal{L}_6)$  of index 6 is shown. The corresponding rational function  $R(z)$ , obtained from the specific choice of the 6 distinct ordered critical values  $\mathcal{W}_6$ , has 6 simple critical points, one over each of the 6 distinct critical values. Thus, a generic rational function  $R(z)$ . This corresponds to the the two colored tilling of [2] that appears in figure 5 (a).

With this in mind, the following result is useful and follows immediately from Table 1, Proposition 6.11, Theorem 7.1, and the bounds (20) and (21).

**Lemma 8.2.** *Given a  $t$ -graph  $\Gamma$  or a pre-Speiser graph  $\mathfrak{S}$ , upper and lower bounds for  $q \geq 2$ , in order that they extend to a Speiser  $q$ -tessellation  $(\mathcal{T}(\widehat{\Gamma}_q), \mathcal{L}_{\mathcal{W}_q})$  or an analytic Speiser graph  $(\mathfrak{S}_q, \mathcal{L}_{\mathcal{W}_q})$  of index  $q$ , are as follow*

$$\max \# \left\{ \begin{array}{l} \text{vertices on } \partial \overline{T}_\alpha, \\ \text{for } T_\alpha \in \mathcal{T}(\Gamma) \end{array} \right\} \leq q \leq \# \left\{ \begin{array}{l} \text{vertices of } \Gamma \text{ with} \\ \text{valence } \geq 4 \end{array} \right\}, \quad (20)$$

$$\max \left\{ \begin{array}{l} \text{valence of the} \\ \text{vertices of } \mathfrak{S} \end{array} \right\} \leq q \leq \# \left\{ \begin{array}{l} \text{faces of } \mathfrak{S}, \\ \text{that are not digons} \end{array} \right\}. \quad (21)$$

□

In the case of  $t$ -graphs with  $2n < \infty$  tiles (presumably corresponding to rational functions, say of degree  $n \geq 2$ ), the Riemann–Hurwitz formula implies that the right hand side of Equation (20) is also bounded by  $2n - 2$ . Since the upper bounds (20)–(21) are specific to the particular  $t$ -graph or pre-Speiser graph, it is usually better than that given by the Riemann–Hurwitz formula. Moreover, (20)–(21) also apply to infinite  $t$ -graphs and pre-Speiser graphs.

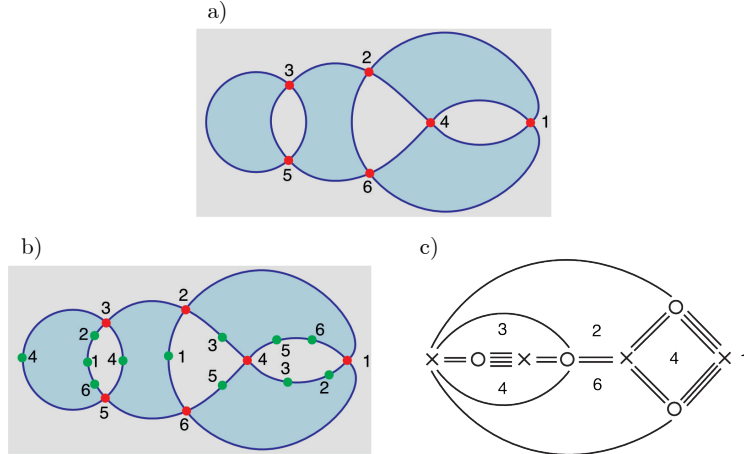


Figure 7: (a) Labelled t-graph with labels  $W_6 \doteq [1, 2, 3, 4, 5, 6]$ . (b) Vertices of valence 2 are added so as to have a consistent labelling  $L_{W_6}$ , thus obtaining a Speiser 6-tessellation. (c) The dual of (b), i.e. a Speiser graph of index 6. (b)–(c) represent a rational function  $R(z)$  with 6 simple critical points and exactly 6 distinct critical values. Thus, a generic rational function  $R(z)$  of degree 4.

### 8.2. Necessary and sufficient conditions for a pre–Speiser graph to be extendable to a Speiser graph of index $q$

Recalling Definition 6.2.1, we shall now proceed to answer Question (2) in terms of pre–Speiser graphs and Speiser graphs. The setup is as follows.

Suppose you have a connected bipartite pre–Speiser graph  $\mathfrak{S} = (V_o \cup V_x, E)$  embedded in the plane with the sets of vertices  $V_o$  and  $V_x$  having the same cardinality, say  $n$  (possibly infinite). The set  $E = E(\mathfrak{S})$  denotes the edges of  $\mathfrak{S}$ . Given a vertex  $v \in V_o \cup V_x$ , denote by  $\deg(v) = \rho_v$  the valence of  $v$ . Further assume that  $2 \leq \rho_v \leq q$  for all vertices and that  $q < \infty$  lies within the bounds (21) given by Lemma 8.2.

We are looking for necessary and sufficient conditions such that  $\mathfrak{S}$  can be extended to a planar  $q$ –regular bipartite multigraph<sup>18</sup>

$$\mathfrak{S}_q = (V_o \cup V_x, E \cup E_{new}),$$

by just adding copies of the edges  $E$  (i.e.  $E_{new}$  are copies of  $E$ ) to  $\mathfrak{S}$ .

**Definition 8.3.** Given a vertex  $v \in V_o \cup V_x$ , with valence  $\deg v = \rho_v$ , we say that  $d_v \doteq q - \rho_v$  is the *deficiency* of vertex  $v$ .

Recalling Definition 6.17.2, we see that.

**Lemma 8.4.** Given a finite set  $S \subset V_o$ , it follows that the neighborhood<sup>19</sup> of  $S$  is a subset of  $V_x$ , in other words  $N(S) \subset V_x$ . Similarly for a finite set  $T \subset V_x$ , the neighborhood of  $T$  is a subset of  $V_o$ , in other words  $N(T) \subset V_o$ .  $\square$

We now have a *bipartite transportation problem*: a classical optimization problem in operation research that models the distribution of resources from multiple supply sources to multiple demand destinations. It can be naturally formulated using bipartite graphs, where supply nodes form one partition and demand nodes form another, with edges representing possible routes and their associated costs (in our case the cost is the same for each edge).

The vertices  $v \in V_o$  have supply  $d_v$  and vertices  $w \in V_x$  have demand  $d_w$ , and it is possible to ship only along existing edges with unlimited capacity.

The question now is, whether we can choose non-negative integers  $x(e)$  for each edge  $e = \overline{x_\alpha \circ \beta} \in E$  (how many parallel copies of  $e$  to add, in order to form edge bundles), such that every vertex  $v \in V_o \cup V_x$  reaches valence  $q$ . For a given edge  $e \in E(\mathfrak{S})$ , the corresponding edge in the extended graph  $\mathfrak{S}_q$  will have multiplicity  $1 + x(e)$ ; recall rows 4 and 5 in Diagram 1.

<sup>18</sup>Recall that a multigraph admits edge bundles, see Remark 6.8.5.

<sup>19</sup>To be completely clear, this is the open neighborhood as in Definition 6.17.3.

The solution for this bipartite transportation problem is classic and well known. See for instance [52], [53], [54] and references therein; for foundational resources see [55], [56].

There exist non-negative integers  $x(e)$  solving the above question if and only if the following conditions are satisfied.

1) Global balance

$$\sum_{v \in V_o} d_v = \sum_{w \in V_x} d_w.$$

2) Local balance / Hall type neighborhood inequalities; for every finite sets  $S \subset V_o$  and  $T \subset V_x$ , the following inequalities hold

$$\begin{aligned} \sum_{v \in S} d_v &\leq \sum_{w \in N(S)} d_w, \\ \sum_{w \in T} d_w &\leq \sum_{v \in N(T)} d_v. \end{aligned}$$

These are the max-flow / min-cut conditions on the bipartite transportation network with capacities  $d_v$  on the vertex arcs and infinite capacities on edge arcs; by unimodularity, a feasible real solution is integral.

For countably infinite graphs with finite  $q$ , the same conditions, required for all finite subsets  $S \subset V_o$  and  $T \subset V_x$  are necessary and sufficient (sufficiency follows by an exhaustion by finite induced subgraphs and a compactness/limit argument).

The above proves the result below, which completes Diagram 1.

**Theorem 8.5** (Pre-Speiser graph extension to Speiser graph of index  $q$ ). *A pre-Speiser graph  $\mathfrak{S} = (V_o \cup V_x, E)$  embedded in the plane extends to a Speiser graph  $\mathfrak{S}_q$  of index  $q$  if and only if  $\mathfrak{S}$  satisfies the following conditions:*

1) Global balance

$$\sum_{v \in V_o} (q - \rho_v) = \sum_{w \in V_x} (q - \rho_w).$$

2) Local balance / Hall neighborhood inequalities: for every finite sets  $S \subset V_o$  and  $T \subset V_x$ ,

$$\sum_{v \in S} (q - \rho_v) \leq \sum_{w \in N(S)} (q - \rho_w), \quad (22)$$

$$\sum_{w \in T} (q - \rho_w) \leq \sum_{v \in N(T)} (q - \rho_v). \quad (23)$$

□

Finally a use of Lemma 6.13 proves.

**Corollary 8.6.** *A pre-Speiser graph  $\mathfrak{S}$  represents a Speiser function if and only if it satisfies conditions (1) and (2) of Theorem 8.5.* □

### 8.3. W. P. Thurston et al.'s approach

In [2], they consider a planar tessellation with alternating colors, which in our language corresponds to  $\mathcal{T}(\Gamma)$  arising from a  $\mathbf{t}$ -graph  $\Gamma$ . Three conditions are required in order to characterize the planar tessellations that represent generic rational functions.

- i) The tiles/faces of  $\mathcal{T}(\Gamma)$  are Jordan regions.
- ii) Global balance. For finite graphs  $\Gamma$ , with an alternating blue-gray colouring of the faces of  $\mathcal{T}(\Gamma)$ , there are the same number of blue faces as there are of gray faces.
- iii) Local balance. For any oriented simple closed path in  $\Gamma$ , say  $\Upsilon$ , that is bordered by blue faces on the left and grey on the right (except at the corners), there are strictly more blue faces than grey faces on the left side of  $\Upsilon$ .

In figure 3 of [2], a tessellation that is globally balanced but not locally balanced is shown. The next example illustrates that lack of local balance is actually very easy to obtain.

**Example 8.2** (Every  $\mathbf{t}$ -graph can be modified to one without local balance). Let  $\mathcal{T}(\Gamma)$  be a globally and locally balanced tessellation, finite or infinite. Consider any edge of  $\Gamma$  as in Figure 8.a. Replace the edge with the graph shown in Figure 8.c, to obtain the graph of Figure 8.b. This new  $\mathbf{t}$ -graph  $\Gamma'$  is still globally balanced, but it is not locally balanced; the path  $\alpha$ , that does not satisfy the requirements for local balance, is colored green in the figures. Note that one could also use Figure 8.d, instead of Figure 8.c.

By duality, the corresponding statement for the pre-Speiser graph is: replace the single horizontal edge by the dual graph of Figure 8.c, as indicated in Figures 8.e–f.

We shall use Theorem 8.5, particularly (23), to show that it is not possible to add edges to the pre-Speiser graph  $\mathfrak{S}'$  to make it a regular graph (thus a Speiser graph  $\mathfrak{S}_q$  of index  $q$ ). The problem lies with the vertices inside the green area. We shall work with Figure 8.f: a subset of the pre-Speiser graph  $\mathfrak{S}$ , dual to  $\Gamma'$ . The vertices of the subset of  $\mathfrak{S}$ , have been labelled as  $\{o_1, \dots, o_5\} \subset V_o$  and  $\{x_1, \dots, x_5\} \subset V_x$ . Consider the set  $T = \{x_2, x_3\}$ , thus  $N(T) = \{o_4, o_5\}$ , and observe that

$$\sum_{w \in T} (q - \rho_w) > \sum_{v \in N(T)} (q - \rho_v), \quad \text{for } 5 \leq q \leq 8.$$

Thus,  $\mathfrak{S}$  can not be extended to a Speiser graph of index  $q$ , for  $5 \leq q \leq 8$  (and consequently by Lemma 8.2, for any  $q$ ). Equivalently,  $\Gamma'$  can not be extended to an A-map  $\widehat{\Gamma}'_q$ .

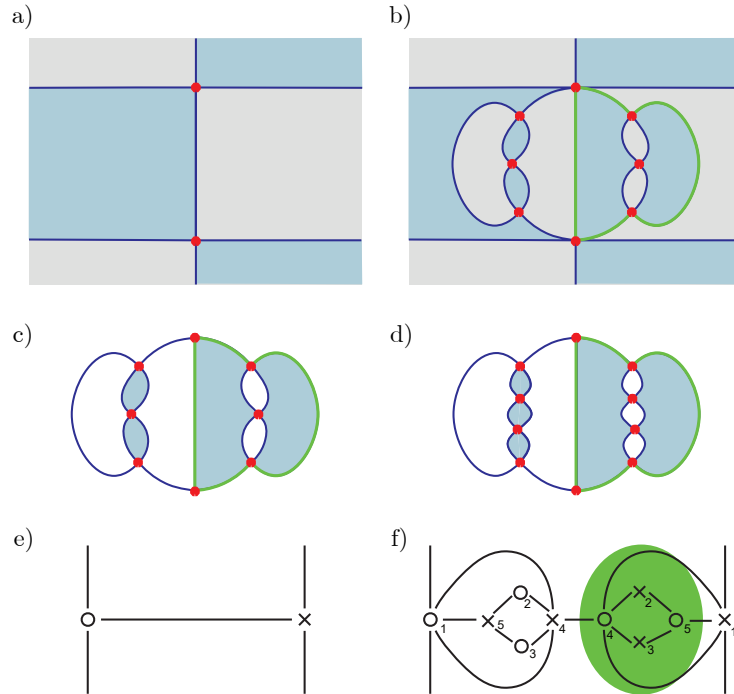


Figure 8: Modifying a  $t$ -graph to make it non locally balanced. (a) An edge  $e$  of an arbitrary  $t$ -graph  $\Gamma$ , that is globally and locally balanced. (b) By replacing the edge  $e$  with the graph in (c), we obtain a globally balanced but not locally balanced  $t$ -graph. Of course one could also use (d) to make another different  $t$ -graph that is not locally balanced. In all cases, the green path is the one that does not satisfy the local balance requirement. By duality, in (e) is the pre-Speiser graph, corresponding to (a) and (f) is the modified pre-Speiser graph, corresponding to (b). In (f) it is impossible to make the subgraph, enclosed by the green area, a regular subgraph.

Recalling Definition 5.1 of tessellation, the above example shows that:

**Corollary 8.7.** *There are finite and infinite tessellations  $\mathcal{T}(\Gamma)$  that do not represent any Speiser function.*  $\square$

#### 8.4. J. Tomasini's approach

In [51], an intermediate approach between considering tessellations or their duals the Speiser graphs, is taken.

Instead of considering the pullback of a Jordan path that traverses the labelled singular values, J. Tomasini considers the pullback via the rational function  $w(z) = R(z)$  of a “spider”,  $T_q$ , consisting of a central black vertex (corresponding to a regular point), and simple edges to labelled red vertices (the singular values). From this *increasing bipartite map* (a planar labelled bipartite graph)  $w(z)^* T_q$ , he erases the labels and the valence 1 (red) vertices, together

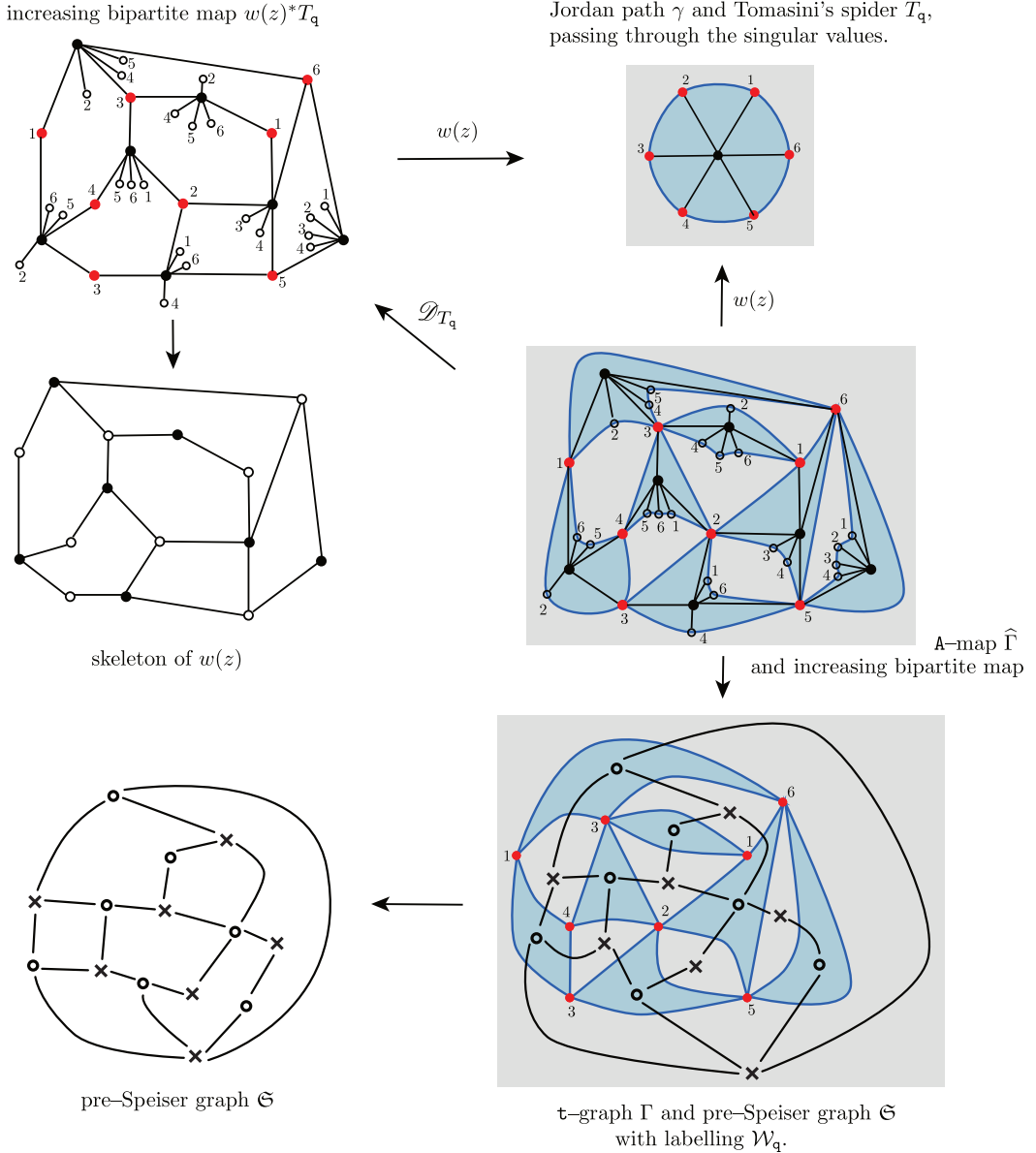


Figure 9: Starting on the top left is Tomasini's increasing bipartite map  $w(z)^*T_q$ ; below it is the skeleton of  $w(z)$ . On the top right are the Jordan path  $\gamma$  and the spider  $T_q$ , passing through the singular values. Middle right is the  $\mathfrak{A}$ -map  $\widehat{\Gamma}_q$  superimposed with the increasing bipartite map  $w(z)^*T_q$  to exemplify the deformation retract  $\mathcal{D}_{T_q}$ . Bottom row contains the pre-Speiser graph and the  $\mathfrak{t}$ -graph  $\Gamma$  for comparison with Tomasini's combinatorial objects.

with their incident edges; obtaining a *skeleton* of  $w(z)$ . See Figure 9, specifically the top row and first two left hand figures.

Using the above he proves.

**Theorem** (Tomasini's characterization of finite branched self covers of  $\mathbb{S}^2$  [51]). A finite planar bipartite graph  $G$  is realized as a skeleton of a branched self cover of  $\mathbb{S}^2$  if and only if  $G$  is

- 1) Globally balanced; there are the same number of black vertices as faces of  $G$ .
- 2) Locally balanced; for any subgraph  $H$  of  $G$  with more than one black vertex, the number of black vertices of  $H$  is greater than or equal to the number of faces of  $H$ .

Roughly speaking, the relationship between the tessellation scheme of §5 and Tomasini's planar bipartite graphs is through a deformation retract  $\mathcal{D}_{T_q}$  of the Speiser  $q$ -tessellation  $\mathcal{T}(w(z)^*\gamma)$  (equivalently the A-map  $\widehat{\Gamma}_q = w(z)^*\gamma$ ) to the increasing bipartite map  $w(z)^*T_q$ . Thus,  $\mathcal{D}_{T_q}$  retracts each blue tile/face to a regular point in a blue face (obtaining a black vertex for each blue face), fixing the vertices and coloring them red. The same deformation retract  $\mathcal{D}_{T_q}$  can be applied to the t-graph  $\Gamma$  to obtain the skeleton  $G$ . Of course the labelling of the increasing bipartite map  $w(z)^*T_q$  coincides with the consistent  $q$ -labelling  $\mathcal{L}_{W_q}$  of the A-map  $\widehat{\Gamma}_q = w(z)^*\gamma$  and its dual the Speiser graph  $\mathfrak{S}_q$  of index  $q$ . See Figure 9.

Corollary 8.7 together with all of the above suggest the following.

**Conjecture 8.8.** *The three local balance conditions of Theorem 8.5, section §8.3, and section §8.4, are equivalent.*

## 9. Geometrical decomposition of Speiser functions

Let  $w(z)$  be a Speiser function with Riemann surface  $\mathcal{R}_{w(z)}$ . In this section we revisit Speiser Riemann surfaces, as in §4, in order to obtain a unique geometrical decomposition of  $\mathcal{R}_{w(z)}$  into *maximal logarithmic towers* and a *soul*, closely related to its Speiser graph  $\mathfrak{S}_q$ . The notation differs slightly from that of §4, where we were interested in obtaining a decomposition of  $\mathcal{R}_{w(z)}$  in maximal domains of single-valuedness of  $w^{-1}(z)$ .

As a first step, recall notation previous to Remark 3.8;  $\delta = p + r$  indicates the number<sup>20</sup> of singularities of  $w^{-1}(z)$ , i.e. the number of branch points of  $\mathcal{R}_{w(z)}$ .

If  $p = 0$ , then there are no logarithmic singularities; thus  $w(z)$  only has  $r$  algebraic singularities.

Furthermore, since logarithmic singularities occur only on the ideal boundary of  $\Omega_z$ , it follows that  $\Omega_z = \widehat{\mathbb{C}}_z$  does not support meromorphic functions  $w(z)$  with logarithmic singularities. Thus the case  $p \neq 0$ , does not occur for  $\Omega_z = \widehat{\mathbb{C}}_z$ .

### 9.1. The pieces: flat p-gons, maximal logarithmic towers, the soul

The following definitions, describing flat p-gon, logarithmic tower, soul, rational block, exponential and  $h$ -tangent blocks, are the elementary pieces of our decomposition of the Riemann surface  $\mathcal{R}_{w(z)}$ .

**Definition 9.1.** Let  $p \geq 2$ , a *flat p-gon*  $(\overline{\mathcal{P}}, w(\zeta))$  is a pair consisting of a Riemann surface with boundary  $\overline{\mathcal{P}}$  furnished with a meromorphic function  $w(\zeta) : \mathcal{P} \rightarrow \widehat{\mathbb{C}}_w$ , with  $0 \leq \rho \leq \infty$  critical points, satisfying the following.

- i) The interior  $\mathcal{P}$  of  $\overline{\mathcal{P}}$  is an open Jordan domain, with oriented boundary  $\partial\overline{\mathcal{P}}$  homeomorphic to  $\mathbb{S}^1$ .
- ii)  $\mathcal{P}$  is on the left side of the boundary.
- iii) The boundary  $\partial\overline{\mathcal{P}}$  has

vertices  $\{\zeta_\beta \mid \beta \in 1, \dots, p\}$  and sides  $\{S_\beta = \overline{\zeta_\beta \zeta_{\beta+1}} \mid \beta \in 1, \dots, p\}$ ,  
cyclically enumerated.

- iv) The directional derivative of  $w(\zeta)$  in the interior of the sides  $\{S_\beta\}$  is non zero.
- v) The image  $w(S_\beta)$  is a geodesic segment in  $(\widehat{\mathbb{C}}_w, \frac{\partial}{\partial w})$  with extreme points

$$w(\zeta_\beta) = a_\beta, \quad w(\zeta_{\beta+1}) = a_{\beta+1}, \quad a_\beta \neq a_{\beta+1}.$$

<sup>20</sup>Both,  $p$  and  $r$ , can be infinite or zero.

Consider the sides  $\{S_\beta\}_{\beta=1}^p$  of a flat  $p$ -gon  $\bar{\mathcal{P}}$ , with extreme points  $\{\zeta_\beta, \zeta_{\beta+1}\} \subset S_\beta$ . By identifying  $\sim$  all the vertices  $\{\zeta_\beta\}$  to one point, say  $\infty_\sim$ , we obtain a Riemann surface  $\bar{\mathcal{P}}/\sim$ , which is homeomorphic to a sphere  $\mathbb{S}^2$  with  $p$  open discs  $U_\beta$  removed; the closure of the disks share only one common point. This common point is also denoted as  $\infty_\sim$  in  $\bar{\mathcal{P}}/\sim$ .

Note that a flat  $\rho$ -gon contains  $\rho$  critical points; the case when  $\rho < \infty$  will be relevant. To see this, consider the following equivalence relation.

**Definition 9.2.** Two meromorphic functions  $w_\ell(z) : V_\ell \rightarrow \widehat{\mathbb{C}}_w$ ,  $\ell = 1, 2$ , are right-left equivalent when there exist biholomorphisms  $\phi : V_1 \rightarrow V_2$ , and  $\varphi : w_2(V_2) \rightarrow w_1(V_1)$  such that

$$w_1 = \varphi \circ w_2 \circ \phi. \quad (24)$$

**Lemma 9.3.** Let  $(\bar{\mathcal{P}}, w(\zeta))$  be a flat  $p$ -gon with  $\rho < \infty$  critical points. Then  $w(\zeta) : \mathcal{P} \rightarrow \widehat{\mathbb{C}}_w$  is right-left equivalent to a rational function

$$R(z) : \mathcal{P} \subset \widehat{\mathbb{C}}_z \rightarrow \widehat{\mathbb{C}}_w,$$

where  $\mathcal{P}$  is an appropriate Jordan domain.

*Proof.* Recall that the sides  $\overline{\zeta_\beta \zeta_{\beta+1}}$  of  $\mathcal{P}$  are straight line segments.

There exists an embedding  $\varphi(z) : \mathcal{P} \hookrightarrow \widehat{\mathbb{C}}_z \times \widehat{\mathbb{C}}_w$  such that  $w(z) = \pi_2 \circ \varphi(z)$ , according to Diagram (5). Moreover, the critical points of  $w(z)$  correspond to finitely ramified branch points of the Riemann surface with boundary  $\varphi(\mathcal{P})$ . Because of (v) of Definition 9.1, it is clear that  $\varphi(\overline{\zeta_\beta \zeta_{\beta+1}}) = \overline{a_\beta a_{\beta+1}}$ . Thus the Riemann surface with boundary  $\varphi(\mathcal{P})$  can be extended, in  $\widehat{\mathbb{C}}_z \times \widehat{\mathbb{C}}_w$ , to a Riemann surface  $\widehat{\mathcal{P}}$  without boundary such that  $\pi_1(\widehat{\mathcal{P}}) = \widehat{\mathbb{C}}_z$  which has at most  $\rho$  finitely ramified branch points and no infinitely ramified branch points. Since  $\rho < \infty$ , this proves the existence of a rational function  $R(z)$  on  $\widehat{\mathbb{C}}_z$  such that on  $\mathcal{P} = \pi_1(\mathcal{P})$ , and  $R(z)$  is right-left equivalent to  $w(z)$  on  $\mathcal{P}$ .  $\square$

**Definition 9.4.** A function  $w(\zeta) : \mathcal{P} \rightarrow \widehat{\mathbb{C}}_w$  arising from a flat  $p$ -gon, with  $\rho < \infty$  critical points, is a *rational block*  $R(z) : \mathcal{P} \subset \widehat{\mathbb{C}}_z \rightarrow \widehat{\mathbb{C}}_w$ .

**Lemma 9.5** (Surgery of a flat  $p$ -gon to pairs of logarithmic singularities). Let  $(\bar{\mathcal{P}}, w(\zeta))$  be a flat  $p$ -gon, and let  $S_\beta$  be a side on the boundary of  $\bar{\mathcal{P}}$ , where its extreme points has values

- i)  $w(\zeta_\beta) = a_\beta \in \mathbb{C}_w$ ,  $w(\zeta_{\beta+1}) = a_{\beta+1} = \infty \in \widehat{\mathbb{C}}_w$ , or
- ii)  $w(\zeta_\beta) = a_\beta$ ,  $w(\zeta_{\beta+1}) = a_{\beta+1} \in \mathbb{C}_w$ .

Then, there exist an extension of  $w(\zeta)$ , in  $\mathcal{P}$ , to the interior of the corresponding open disk  $U_\beta$ , the  $\beta$ -th component of the boundary in  $\mathcal{P}/\sim$ , such that  $w(\zeta)|_{U_\beta}$  is right-left equivalent to

- i)  $\exp(\zeta)$  or
- ii)  $\tanh(\zeta)$ ,

respectively.

Figure 10 illustrates the Lemma.

*Proof.* By (v) in Definition 9.1, we have that  $a_\beta \neq a_{\beta+1}$ .

When  $a_\beta, a_{\beta+1} \in \mathbb{C}_w$ , then there is an affine biholomorphism  $\varphi_\beta$  that takes the oriented segment  $[-1, 1]$  to the oriented side  $S_\beta = \overline{\zeta_\beta \zeta_{\beta+1}}$ , with  $\varphi_\beta^{-1}(a_\beta) = -1$  and  $\varphi_\beta^{-1}(a_{\beta+1}) = 1$ . The required analytic extension of  $w(\zeta)$  is

$$w(\zeta) : ((\bar{\mathcal{P}}/\sim) \cup \overline{U_\beta}) \setminus \{\infty_\sim\} \subset \mathbb{S}^2 \rightarrow \widehat{\mathbb{C}}_w$$

$$\zeta \mapsto \begin{cases} w(\zeta) & \zeta \in \bar{\mathcal{P}} \setminus \{\infty_\sim\} \\ (\varphi_\beta \circ \tanh)(\zeta) & \zeta \in \overline{U_\beta} \setminus \{\infty_\sim\}. \end{cases}$$

The argument is as follows. Since  $\mathcal{P}$  is a Riemann surface, let  $J$  denote its complex structure. By using the affine map  $\varphi_\beta$ , it is enough to perform the extension of  $J$  to a complex structure  $J_\beta$  on  $\overline{U_\beta} \setminus \{\infty_\sim\}$ . We can recognize that  $(U_\beta, J_\beta)$  is biholomorphic to the lower half plane  $\mathbb{H}_- = \{\Im(\zeta) < 0\}$ . Hence the function  $\tanh(\zeta)$  makes sense.

When  $w(a_\beta) \in \mathbb{C}_w$ ,  $w(a_{\beta+1}) = \infty \in \widehat{\mathbb{C}}_w$ , then there is a biholomorphism  $\varphi_\beta$  taking  $[0, +\infty]$  to the oriented side  $S_\beta = \overline{a_\beta a_{\beta+1}}$ . By an analogous argument, the required extension of  $w(\zeta)$  is  $(\varphi_\beta \circ \exp)(\zeta)$ .  $\square$

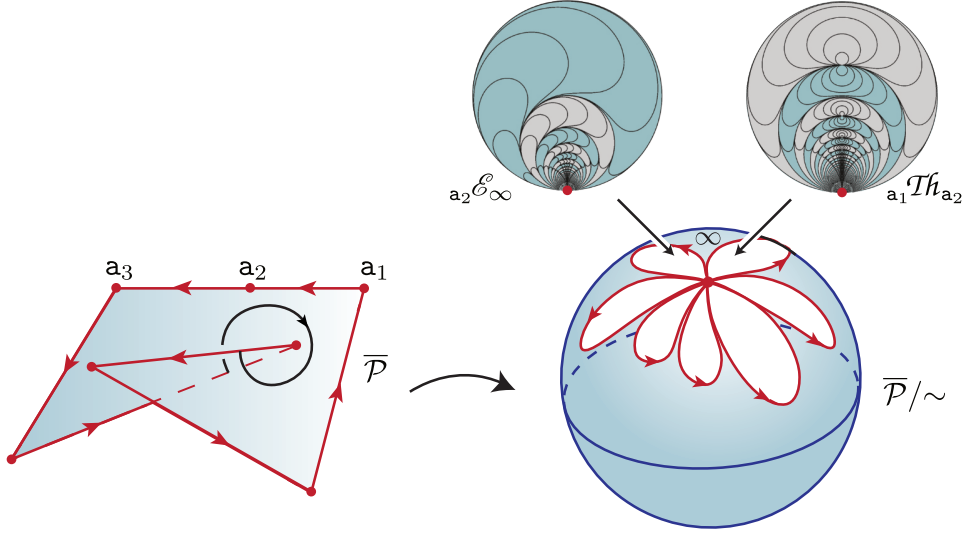


Figure 10: A flat  $p$ -gon  $(\bar{P}, w(\zeta))$ , whose vertices have been identified to one point  $\infty_\sim$ , obtaining a Riemann surface  $\bar{P}/\sim$  homeomorphic to a sphere  $S^2$  with  $p$  open disks removed. As second step, we glue an  $h$ -tangent block  $a_1 \mathcal{Th}_{a_2}$  or an exponential block  $a_2 \mathcal{E}_\infty$  on each boundary component. We sketch a 7-gon with a vertex  $a_5$  of cone angle  $> 2\pi$ . Note that  $a_3 = \infty \in \widehat{\mathbb{C}}_w$ .

In view of Lemma 9.5, the following is natural.

**Definition 9.6** (Exponential and  $h$ -tangent blocks). Consider  ${}_{a_\alpha} U_{a_\beta} \subset \widehat{\mathbb{C}}_z$  a Jordan domain, and  $a_\alpha \neq a_\beta \in \widehat{\mathbb{C}}_w$ . Let  $w(z) : {}_{a_\alpha} U_{a_\beta} \rightarrow \widehat{\mathbb{C}}_w$ ,

be a meromorphic function with an essential singularity at  $e = \infty \in \partial({}_{a_\alpha} U_{a_\beta})$  and exactly two distinct asymptotic values  $a_\alpha, a_\beta \in \widehat{\mathbb{C}}_w$ .

1. An *exponential block*  ${}_\infty \mathcal{E}_{a_\beta}$  is a function  $w(z)$  on  ${}_\infty U_{a_\beta}$  right-left equivalent to  $e^z : \overline{\mathbb{H}} \rightarrow \widehat{\mathbb{C}}$ , i.e. there are biholomorphisms, as in Equation (24),

- i)  $\phi(z) : {}_\infty \overline{U}_{a_\beta} \rightarrow \overline{\mathbb{H}}$  taking  $e$  to  $\infty$ , and
- ii)  $\varphi(w) : \widehat{\mathbb{C}}_w \rightarrow \widehat{\mathbb{C}}_w$  taking  $0$  to  $a_\beta$  and  $\infty$  to  $a_\alpha$ .

The *exponential block*  ${}_{a_\alpha} \mathcal{E}_\infty$  is defined in an analogous way.

2. An  *$h$ -tangent block*  ${}_{a_\alpha} \mathcal{Th}_{a_\beta}$  is a function  $w(z)$  on  ${}_{a_\alpha} U_{a_\beta}$  right-left equivalent to  $\tanh(z) : \overline{\mathbb{H}} \rightarrow \widehat{\mathbb{C}}$ , i.e. there are biholomorphisms, as in Equation (24),

- i)  $\phi(z) : {}_{a_\alpha} \overline{U}_{a_\beta} \rightarrow \overline{\mathbb{H}}$  taking  $e$  to  $\infty$ , and
- ii)  $\varphi(w) : \widehat{\mathbb{C}}_w \rightarrow \widehat{\mathbb{C}}_w$  taking  $-1$  to  $a_\alpha$  and  $1$  to  $a_\beta$ .

The elementary blocks  ${}_{a_\alpha} \mathcal{E}_{a_\beta}$  and  ${}_{a_\alpha} \mathcal{Th}_{a_\beta}$  can be easily understood with the following commutative diagram

$$\begin{array}{ccc}
 {}_{a_\alpha} \overline{U}_{a_\beta} \subset \widehat{\mathbb{C}}_z & \xrightarrow{w(z)} & \widehat{\mathbb{C}}_w \\
 \phi \downarrow & & \uparrow \varphi \\
 \overline{\mathbb{H}} & \xrightarrow{e^\zeta \text{ or } \tanh(\zeta)} & \widehat{\mathbb{C}}_w.
 \end{array} \tag{25}$$

**Remark 9.7** (Using vector fields to distinguishing between topologically equivalent functions). Note that the elementary blocks  ${}_{a_\alpha} \mathcal{E}_{a_\beta}$  and  ${}_{a_\alpha} \mathcal{Th}_{a_\beta}$  are all right-left equivalent functions; in particular topologically indistinguishable (their underlying tessellations, and/or pre Speiser graphs, are equivalent under homeomorphisms). However, as meromorphic functions, they are very different: the exponential block  ${}_{a_\alpha} \mathcal{E}_{a_\beta}$  has one finite and one infinite asymptotic values

defining it, but the  $h$ -tangent block  ${}_{a_\alpha}T_{a_\beta}$  has two finite asymptotic values defining it, and is strictly meromorphic in the interior of its domain. The use of the associated canonical vector fields<sup>21</sup>

$$X_{{}_{a_\alpha}E_{a_\beta}}(z) \doteq \frac{1}{{}_{a_\alpha}E'_{a_\beta}(z)} \frac{\partial}{\partial z} \quad \text{and} \quad X_{{}_{a_\alpha}T_{a_\beta}}(z) \doteq \frac{1}{{}_{a_\alpha}T'_{a_\beta}(z)} \frac{\partial}{\partial z}$$

see [18] prop. 2.5, allows us to very easily distinguish between them by considering their phase portraits. See Figure 13, and Example 9.1.c for further details.

The next definition is illustrated in Figure 11.

**Definition 9.8.** Let  $\mathcal{R}_{w(z)}$  be the Speiser Riemann surface associated to a Speiser function  $w(z)$  provided with a cyclic order  $\mathcal{W}_q$  for its  $q$  singular values. By Remark 5.6,

$$\gamma = \overline{a_\alpha a_\beta} \cup \overline{a_\beta a_\alpha} \subset \widehat{\mathbb{C}}_w$$

is a Jordan path, the union of two geodesic polygonals, as in Definition 5.4, that runs through  $\mathcal{W}_q$ .

1) The *closed hemispheres*  $\mathfrak{H}^\pm$  associated to  $\gamma$  satisfy

$$\mathfrak{H}^+ \cap \mathfrak{H}^- = \gamma, \quad \text{and} \quad \widehat{\mathbb{C}}_w = \mathfrak{H}^+ \cup \mathfrak{H}^-,$$

with  $\mathfrak{H}^+$  on the left hand side of  $\gamma$ . Let  $\Xi = \{\overline{w_{j(a)} w_{j(r)}} \mid j(a) \neq j(r)\} \subsetneq \gamma$  be a non-empty collection of polygonal branch cuts. A *positive half-sheet*  $\mathfrak{L}_\Xi^+$  is

$$\mathfrak{H}^+ \setminus \Xi.$$

Analogously, a *negative half-sheet*  $\mathfrak{L}_\Xi^-$  is  $\mathfrak{H}^- \setminus \Xi$ .

2) Let  $\overline{a_\alpha a_\beta}$  be a polygonal branch cut, a *logarithmic tower*<sup>22</sup>  $\mathcal{T}(a_\alpha, a_\beta)$  of  $\mathcal{R}_{w(z)}$  is a Riemann surface

- i) associated to an exponential or an  $h$ -tangent block on  ${}_{a_\alpha}U_{a_\beta}$  of  $w(z)$ ,
- ii) whose boundary is an element of  $\pi_2^{-1}(\overline{a_\alpha a_\beta})$ .

3) A  $\mathcal{T}(a_\alpha, a_\beta)$  is a *maximal logarithmic tower* in  $\mathcal{R}_{w(z)}$  if given any logarithmic tower  $\widehat{\mathcal{T}}(a_\alpha, a_\beta)$  such that  $\mathcal{T}(a_\alpha, a_\beta) \subset \widehat{\mathcal{T}}(a_\alpha, a_\beta)$ , then  $\mathcal{T}(a_\alpha, a_\beta) = \widehat{\mathcal{T}}(a_\alpha, a_\beta)$ .

**Remark 9.9** (Construction and notation for logarithmic towers). 1. A logarithmic tower  $\mathcal{T}(a_\alpha, a_\beta)$  is determined by a pair  $(a_\alpha, a_\beta)$  of asymptotic values of  $w(z)$ , however, not all pairs of asymptotic values of  $w(z)$  determine logarithmic towers. However, four abstract and qualitatively distinct cases appear:

$$\begin{aligned} \mathcal{T}_+^\circ(a_\alpha, a_\beta) &= \left[ (\mathfrak{H}^+ \setminus \overline{a_\alpha a_\beta}) \cup \left( \bigcup_{\theta=2}^{\infty} (\mathfrak{H}^- \setminus \overline{a_\alpha a_\beta} \cup \mathfrak{H}^+ \setminus \overline{a_\alpha a_\beta})_\theta \right) \right] / \sim, \\ \mathcal{T}_+^\times(a_\alpha, a_\beta) &= \left[ \bigcup_{\theta=1}^{\infty} (\mathfrak{H}^- \setminus \overline{a_\alpha a_\beta} \cup \mathfrak{H}^+ \setminus \overline{a_\alpha a_\beta})_\theta \right] / \sim, \\ \mathcal{T}_-^\times(a_\alpha, a_\beta) &= \left[ (\mathfrak{H}^- \setminus \overline{a_\alpha a_\beta}) \cup \left( \bigcup_{\theta=2}^{\infty} (\mathfrak{H}^+ \setminus \overline{a_\alpha a_\beta} \cup \mathfrak{H}^- \setminus \overline{a_\alpha a_\beta})_\theta \right) \right] / \sim, \\ \mathcal{T}_-^\circ(a_\alpha, a_\beta) &= \left[ \bigcup_{\theta=1}^{\infty} (\mathfrak{H}^+ \setminus \overline{a_\alpha a_\beta} \cup \mathfrak{H}^- \setminus \overline{a_\alpha a_\beta})_\theta \right] / \sim. \end{aligned} \tag{26}$$

The super index  $\circ$  or  $\times$  indicates that the first hemisphere of the tower is blue  $\mathfrak{H}^+$  or gray  $\mathfrak{H}^-$ . As for notation, when the context is clear, we shall sometimes drop the pair of asymptotic values and simply write  $\mathcal{T}_+^\circ$  instead of  $\mathcal{T}_+^\circ(a_\alpha, a_\beta)$ , the other cases are analogous.

2. Recalling Definitions 4.3 and 4.4, together with Proposition 4.7, some useful features of the construction of logarithmic towers, by gluing, are the following. The use of Figure 11 is recommended.

i) The isometric glueing<sup>23</sup> for

$$\mathcal{T}_-^\circ = \left[ \bigcup_{\theta=1}^{\infty} (\mathfrak{H}^+ \setminus \overline{a_\alpha a_\beta} \cup \mathfrak{H}^- \setminus \overline{a_\alpha a_\beta})_\theta \right] / \sim$$

is as follows.

<sup>21</sup>We will drop the subindices when those are not essential, thus  $X_E(z)$ ,  $X_{T_H}(z)$ .

<sup>22</sup>See also [20] p. 152 and [18] p. 22, where the term ‘semi-infinite helicoid’ is used.

<sup>23</sup>Recall Corollary 4.2, this technique also appeared in [18] pp. 60 and 61.

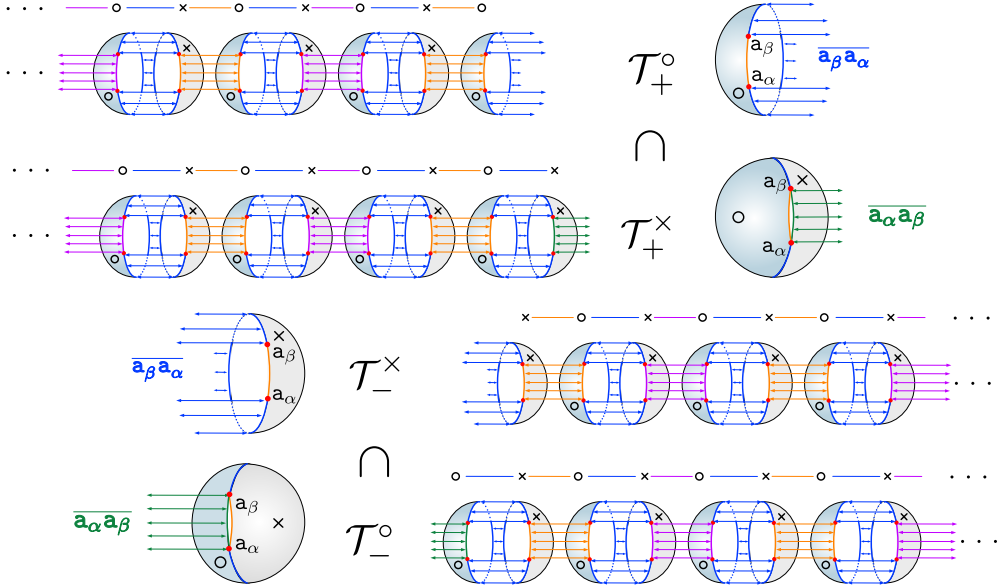


Figure 11: Accurate construction of logarithmic towers by surgery, four abstract and qualitatively distinct cases appear. Consider  $\gamma = \overline{a_\alpha a_\beta} \cup \overline{a_\beta a_\alpha}$ , the blue (resp. gray) hemisphere is on the left (resp. right) side of  $\overline{a_\alpha a_\beta}$ . The gluing is denoted by the same horizontal colored lines. The towers  $\mathcal{T}_+^o$  and  $\mathcal{T}_+^x$  have boundary  $\overline{a_\alpha a_\beta}$  (in green), while the towers  $\mathcal{T}_-^x$  and  $\mathcal{T}_-^o$  have boundary  $\overline{a_\beta a_\alpha} \dot{=} \gamma \setminus \overline{a_\alpha a_\beta}$  (in blue).

- a) First consider  $(\mathfrak{H}^+ \setminus \overline{a_\alpha a_\beta} \cup \mathfrak{H}^- \setminus \overline{a_\alpha a_\beta})_\theta$  for fixed  $\theta \geq 1$ , and glue the half sheets  $\mathfrak{H}^+ \setminus \overline{a_\alpha a_\beta}$  to  $\mathfrak{H}^- \setminus \overline{a_\alpha a_\beta}$  along their common boundary  $\overline{a_\beta a_\alpha} \dot{=} \gamma \setminus \overline{a_\alpha a_\beta}$ .
- b) Clearly, after gluing as in (a),  $(\mathfrak{H}^+ \setminus \overline{a_\alpha a_\beta} \cup \mathfrak{H}^- \setminus \overline{a_\alpha a_\beta})_\theta / \sim$  is a sheet<sup>24</sup>  $(\widehat{\mathbb{C}}_w \setminus \overline{a_\alpha a_\beta})_\theta$ , with boundary consisting of two copies of the polygonal geodesic segment  $\overline{a_\alpha a_\beta}$ , namely  $\overline{a_\alpha a_{\beta+}}$  and  $\overline{a_\alpha a_{\beta-}}$ .
- c) Next, for each  $j \geq 1$ , glue one copy, say  $\overline{a_\alpha a_{\beta+}}$  from the  $j$ -th sheet  $(\widehat{\mathbb{C}}_w \setminus \overline{a_\alpha a_\beta})_{\theta=j}$ , to a copy  $\overline{a_\alpha a_{\beta-}}$  from the  $(j+1)$ -th sheet  $(\widehat{\mathbb{C}}_w \setminus \overline{a_\alpha a_\beta})_{\theta=j+1}$ ; this leaves the geodesic segment  $\overline{a_\alpha a_{\beta-}}$  as the boundary of the sheet  $(\widehat{\mathbb{C}}_w \setminus \overline{a_\alpha a_\beta})_{\theta=1}$ ; no other boundaries are left.
- d) Thus, the boundary of  $\mathcal{T}_-^o$  is the open polygonal  $\overline{a_\alpha a_{\beta-}}$  coming from the 1-st sheet  $(\widehat{\mathbb{C}}_w \setminus \overline{a_\alpha a_\beta})_{\theta=1}$ .
- ii) The construction of the logarithmic tower

$$\mathcal{T}_-^x = \left[ (\mathfrak{H}^- \setminus \overline{a_\alpha a_\beta}) \cup \left( \bigcup_{\theta=2}^{\infty} (\mathfrak{H}^+ \setminus \overline{a_\alpha a_\beta} \cup \mathfrak{H}^- \setminus \overline{a_\alpha a_\beta})_\theta \right) \right] / \sim$$

is similar with the following modifications: Steps (a)–(d) are the same as above, with  $\theta \geq 2$ ; obtaining a logarithmic tower with boundary  $\overline{a_\alpha a_{\beta-}}$  coming from the 2-nd sheet  $(\widehat{\mathbb{C}}_w \setminus \overline{a_\alpha a_\beta})_{\theta=2}$ .

d) Finally, glue a half sheet  $(\mathfrak{H}^- \setminus \overline{a_\alpha a_\beta})$  along the boundary  $\overline{a_\alpha a_{\beta+}}$  leaving the boundary  $\overline{a_\beta a_\alpha}$  as the only boundary of  $\mathcal{T}_-^x$ .

- iii) The construction/glueing of the logarithmic towers  $\mathcal{T}_+^x$  and  $\mathcal{T}_+^o$  is analogous to the above, recall Equation (26).
- 3. It is clear from the above construction and from Figure 11, that given a pair  $(a_\beta, a_\alpha)$  of asymptotic values:
  - a) there are an infinite number of logarithmic towers in  $\mathcal{R}_{w(z)}$  of each type,
  - b) containment, and thus maximality as in Definition 9.8.3, only makes sense when the logarithmic towers are considered in  $\mathcal{R}_{w(z)}$ , see Examples 9.1.b and 10.1.b.

<sup>24</sup>Note that Definition 4.4 of sheet with branch cuts satisfies  $\mathfrak{L}_\Xi = \widehat{\mathbb{C}} \setminus \Xi = (\mathfrak{H}^+ \cup \mathfrak{H}^-) \setminus \Xi = \mathfrak{L}_\Xi^+ \cup \mathfrak{L}_\Xi^-$ .

**Definition 9.10.** The *soul*  $\mathfrak{N}_{w(z)}$ , of a Riemann surface  $\mathcal{R}_{w(z)}$ , is the subset obtained as the complement, in  $\mathcal{R}_{w(z)}$ , of the maximal logarithmic towers of  $\mathcal{R}_{w(z)}$ .

**Remark 9.11.** The above concepts appear as “logarithmic end” and “nucleus” in the classic literature (recall Remark 6.16), both for the combinatorial objects as for their corresponding Riemann surfaces analogous, surely because of the bijection between them (recall Definition 6.18.1–2 and see Lemma 9.13 below). However, the term “kernel” is used by [10] instead of nucleus when speaking of the complement of the logarithmic towers on the Riemann surface. We prefer to make the distinction clear and thus use

- “logarithmic end” and “nucleus” when considering the combinatorial objects (Speiser graphs), and
- “logarithmic towers” and “soul” when considering the analytic objects (Riemann surfaces).

**Example 9.1** (Two elementary  $N$ –functions).

a) The functions

$$e^z \doteq \mathcal{E}(z) \text{ and } \tanh(z) \doteq \mathcal{T}\mathcal{H}(z),$$

have asymptotic values

$$\mathcal{AV}_{\mathcal{E}} = \{a_1, a_2\} = \{0, \infty\} \text{ and } \mathcal{AV}_{\mathcal{T}\mathcal{H}} = \{a_1, a_2\} = \{-1, 1\}$$

respectively, as their only singular values, compare also with Definition 9.6. Further note that  $\tanh(z) = \frac{e^{2z}-1}{e^{2z}+1}$ , thus they are right–left  $Aut(\widehat{\mathbb{C}})$ –equivalent, as in Definition 9.2, so both have constant Schwarzian derivative

$$Sw\{e^z, z\} = -\frac{1}{2}, \quad Sw\{\tanh(z), z\} = -2.$$

Thus, they are  $N$ –functions.

b) Their Riemann surfaces  $\mathcal{R}_{w(z)}$ , have two infinitely ramified branch points, by Remark 4.1.2 they are denoted as,

$$\textcircled{1} = (\infty_1, a_1, \infty) \text{ and } \textcircled{2} = (\infty_2, a_2, \infty).$$

For  $\mathcal{R}_{\mathcal{E}(z)}$  one of the branch points lies over  $\infty \in \widehat{\mathbb{C}}_w$ , the other over the finite asymptotic value 0. For  $\mathcal{R}_{\mathcal{T}\mathcal{H}(z)}$  the branch points lie over the finite asymptotic values  $\{-1, 1\}$ . The diagonals<sup>25</sup> are  $\{\Delta_{\vartheta_0 \infty} = [0, +\infty]_{\vartheta}\}_{\vartheta \in \mathbb{Z}}$  and  $\{\Delta_{\vartheta -11} = [-1, 1]_{\vartheta}\}_{\vartheta \in \mathbb{Z}}$  for  $\mathcal{R}_{\mathcal{E}(z)}$  and  $\mathcal{R}_{\mathcal{T}\mathcal{H}(z)}$ , respectively.

According to Proposition 4.7, the decomposition in sheets (maximal domains of single–valuedness) is

$$\mathcal{R}_{w(z)} = \left( \bigcup_{\vartheta_1 = -\infty}^{\infty} (\widehat{\mathbb{C}}_w \setminus \overline{a_1 a_2})_{\vartheta_1} \right) / \sim,$$

where we can immediately recognize  $\mathcal{R}_{w(z)}$  as the union of two logarithmic towers. In fact, considering the cyclic order  $\mathcal{W}_2 = [a_1, a_2]$ , there are basically two choices for the decomposition:

$$\mathcal{R}_{w(z)} = \mathcal{T}_+^{\times}(a_1, a_2) \cup \mathcal{T}_-^{\circ}(a_1, a_2)$$

or

$$\mathcal{R}_{w(z)} = \mathcal{T}_+^{\circ}(a_1, a_2) \cup \mathcal{T}_-^{\times}(a_1, a_2).$$

Note that, both  $\mathcal{R}_{\mathcal{E}(z)}$ ,  $\mathcal{R}_{\mathcal{T}\mathcal{H}(z)}$ , are exceptional in the sense that there are no maximal logarithmic towers, and hence the soul is empty.

c) For the tessellation, with the cyclic order  $\mathcal{W}_2$ , it follows that  $\gamma = \mathbb{R} \cup \{\infty\}$  and the Speiser 2–tessellation

$$((\mathbb{C}_z \cup \{\infty_{a_1}, \infty_{a_2}\}) \setminus w(z)^* \gamma, w(z)^* \mathcal{L}_\gamma)$$

is shown in Figure 12.a–b. Note that the difference between the case for  $e^z$  and  $\tanh(z)$  is the actual choice of the asymptotic values. The two vertices of infinite valence of the graph  $w(z)^* \gamma$  are the points  $\infty_{a_1}, \infty_{a_2}$  in the non Hausdorff compactification

$$\mathbb{C}_z \cup \{\infty_{a_1}, \infty_{a_2}\}$$

determined by the two asymptotic values  $\{a_1, a_2\}$ .

d) Their analytic Speiser graph of index  $q = 2$  is drawn in Figure 12.c. Note that the tessellations and Speiser graphs for the two functions  $e^z$  and  $\tanh(z)$  only differ in the choice of singular values, *i.e.* the cyclically ordered asymptotic values  $\mathcal{W}_2$ .

e) Moreover, by considering the canonical vector fields

$$X_{\mathcal{E}}(z) \doteq \frac{1}{\mathcal{E}'(z)} \frac{\partial}{\partial z} = e^{-z} \frac{\partial}{\partial z} \quad \text{and} \quad X_{\mathcal{T}\mathcal{H}}(z) \doteq \frac{1}{\mathcal{T}\mathcal{H}'(z)} \frac{\partial}{\partial z} = \cosh^2(z) \frac{\partial}{\partial z}$$

<sup>25</sup>Recall Definition 4.6. In particular that if two diagonals have the same  $\vartheta$ , then their corresponding branch points share the same sheet.

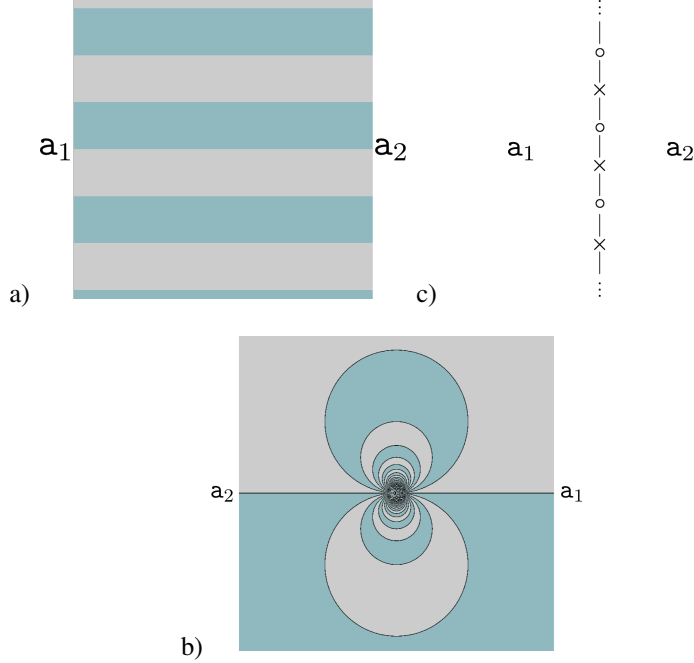


Figure 12: Consider  $((\mathbb{C}_z \cup \{\infty_{a_1}, \infty_{a_2}\}) \setminus w(z)^* \gamma, w(z)^* \mathcal{L}_\gamma)$  the tessellation corresponding to the  $N$ -functions  $w(z) = e^z$  (when  $a_1 = 0, a_2 = \infty$ ) and  $w(z) = \tanh(z)$  (when  $a_1 = -1, a_2 = 1$ ), for  $\gamma = \mathbb{R} \cup \{\infty\}$ . (a) The tessellation near the origin, (b) near the essential singularity at  $\infty \in \widehat{\mathbb{C}}_z$ . (c) The corresponding Speiser graph of index 2.

associated to  $e^z$  and  $\tanh(z)$  respectively, we can observe a correspondence<sup>26</sup> between the elementary blocks (left column) and the pairs (domain, vector field):

$$\begin{aligned} (\overline{\mathbb{H}}, \mathcal{E}(z)) &\longleftrightarrow (\overline{\mathbb{H}}, X_{\mathcal{E}}(z)) \\ (\overline{\mathbb{H}}, \mathcal{T}_h(z)) &\longleftrightarrow (\overline{\mathbb{H}}, X_{\mathcal{T}_h}(z)). \end{aligned} \tag{27}$$

With this correspondence, we can now visualize the phase portrait of  $\Re(X_{\mathcal{E}})(z)$  and  $\Re(X_{\mathcal{T}_h})(z)$  as shown in Figure 13. In order to distinguish the two elementary blocks, we abuse notation and use the visualization of the corresponding vector fields instead of the usual (indistinguishable) tessellations.

Recalling the decomposition of a sheet into half sheets,

$$\mathfrak{L}_\Xi = \widehat{\mathbb{C}} \setminus \Xi = (\mathfrak{H}^+ \cup \mathfrak{H}^-) \setminus \Xi = \mathfrak{L}_\Xi^+ \cup \mathfrak{L}_\Xi^-,$$

we can now decompose  $\mathcal{R}_{w(z)}$  in a different way than that of Proposition 4.7.

**Theorem 9.12** (Decomposition of  $\mathcal{R}_{w(z)}$  into the soul and maximal logarithmic towers). *Let  $w(z)$  be a Speiser function provided with a cyclic order  $\mathcal{W}_q$  for its  $q \geq 2$  distinct singular values.*

1) *The Riemann surface  $\mathcal{R}_{w(z)}$  associated to  $w(z)$  can be constructed by isometric glueing of half sheets  $\mathfrak{H}^+ \setminus \Xi$  and*

<sup>26</sup>See [18] proposition 2.5 for the complete correspondence.

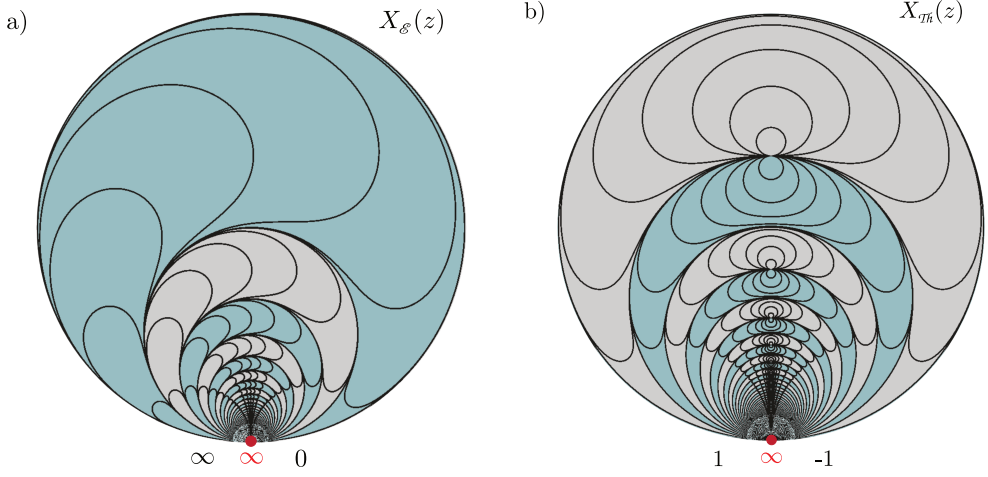


Figure 13: Two elementary blocks. (a) Exponential block  $0E_\infty$  corresponding to  $E(z) = e^z : \mathbb{H} \rightarrow \widehat{\mathbb{C}}_w$ . (b)  $h$ -tangent block  $-fTanh_1$  corresponding to  $T(z) = \tanh(z) : \mathbb{H} \rightarrow \widehat{\mathbb{C}}_w$ . Visualized using the associated vector fields  $X_E(z) = e^{-z} \frac{\partial}{\partial z}$  and  $X_T(z) = \cosh^2(z) \frac{\partial}{\partial z}$ . Note that since the Riemann surfaces  $R_{E(z)}$  and  $R_{T(z)}$ , do not have maximal logarithmic towers, there is no first blue or gray region; the blue-gray coloring is not canonical. The asymptotic values are indicated on each side of the essential singularity (marked red) at  $\infty \in \partial \mathbb{H}$ . The ‘dipoles’ in (b) correspond to the simple poles of  $\tanh(z)$ .

$\mathfrak{H}^- \setminus \Xi'$ , denoted by  $\sim$ , as follows

$$\mathcal{R}_{w(z)} = \left( \underbrace{\bigcup_{\vartheta_+ = 1}^{n_+} \left[ \mathfrak{H}^+ \setminus \left( \bigcup_{j(a), j(r) \in \Xi_{\vartheta_+}} \overline{w_{j(a)} w_{j(r)}} \right) \right] \bigcup_{\vartheta_- = 1}^{n_-} \left[ \mathfrak{H}^- \setminus \left( \bigcup_{j(a), j(r) \in \Xi_{\vartheta_-}} \overline{w_{j(a)} w_{j(r)}} \right) \right]}_{\text{soul}} \cup \right. \\ \left. \underbrace{\underbrace{\mathcal{T}(a_{\alpha_1}, a_{\beta_1})}_{1^{\text{st}} \text{ logarithmic tower}} \cup \dots \cup \underbrace{\mathcal{T}(a_{\alpha_p}, a_{\beta_p})}_{p^{\text{th}} \text{ logarithmic tower}}}_{\text{ }} \right) \sim . \quad (28)$$

In the above expression the following conventions are observed.

- The singular values of  $w(z)$  are denoted by  $\{w_{j(t)}\}_{t=1}^\delta$ , and as usual the asymptotic values are  $\{a_{\alpha_\sigma}, a_{\beta_\sigma}\}_{\sigma=1}^p$ , recall Equation (10).
- The number of half sheets in the soul is  $(n_+ + n_-) \in \mathbb{N} \cup \{\infty\}$ , the half sheets  $\mathfrak{H}^\pm \setminus \Xi_{\vartheta_\pm}$  are indexed by  $\vartheta_\pm$ .
- The  $p$  maximal logarithmic towers of  $\mathcal{R}_{w(z)}$  are distinguished by suitable pairs of asymptotic values

$$\underbrace{\{a_{\alpha_1} a_{\beta_1}, \dots, a_{\alpha_p} a_{\beta_p}\}}_{\star\text{-boundary}} \subseteq \{w_{j(a)} w_{j(r)}\},$$

where  $\star$ -boundary coincides with the boundary of the maximal logarithmic towers.

- 2) On each maximal logarithmic tower

$$\mathcal{T}(a_{\alpha_j}, a_{\beta_j}), \quad j \in \{1, \dots, p\},$$

the function  $w(z)$  is an exponential or an  $h$ -tangent block, i.e. is right-left equivalent to

- the function  $\exp(z) : \mathbb{H} \rightarrow \widehat{\mathbb{C}}$  when one of the asymptotic values  $a_{\alpha_j}, a_{\beta_j} \in \widehat{\mathbb{C}}_w$  is infinite,
- the function  $\tanh(z) : \mathbb{H} \rightarrow \widehat{\mathbb{C}}$  when both asymptotic values  $a_{\alpha_j}, a_{\beta_j} \in \mathbb{C}_w$  are finite.

- 3) The soul is a flat  $p$ -gon, with at most  $0 \leq r + p \leq \infty$  critical points. Furthermore, the soul determines the Riemann surface  $\mathcal{R}_{w(z)}$ .
- 4) Assume in addition that  $w(z)$  is a finite Speiser function.
  - The number  $p$  of maximal logarithmic towers is zero if and only if  $w(z)$  is a rational function on  $\widehat{\mathbb{C}}_z$ , otherwise  $2 \leq p < \infty$ .
  - The soul is a flat  $p$ -gon, with at most  $0 \leq r + p < \infty$  critical points, i.e. the function  $w(z)$  is right-left equivalent to a rational function  $R(z)$  restricted to a certain Jordan domain  $\mathcal{P} \subset \widehat{\mathbb{C}}_z$ .

*Proof of Theorem 9.12.* The proof is basically a direct application of Theorem 7.1, specifically (4)  $\iff$  (2). Thus the converse: a Riemann surface as in (28) produces a Speiser function  $w(z)$ , is also immediate.

In full detail, recall Diagram (5), particularly that  $\pi_1$  is a biholomorphism. Thus the analytic Speiser graph  $(\mathfrak{S}_q, \mathcal{L}_{W_q})$ , together with the cell decomposition  $\Omega_z \setminus \mathfrak{S}_{w(z)}$ , and Proposition 6.11, provide an accurate representation of  $\mathcal{R}_{w(z)}$ :

- i) each vertex  $v = \circ$ , of the Speiser graph  $(\mathfrak{S}_{w(z)}, \mathcal{W}_q)$ , corresponds to a half sheet  $(\mathfrak{H}^+ \setminus \overline{a_\alpha a_\beta}) \subset \mathcal{R}_{w(z)}$ ,
- ii) each vertex  $v = \times$ , of the Speiser graph  $(\mathfrak{S}_{w(z)}, \mathcal{W}_q)$ , corresponds to a half sheet  $(\mathfrak{H}^- \setminus \overline{a_\alpha a_\beta}) \subset \mathcal{R}_{w(z)}$ ,
- iii) each edge of the Speiser graph indicates the gluing of the corresponding half sheets,
- iv) each  $w_j$ -face of  $\Omega_z \setminus \mathfrak{S}_{w(z)}$  represents a branch point of the surface  $\mathcal{R}_{w(z)}$ , with ramification index half the number of sides of the  $w_j$ -face.

Denote the set of asymptotic values (counted with multiplicity) by  $\{a_\beta\} \subset \{w_{j(i)}\}_{i=1}^\delta$ ; necessarily its cardinality is  $0 \leq p \leq \delta < \infty$ .

Given (an arbitrary) Speiser function  $w(z)$ , the following result relates logarithmic ends of the Speiser graph  $(\mathfrak{S}_{w(z)}, \mathcal{W}_q)$ , see Definition 6.18, to the logarithmic towers of the Riemann surface  $\mathcal{R}_{w(z)}$ , see Definition 9.8.

**Lemma 9.13.** *Let  $w(z) : \Omega_z \rightarrow \widehat{\mathbb{C}}_w$  be a Speiser function with  $q \geq 2$  singular values.*

1) *There is a bijection between:*

- i) *the logarithmic ends  $\mathcal{T}$  of the analytic Speiser graph  $(\mathfrak{S}_{w(z)}, \mathcal{W}_q)$ , determined by  $a_\alpha$  and  $a_\beta$ , the asymptotic values corresponding to the unbounded  $a_\alpha$  and  $a_\beta$ -faces of  $\mathcal{T}$ ,*
- ii) *the maximal logarithmic towers of  $\mathcal{R}_{w(z)}$ ,  $\mathcal{T}(a_\alpha, a_\beta)$ , determined by the pair  $(a_\alpha, a_\beta)$  of asymptotic values of  $w(z)$ .*

2) *The analogous statement applies for the nucleus of  $(\mathfrak{S}_{w(z)}, \mathcal{W}_q)$  and the soul of  $\mathcal{R}_{w(z)}$ .*

*Proof.* By Proposition 6.11.2.c,  $\mathcal{T}$  has associated to itself asymptotic values  $a_\alpha$  and  $a_\beta$ , where  $a_\alpha \neq a_\beta$ . Furthermore, it is easy to check that the edge bundle in  $\mathfrak{S}_{w(z)}$  between the pair of vertices  $(v_{2\tau-1}, v_{2\tau})$  and the pair  $(v_{2(\tau+1)-1}, v_{2(\tau+1)})$  corresponds to the isometric glueing of the sheets  $(\widehat{\mathbb{C}} \setminus \overline{a_\alpha a_\beta})_\vartheta$  and  $(\widehat{\mathbb{C}} \setminus \overline{a_\alpha a_\beta})_{\vartheta+1}$  in  $\mathcal{R}_{w(z)}$ , with  $\vartheta = \tau$ , recall Corollary 4.2. Thus, each pair  $(v_{2\tau-1}, v_{2\tau})$  of adjacent vertices, represents a sheet  $(\widehat{\mathbb{C}} \setminus \overline{a_\alpha a_\beta})_\vartheta$ , with  $\vartheta = \tau$ .

The rest of the proof is left to the reader.  $\square$

Recalling Example 6.4, note that the set of logarithmic towers may be empty.

From Definition 9.10, the complement of the  $p$  maximal logarithmic towers in the decomposition (14), is the soul, proving statement (1).

Statement (2) follows immediately from Lemma 9.5, where the pair of logarithmic singularities can be recognized as an exponential or  $h$ -tangent block.

Statement (3) follows from the definition of the soul as the complement of the maximal logarithmic towers, and an accurate interpretation of Lemma 9.5.

For statement (4), since  $w(z)$  is a finite Speiser function, its Speiser graph has a finite number of bounded and unbounded faces, thus it follows that the ends are in fact logarithmic ends, say  $0 \leq p < \infty$ ,  $p \neq 1$  of them (see below). A simple argument, shows that the nucleus  $\mathfrak{N}$  is connected and has  $p$  logarithmic ends as its boundary. Hence by Remark 9.11 and Lemma 9.13, the soul is connected and can be recognized as a flat  $p$ -gon, thus Lemma 9.3 proves statement (4.b).

Finally, staying in the finite Speiser case, let us describe the Riemann surfaces  $\mathcal{R}_{w(z)}$  appearing for different values of  $p$ .

- Case  $p = 0$ . In this case, the cell decomposition arising from the Speiser graph  $\mathfrak{S}_{w(z)}$  consists of a finite number of bounded  $w_j$ -faces. Thus  $\mathfrak{S}_{w(z)}$  is finite and we conclude that  $w(z)$  is a rational function. Moreover,  $\mathcal{R}_{w(z)}$  is the soul.
- Case  $p = 1$  does not appear. Suppose the contrary, hence  $\mathcal{R}_{w(z)}$  has exactly one infinitely ramified branch point, thus  $\mathcal{R}_{w(z)}$  has an infinite number of sheets, and hence an infinite number of finitely ramified branch points. A contradiction, since  $w(z)$  is a finite Speiser function.
- Case  $p = 2$  and no bounded faces other than digons. By Lemma 6.20 the cell decomposition arising from the Speiser graph  $\mathfrak{S}_{w(z)}$ , has two unbounded faces, as in Figure 12.c. Note that the nucleus  $\mathfrak{N}_\infty$  of  $\mathfrak{S}_{w(z)}$  is empty; thus the soul  $\mathfrak{N}_{w(z)}$  of  $\mathcal{R}_{w(z)}$  is also empty. Example 9.1 describes explicitly the possible functions  $w(z)$ .

- Case  $p \geq 3$ . The proof for the generic cases uses the arguments presented before Lemma 9.13 and is as follows.  
Step 1. The Speiser graph has exactly  $p$  logarithmic ends. Thus, from the fact that there are only a finite number of singularities of  $w^{-1}(z)$  and Proposition 6.11.2, the number of bounded faces that are not digons, and the number of unbounded faces, are both finite. From this, it is easy to see that the only way that the cell decomposition arising from a Speiser graph  $\mathfrak{S}_{w(z)}$  has  $p$  unbounded faces, is that it has exactly  $p$  logarithmic ends.  
Step 2. By Lemma 9.13, we see that  $\mathcal{R}_{w(z)}$  has exactly  $p$  maximal logarithmic towers  $\mathcal{T}(a_\alpha, a_\beta)$  of  $\mathcal{R}_{w(z)}$ .  $\square$

## 9.2. Characterization of finite Speiser functions on $\Omega_z = \mathbb{C}_z, \widehat{\mathbb{C}}_z$

Recall that a *finite Speiser function* is a Speiser function with a finite number  $\delta = p + r$  of singularities of  $w^{-1}(z)$ . It is a classical result of R. Nevanlinna that only  $\Omega_z = \mathbb{C}_z$  appears. See [13] §8 and [6] p. 301.

Considering Theorem 7.1, Theorem 9.12, Lemma 9.5 and Definition 9.6, we have proved.

**Corollary 9.14** (Characterization of finite Speiser functions on  $\Omega_z = \mathbb{C}_z, \widehat{\mathbb{C}}_z$ ). *The following objects are equivalent.*

- 1) A finite Speiser function  $w(z) : \Omega_z \rightarrow \widehat{\mathbb{C}}_w$ .
- 2) A meromorphic function  $w(z) : \Omega_z \rightarrow \widehat{\mathbb{C}}_w$ , constructed by surgery of:
  - a) a rational block  $R(z) : \overline{\mathcal{P}} \subset \widehat{\mathbb{C}}_z \rightarrow \widehat{\mathbb{C}}_w$ , and
  - b) a finite number of
    - exponential blocks,  $\exp(z) : \overline{\mathbb{H}} \rightarrow \widehat{\mathbb{C}}_w$ ,
    - $h$ -tangent blocks,  $\tanh(z) : \overline{\mathbb{H}} \rightarrow \widehat{\mathbb{C}}_w$ .
- 3) A flat  $p$ -gon  $(\overline{\mathcal{P}}, w(\zeta))$ , with  $2 \leq p < \infty$ , whose function  $w(\zeta)$  has a finite number of critical points in the interior of  $\overline{\mathcal{P}}$ , with an exponential or  $h$ -tangent blocks glued to each side.
- 4) A Speiser Riemann surface  $\mathcal{R}_{w(z)}$  with a finite number of branch points.
- 5) A Speiser graph of index  $q$  with only a finite number of faces that are not digons.
- 6) A Speiser  $q$ -tessellation with a finite number of vertices of valence greater than or equal to 4.  $\square$

The above result extends the notion of *structurally finite entire functions* considered by M. Taniguchi [16], [17].

**Remark 9.15.** 1. Note that if the set of logarithmic towers is empty, *i.e.*  $p = 0$ , the soul of  $\mathcal{R}_{w(z)}$  is itself. Moreover, Statement (3) is empty (there is no flat  $p$ -gon). In particular, if  $w(z)$  has no asymptotic values (for instance if  $w(z)$  is rational) then the set of logarithmic towers is empty.

2. An immediate consequence of Corollary 9.14, is that  $N$ -functions, can be constructed via surgery of:

- a rational block, without interior singular points, and
- a finite number  $2 \leq p < \infty$  of exponential and  $h$ -tangent blocks.

3. If we consider *non finite Speiser functions*, other cases appear:

- $w(z) = \varphi(z)$  on  $\mathbb{C}_z$ , with  $p = 0$ ,  $r = \infty$  and  $q = 4$ , its associated Riemann surface has no logarithmic towers (yet it has an infinite number of algebraic branch points, see [9] example 5.1 for the tessellation),
- $w(z) = \cos \sqrt{z}$ , with  $p = 1$ ,  $r = \infty$  and  $q = 3$ , recall Example 3.1.4.b,
- $w(z) = \sin(z)$ , with  $p = 2$ ,  $r = \infty$  and  $q = 3$ ,
- $w(z) = \sin^2(z)$ , with  $p = 4$ ,  $r = \infty$  and  $q = 3$ ,

their Speiser graphs have no logarithmic ends, see [10] p. 360.

4. Speiser functions  $w(z)$  on  $\Omega_z = \Delta$ , always have an infinite number of singularities of  $w^{-1}(z)$ ; a characterization similar to Corollary 9.14 is an open question.

## 10. Examples

**Example 10.1** ( $N$ -function with  $q = 3$ ). Recall the Schwarzian differential equation (11),

$$Sw\{w, z\} = -2z.$$

- a) Up to Möbius transformations, the solutions  $w(z)$  are quotients of two Airy functions, in particular

$$w_{\text{Ai}}(z) = \frac{\text{Bi}(z)}{\text{Ai}(z)},$$

has the asymptotic values

$$\{a_1, a_2, a_3\} = \{-i, i, \infty\}$$

as its only singular values. Thus,  $w_{Ai}(z)$  is an  $N$ -function.

b) The branch points in the Riemann surface  $\mathcal{R}_{w_{Ai}(z)}$  are

$$(-i) = (\infty_1, -i, \infty), \quad (i) = (\infty_2, i, \infty), \quad (\infty) = (\infty_3, \infty, \infty).$$

Amongst the different possible sheets, consider the following 4 different types, with indices  $\Xi = \{1, 2, 3, 4\}$

$$\begin{aligned} \mathfrak{L}_1 &= \widehat{\mathbb{C}}_w \setminus \overline{-i i}, & \mathfrak{L}_2 &= \widehat{\mathbb{C}}_w \setminus \overline{i \infty}, \\ \mathfrak{L}_3 &= \widehat{\mathbb{C}}_w \setminus \overline{-i i \infty}, & \mathfrak{L}_4 &= \widehat{\mathbb{C}}_w \setminus (\overline{-i i} \cup \overline{i \infty} \cup \overline{-i i \infty}). \end{aligned} \quad (29)$$

The sheets  $\mathfrak{L}_3$  and  $\mathfrak{L}_4$  are different in the following sense:

- the boundary of  $\mathfrak{L}_3$  consists of two copies of the segment  $\overline{-i i \infty}$ ,
- the boundary of  $\mathfrak{L}_4$  consists of a copy of the segment  $\overline{-i i \infty}$ , and a copy of the segments  $\overline{-i i}$  and  $\overline{i \infty}$ .

In both cases,  $i$  is a co-singular value.

The diagonals in  $\mathcal{R}_{w_{Ai}(z)}$  are:

$$\begin{aligned} \Delta_{\vartheta_1 - i i}, \text{ with } \vartheta_1 \in \mathbb{N}, \text{ note that } \pi_2(\Delta_{\vartheta_1 - i i}) &= \overline{-i i}, \\ \Delta_{\vartheta_2 i \infty}, \text{ with } \vartheta_2 \in \mathbb{N}, \text{ note that } \pi_2(\Delta_{\vartheta_2 i \infty}) &= \overline{i \infty}, \\ \Delta_{\vartheta_3 - i \infty}, \text{ with } \vartheta_3 \in \mathbb{N}, \text{ note that } \pi_2(\Delta_{\vartheta_3 - i \infty}) &= \overline{-i i \infty}, \\ \Delta_{\vartheta_4 - i i} \cup \Delta_{\vartheta_4 i \infty} \cup \Delta_{\vartheta_4 - i \infty}, \text{ with } \vartheta_4 &= 1. \end{aligned}$$

Thus, the actual sheets that appear in  $\mathcal{R}_{w_{Ai}(z)}$  are:

$$\begin{aligned} \mathfrak{L}_{1,\vartheta_1} &= \widehat{\mathbb{C}}_w \setminus (\pi_2(\Delta_{\vartheta_1 - i i})) = (\widehat{\mathbb{C}}_w \setminus \overline{-i i})_{\vartheta_1}, \text{ with } \vartheta_1 \in \mathbb{N}, \\ \mathfrak{L}_{2,\vartheta_2} &= \widehat{\mathbb{C}}_w \setminus (\pi_2(\Delta_{\vartheta_2 i \infty})) = (\widehat{\mathbb{C}}_w \setminus \overline{i \infty})_{\vartheta_2}, \text{ with } \vartheta_2 \in \mathbb{N}, \\ \mathfrak{L}_{3,\vartheta_3} &= \widehat{\mathbb{C}}_w \setminus (\pi_2(\Delta_{\vartheta_3 - i \infty})) = (\widehat{\mathbb{C}}_w \setminus \overline{-i i \infty})_{\vartheta_3}, \text{ with } \vartheta_3 \in \mathbb{N}, \\ \mathfrak{L}_{4,\vartheta_4} &= \widehat{\mathbb{C}}_w \setminus (\pi_2(\Delta_{\vartheta_4 - i i}) \cup \pi_2(\Delta_{\vartheta_4 i \infty}) \cup \pi_2(\Delta_{\vartheta_4 - i \infty})) \\ &= (\widehat{\mathbb{C}}_w \setminus (\overline{-i i} \cup \overline{i \infty} \cup \overline{-i i \infty}))_{\vartheta_4}, \text{ with } \vartheta_4 = 1. \end{aligned}$$

Thus by gluing  $\mathfrak{L}_{4,1}$  to  $\mathfrak{L}_{1,1}$ ,  $\mathfrak{L}_{2,1}$  and  $\mathfrak{L}_{3,1}$ , along their common boundaries, we obtain a decomposition of  $\mathcal{R}_{w_{Ai}(z)}$  into maximal domains of single-valuedness, as in Proposition 4.7, namely

$$\mathcal{R}_{w_{Ai}(z)} = \left( \mathfrak{L}_{4,1} \cup \bigcup_{\vartheta_1=1}^{\infty} \mathfrak{L}_{1,\vartheta_1} \cup \bigcup_{\vartheta_2=1}^{\infty} \mathfrak{L}_{2,\vartheta_2} \cup \bigcup_{\vartheta_3=1}^{\infty} \mathfrak{L}_{3,\vartheta_3} \right) / \sim. \quad (30)$$

Clearly, we could have chosen different types of sheets in Equation (29); for instance by choosing  $\mathfrak{L}_3 = \widehat{\mathbb{C}}_w \setminus \overline{\infty - i}$ ,  $\mathfrak{L}_1 = \widehat{\mathbb{C}}_w \setminus \overline{i \infty - i}$  and  $\mathfrak{L}_4 = \widehat{\mathbb{C}}_w \setminus (\overline{i \infty - i} \cup \overline{i \infty} \cup \overline{\infty - i})$ , the decomposition (30) into maximal domains of single-valuedness would be different.

On the other hand, considering the cyclic order

$$\mathcal{W}_3 = [-i, i, \infty],$$

the decomposition of  $\mathcal{R}_{w_{Ai}(z)}$  into  $p = 3$  maximal logarithmic towers and the unique soul is

$$\mathcal{R}_{w_{Ai}(z)} = \left[ \underbrace{\mathfrak{H}^+ \setminus (\overline{-i i} \cup \overline{i \infty} \cup \overline{\infty - i})}_{\text{soul}} \cup \underbrace{\mathcal{T}_-^\times(-i, i)}_{\text{logarithmic tower}} \cup \underbrace{\mathcal{T}_-^\times(i, \infty)}_{\text{logarithmic tower}} \cup \underbrace{\mathcal{T}_-^\times(\infty, -i)}_{\text{logarithmic tower}} \right] / \sim.$$

c) For the tessellation, with the cyclic order  $\mathcal{W}_3$ , it follows that  $\gamma = i\mathbb{R} \cup \{\infty\}$  and the Speiser 3-tessellation  $(\mathbb{C}_z \setminus w_{Ai}(z)^* \gamma, w_{Ai}(z)^* \mathcal{L}_\gamma)$  is drawn in Figure 14.a–b. The tiles are 3-gons, with vertices of valence two represented by green dots (the cosingular points). The three vertices of infinite valence of the graph  $w_{Ai}(z)^* \gamma$  are the points in the non Hausdorff compactification

$$\mathbb{C}_z \cup \{\infty_{a_1}, \infty_{a_2}, \infty_{a_3}\}$$

determined by the three asymptotic values.

d) Its Speiser graph of index 3 is drawn in Figure 14.c. Note that the nucleus consists of one vertex  $v = \circ$  with three edges (in red), surrounded by three logarithmic ends (in black).

**Example 10.2.** Consider the function

$$w_4(z) = \frac{12z^4 - 36z^2 + 9}{\sqrt{\pi} (4z^4 - 12z^2 + 3) \operatorname{erfi}(z) - 2e^{z^2} z (2z^2 - 5)}.$$

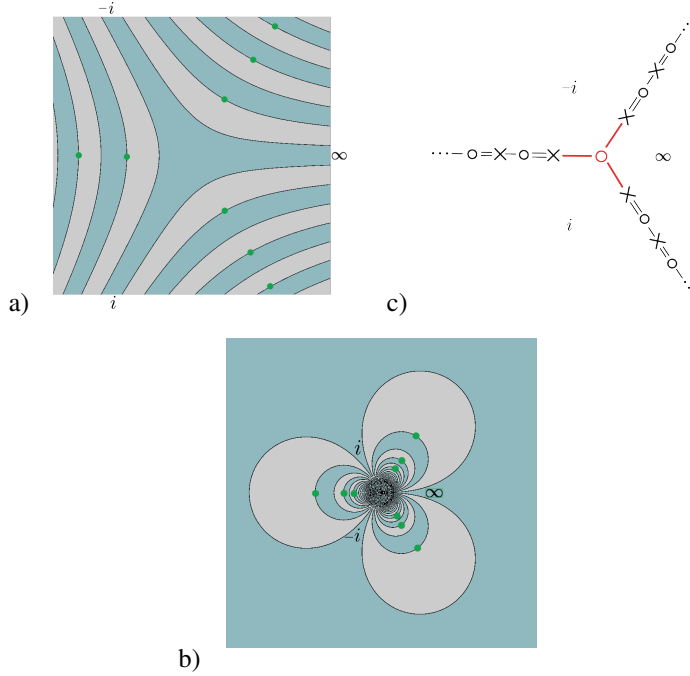


Figure 14: The tessellation  $(\mathcal{T}(w_{Ai}(z)^*\gamma), w_{Ai}(z)^*\mathcal{L}_\gamma)$  corresponding to the  $N$ -function  $w_{Ai}(z) = Bi(z)/Ai(z)$  and  $\gamma = i\mathbb{R} \cup \{\infty\}$ ; (a) near the origin, (b) near the essential singularity at  $\infty \in \widehat{\mathbb{C}}_z$ . (c) The corresponding Speiser graph of index 3. The nucleus is colored red and the p logarithmic ends are colored black.

a) It has the asymptotic values  $\{a_1, a_2, a_3, a_4\} = \left\{0, -\frac{3i}{\sqrt{\pi}}, 0, \frac{3i}{\sqrt{\pi}}\right\}$  as its only singular values. The Schwarzian derivative is  $Sw\{w_4, z\} = -(z^2 + 9)$ , thus it is an  $N$ -function with  $q = 3$ .  
b) The Riemann surface  $\mathcal{R}_{w_4(z)}$  has 4 infinitely ramified branch points, namely  $\textcircled{1} = (\infty_1, 0, \infty)$ ,  $\textcircled{2} = (\infty_2, -\frac{3i}{\sqrt{\pi}}, \infty)$ ,  $\textcircled{3} = (\infty_3, 0, \infty)$ , and  $\textcircled{4} = (\infty_4, \frac{3i}{\sqrt{\pi}}, \infty)$ .

There are 6 different types of diagonals:

$$\Delta_{\theta a_1 a_2}, \Delta_{\theta a_2 a_1}, \Delta_{\theta a_1 a_3}, \Delta_{\theta a_3 a_1}, \Delta_{\theta a_2 a_3}, \text{ and } \Delta_{\theta a_3 a_2}.$$

The actual sheets that appear in  $\mathcal{R}_{w_4(z)}$  are:

$$\begin{aligned} \mathfrak{L}_{1,\vartheta_1} &= \widehat{\mathbb{C}} \setminus (\pi_2(\Delta_{\theta_1 a_1 a_2})) = (\widehat{\mathbb{C}}_w \setminus \overline{a_1 a_2})_{\vartheta_1}, \\ \mathfrak{L}_{2,\vartheta_2} &= \widehat{\mathbb{C}} \setminus (\pi_2(\Delta_{\theta_2 a_2 a_1})) = (\widehat{\mathbb{C}}_w \setminus \overline{a_2 a_1})_{\vartheta_2}, \\ \mathfrak{L}_{3,\vartheta_3} &= \widehat{\mathbb{C}} \setminus (\pi_2(\Delta_{\theta_3 a_1 a_3})) = (\widehat{\mathbb{C}}_w \setminus \overline{a_1 a_3})_{\vartheta_3}, \\ \mathfrak{L}_{4,\vartheta_4} &= \widehat{\mathbb{C}} \setminus (\pi_2(\Delta_{\theta_4 a_3 a_1})) = (\widehat{\mathbb{C}}_w \setminus \overline{a_3 a_1})_{\vartheta_4}, \\ \mathfrak{L}_{5,\vartheta_5} &= \widehat{\mathbb{C}} \setminus (\pi_2(\Delta_{\theta_5 a_2 a_3}) \cup \pi_2(\Delta_{\theta_5 a_3 a_2})) \\ &= \left( \widehat{\mathbb{C}}_w \setminus (\overline{a_2 a_1 a_3} \cup \overline{a_3 a_1 a_2}) \right)_{\vartheta_5}, \\ \mathfrak{L}_{6,\vartheta_6} &= \widehat{\mathbb{C}} \setminus (\pi_2(\Delta_{\theta_6 a_1 a_2}) \cup \pi_2(\Delta_{\theta_6 a_2 a_3}) \cup \pi_2(\Delta_{\theta_6 a_3 a_1})) \\ &= \left( \widehat{\mathbb{C}}_w \setminus (\overline{a_1 a_2} \cup \overline{a_2 a_1 a_3} \cup \overline{a_3 a_1}) \right)_{\vartheta_6}, \text{ with } \vartheta_6 = 1, \text{ and} \\ \mathfrak{L}_{7,\vartheta_7} &= \widehat{\mathbb{C}} \setminus (\pi_2(\Delta_{\theta_7 a_2 a_1}) \cup \pi_2(\Delta_{\theta_7 a_1 a_3}) \cup \pi_2(\Delta_{\theta_7 a_3 a_2})) \\ &= \left( \widehat{\mathbb{C}}_w \setminus (\overline{a_2 a_1} \cup \overline{a_1 a_3} \cup \overline{a_3 a_1 a_2}) \right)_{\vartheta_7}, \text{ with } \vartheta_7 = 1. \end{aligned}$$

The decomposition of  $\mathcal{R}_{w_4(z)}$  into the maximal domains of single-valuedness is

$$\mathcal{R}_{w_4(z)} = \left( \mathfrak{L}_{6,1} \cup \mathfrak{L}_{5,1} \cup \mathfrak{L}_{5,2} \cup \mathfrak{L}_{5,3} \cup \mathfrak{L}_{7,1} \cup \bigcup_{\vartheta_1=1}^{\infty} \mathfrak{L}_{1,\vartheta_1} \cup \bigcup_{\vartheta_2=1}^{\infty} \mathfrak{L}_{2,\vartheta_2} \cup \bigcup_{\vartheta_3=1}^{\infty} \mathfrak{L}_{3,\vartheta_3} \cup \bigcup_{\vartheta_4=1}^{\infty} \mathfrak{L}_{4,\vartheta_4} \right) / \sim .$$

On the other hand, considering the cyclic order

$$\mathcal{W}_3 = [\mathbf{a}_2, \mathbf{a}_1, \mathbf{a}_3] = [-\frac{3i}{\sqrt{\pi}}, 0, \frac{3i}{\sqrt{\pi}}],$$

the decomposition of  $\mathcal{R}_{w(z)}$  into  $p = 4$  maximal logarithmic towers and the unique soul is

$$\begin{aligned} \mathcal{R}_{w_4(z)} = & \left[ \mathfrak{H}^-(\overline{\mathbf{a}_1 \mathbf{a}_3} \cup \overline{\mathbf{a}_2 \mathbf{a}_1} \cup \overline{\mathbf{a}_3 \mathbf{a}_2}) \cup \underbrace{\bigcup_{\vartheta=1}^4 (\mathfrak{H}^+ \setminus \overline{\mathbf{a}_3 \mathbf{a}_2} \cup \mathfrak{H}^- \setminus \overline{\mathbf{a}_3 \mathbf{a}_2})_{\vartheta}}_{\text{soul}} \cup \mathfrak{H}^+(\overline{\mathbf{a}_1 \mathbf{a}_3} \cup \overline{\mathbf{a}_2 \mathbf{a}_1} \cup \overline{\mathbf{a}_3 \mathbf{a}_2}) \right. \\ & \left. \cup \underbrace{\mathcal{T}_-(\mathbf{a}_1, \mathbf{a}_3)}_{\text{logarithmic tower}} \cup \underbrace{\mathcal{T}_-(\mathbf{a}_2, \mathbf{a}_1)}_{\text{logarithmic tower}} \cup \underbrace{\mathcal{T}_+(\mathbf{a}_2, \mathbf{a}_1)}_{\text{logarithmic tower}} \cup \underbrace{\mathcal{T}_+(\mathbf{a}_1, \mathbf{a}_3)}_{\text{logarithmic tower}} \right] / \sim . \end{aligned}$$

c) For the tessellation, with the cyclic order  $\mathcal{W}_3$ , it follows that  $\gamma = i\mathbb{R} \cup \{\infty\}$  and the Speiser 3-tessellation  $(\mathbb{C}_z \setminus w_4(z)^* \gamma, w_4(z)^* \mathcal{L}_\gamma)$  is shown in Figure 15.a–b. The tiles are 3-gons, with the vertices of valence two (the cosingular points) represented by green dots, only a finite number of them are shown. The four vertices of infinite valence of the graph  $w_4(z)^* \gamma$  are the points in the non Hausdorff compactification

$$\mathbb{C}_z \cup \{\infty_1, \infty_2, \infty_3, \infty_4\}$$

determined by the four asymptotic values (with multiplicity)  $\{0, -\frac{3i}{\sqrt{\pi}}, 0, \frac{3i}{\sqrt{\pi}}\}$ .

d) Its analytic Speiser graph  $\mathfrak{S}_{w_4(z)}$  of index 3 is drawn in Figure 15.c. Note that the nucleus consists of ten vertices and four “loose” edges (in red), surrounded by four logarithmic ends (in black).

**Example 10.3.** Consider the function

$$w(z) = \exp(\exp(z)).$$

a) The singular values are  $\mathcal{SV}_w = \{\mathbf{a}_1, \mathbf{a}_2, \mathbf{a}_3\} = \{0, 1, \infty\}$ ; note that all of them are asymptotic values. Thus it is a Speiser function with  $q = 3$ . It is not a finite Speiser function since it has an infinite number of logarithmic singularities of  $w^{-1}(z)$ :

- A singularity  $U_1$  over the asymptotic value 1, with asymptotic path  $\alpha_1(\tau) = -\tau$ , for  $\tau \in (0, \infty)$ .
- An infinite number of singularities,  $\{U_{0,\sigma}\}_{\sigma \in \mathbb{Z}}$ , over the asymptotic value 0, with asymptotic paths  $\alpha_{0,\sigma}(\tau) = (2\sigma + 1)\pi i + \tau$ , for  $\tau \in (0, \infty)$ .
- An infinite number of singularities,  $\{U_{\infty,\sigma}\}_{\sigma \in \mathbb{Z}}$ , over the asymptotic value  $\infty$ , with asymptotic paths  $\alpha_{\infty,\sigma}(\tau) = 2\sigma\pi i + \tau$ , for  $\tau \in (0, \infty)$ .

b) The Riemann surface  $\mathcal{R}_{w(z)}$  has an infinite number of infinitely ramified branch points, namely

$$\textcircled{1} = (\infty_{\textcircled{1}}, 1, \infty), \left\{ \textcircled{0}_\sigma = (\infty_{2\sigma+1}, 0, \infty) \right\}_{\sigma \in \mathbb{Z}}, \text{ and } \left\{ \textcircled{\infty}_\sigma = (\infty_{2\sigma}, \infty, \infty) \right\}_{\sigma \in \mathbb{Z}}.$$

The actual sheets that appear in  $\mathcal{R}_{w(z)}$  are:

$$\begin{aligned} \mathfrak{L}_{1,\vartheta_1} &= \widehat{\mathbb{C}} \setminus (\pi_2(\Delta_{\vartheta_1 \mathbf{a}_1 \mathbf{a}_2}) \cup \pi_2(\Delta_{\vartheta_1 \mathbf{a}_3 \mathbf{a}_1})) = \left( \widehat{\mathbb{C}}_w \setminus (\overline{01} \cup \overline{\infty 0}) \right)_{\vartheta_1}, \\ \mathfrak{L}_{2,\vartheta_2} &= \widehat{\mathbb{C}} \setminus (\pi_2(\Delta_{\vartheta_2 \mathbf{a}_3 \mathbf{a}_1})) = \left( \widehat{\mathbb{C}}_w \setminus \overline{\infty 0} \right)_{\vartheta_2}. \end{aligned}$$

The decomposition of  $\mathcal{R}_{w(z)}$  into maximal domains of single-valuedness is

$$\mathcal{R}_{w(z)} = \left[ \bigcup_{\vartheta_1 \in \mathbb{Z}} \mathfrak{L}_{1,\vartheta_1} \cup \bigcup_{\vartheta_3 \in \mathbb{Z}} \left( \bigcup_{\vartheta_2=1}^{\infty} \mathfrak{L}_{2,\vartheta_2} \right)_{\vartheta_3} \right] / \sim .$$

Considering the cyclic order

$$\mathcal{W}_3 = [0, 1, \infty],$$

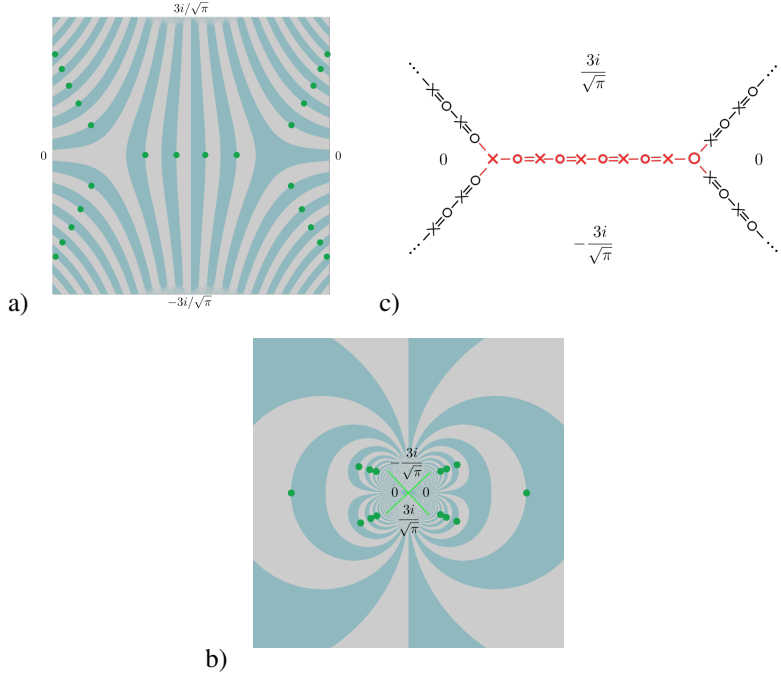


Figure 15: The tessellation  $(\mathbb{C}_z \setminus w_4(z)^* \gamma, w_4(z)^* \mathcal{L}_\gamma)$  corresponding to  $\gamma = i\mathbb{R} \cup \{\infty\}$  and the  $N$ -function  $w_4(z)$ , the green dots indicate the vertices of valence 2; (a) near the origin, (b) near the essential singularity at  $\infty \in \widehat{\mathbb{C}}_z$ ; in (b) the green lines at the center of the drawing have been added to indicate the location of the four vertices of infinite valence. (c) The corresponding Speiser graph of index  $p = 4$ . The nucleus is colored red and the 4 logarithmic ends are colored black.

the decomposition of  $\mathcal{R}_{w(z)}$  into an infinite number of maximal logarithmic towers and the unique soul is

$$\mathcal{R}_{w(z)} = \left[ \underbrace{\bigcup_{\vartheta=-\infty}^{\infty} \left( \mathfrak{H}^+ \setminus (\overline{01} \cup \overline{1\infty} \cup \overline{\infty 0}) \cup \mathfrak{H}^- \setminus (\overline{01} \cup \overline{1\infty} \cup \overline{\infty 0}) \right)_\vartheta}_{\text{soul}} \cup \underbrace{\bigcup_{\vartheta=-\infty}^{\infty} \left( \underbrace{\mathcal{T}_-^o(\infty, 0)}_{\text{logarithmic tower}} \cup \underbrace{\mathcal{T}_+^x(\infty, 0)}_{\text{logarithmic tower}} \right)_\vartheta}_{\text{logarithmic towers}} \right] / \sim .$$

Clearly, the soul is not a rational block.

c) For the tessellation, with the cyclic order  $\mathcal{W}_3$ , it follows that  $\gamma = \mathbb{R} \cup \{\infty\}$  and the Speiser 3-tessellation is  $(\mathcal{T}(w(z)^* \gamma), w(z)^* \mathcal{L}_\gamma)$ , as shown in Figure 16.a. The tiles are topological 3-gons, with vertices of valence two represented by green dots (the cosingular points, with singular values  $a_2 = 1$ ), only two “columns” are drawn, however there are an infinite number of them. There are an infinite number of vertices of infinite valence of the graph  $w(z)^* \gamma$ , these are points in the non Hausdorff compactification

$$\mathbb{C}_z \cup \{\infty_{\bar{1}}, \infty_{\bar{2}}\} \cup \{\infty_{2\sigma}, \infty_{2\sigma+1}\}_{\sigma \in \mathbb{Z}}$$

determined by the asymptotic values.

d) Its analytic Speiser graph of index 3 is drawn in Figure 16.b. In this case the Speiser graph has an unbounded 1-face corresponding to the logarithmic singularity over the asymptotic value 1, an infinite number of unbounded 0-faces and  $\infty$ -faces, which correspond to logarithmic singularities over the asymptotic values 0 and  $\infty$ , respectively. It also has an infinite number of digons corresponding to the coasymptotic value 1. Note that the nucleus consists of an infinite number of vertices and an infinite number of “loose” edges (in red), surrounded by an infinite number of logarithmic ends (in black).

**Example 10.4.** Consider the function

$$w(z) = e^{\sin(z)}.$$

a) The singular values are  $\mathcal{SV}_w = \{w_1, w_2, a_1, a_2\} = \{e, e^{-1}, 0, \infty\}$ . Thus it is a Speiser function with  $q = 4$ . It is not a finite Speiser function since:

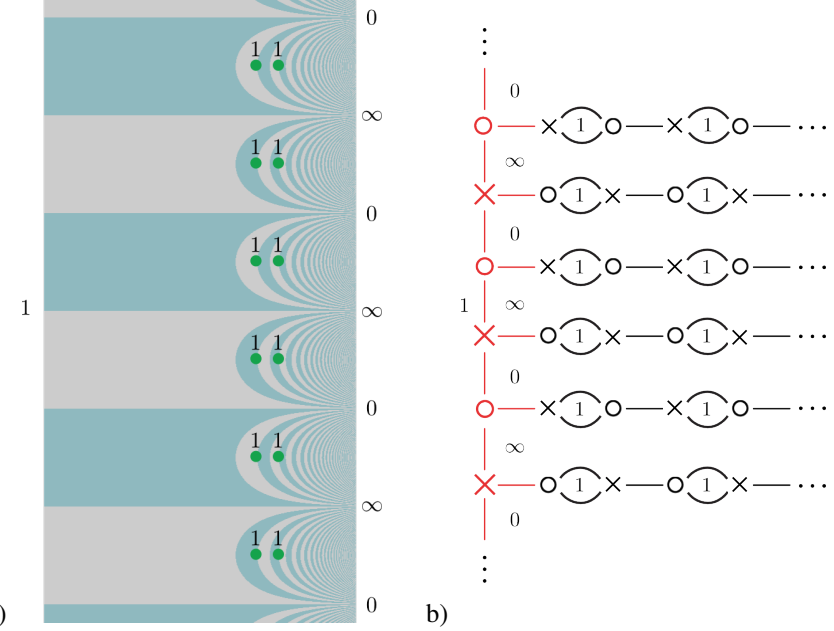


Figure 16: Consider the Speiser function  $w(z) = \exp(\exp(z))$  whose singular values are  $\{0, 1, \infty\}$ , note that all of them are asymptotic values. a) Speiser 3-tessellation  $\mathcal{T}_\gamma(w(z))$ , here  $\gamma = \mathbb{R} \cup \{\infty\}$ . The green dots are the cosingular points labelled with the corresponding cosingular value ‘1’; these continue indefinitely to the right as suggested. b) Speiser graph  $\mathfrak{S}_{w(z)}$  of index  $q = 3$ ; the digons are labelled ‘1’ since they are the dual of the cosingular points. The nucleus is colored red and the logarithmic ends are colored black.

- It has an infinite number of critical points  $\mathcal{CP}_w \doteq \{z_k = \frac{2k+1}{2}\pi \mid k \in \mathbb{Z}\}$  corresponding to the critical values  $\mathcal{CV}_w \doteq \{e, e^{-1}\}$ .
- It has an infinite number of logarithmic singularities  $\{U_{0,\sigma\pm}\}_{\sigma \in \mathbb{Z}}$  over the asymptotic value 0, and an infinite number of logarithmic singularities  $\{U_{\infty,\sigma\pm}\}_{\sigma \in \mathbb{Z}}$  over the asymptotic value  $\infty$ . The asymptotic paths are  $\alpha_{a_{\sigma\pm}}(\tau) = (2\sigma + 1)\frac{\pi}{2} \pm i\tau$ , for  $\sigma \in \mathbb{Z}$ ,  $\tau \in (0, \infty)$  associated to the asymptotic values

$$a_{\sigma\pm} = \begin{cases} 0_{\sigma\pm} = 0, & \text{for odd } \sigma, \\ \infty_{\sigma\pm} = \infty, & \text{for even } \sigma. \end{cases}$$

b) The Riemann surface has an infinite number of finitely ramified branch points

$$\circledcirc_k = \begin{cases} (z_k, e^{-1}, 2), & \text{for odd } k, \\ (z_k, e, 2), & \text{for even } k, \end{cases} \quad k \in \mathbb{Z},$$

and an infinite number of infinitely ramified branch points

$$\circledcirc_\pm = \begin{cases} (\infty_{\sigma\pm}, 0, \infty), & \text{for odd } \sigma, \\ (\infty_{\sigma\pm}, \infty, \infty), & \text{for even } \sigma, \end{cases} \quad \sigma \in \mathbb{Z}.$$

The actual sheets that appear in  $\mathcal{R}_{w(z)}$  are:

$$\begin{aligned} \mathfrak{L}_{1,\theta_1} &= \widehat{\mathbb{C}} \setminus (\pi_2(\Delta_{\theta_1 a_2 a_1})) = (\widehat{\mathbb{C}}_w \setminus \overline{\infty 0})_{\theta_1}, \\ \mathfrak{L}_{2,\theta_2} &= \widehat{\mathbb{C}} \setminus (\pi_2(\Delta_{\theta_2 a_2 a_1})) = (\widehat{\mathbb{C}}_w \setminus \overline{0 \infty})_{\theta_2}, \\ \mathfrak{L}_{3,\theta_3} &= \widehat{\mathbb{C}} \setminus (\pi_2(\Delta_{\theta_3 a_1 w_1}) \cup \pi_2(\Delta_{\theta_3 w_2 a_2}) \cup \pi_2(\Delta_{\theta_3 a_2 a_1})) \\ &= (\widehat{\mathbb{C}}_w \setminus (\overline{0 e^{-1}} \cup \overline{e \infty} \cup \overline{\infty 0}))_{\theta_3}. \end{aligned}$$

The decomposition of  $\mathcal{R}_{w(z)}$  into maximal domains of single-valuedness is

$$\mathcal{R}_{w(z)} = \left[ \bigcup_{\theta_3 \in \mathbb{Z}} \mathfrak{L}_{3,\theta_3} \cup \bigcup_{\theta_3 \in \mathbb{Z}} \left( \bigcup_{\theta_1=1}^{\infty} \mathfrak{L}_{1,\theta_1} \cup \bigcup_{\theta_2=1}^{\infty} \mathfrak{L}_{2,\theta_2} \right)_{\theta_3} \right] / \sim .$$

Considering the cyclic order

$$\mathcal{W}_4 = [a_1, w_2, w_1, a_2] = [0, e^{-1}, e, \infty],$$

the decomposition of  $\mathcal{R}_{w(z)}$  into an infinite number of maximal logarithmic towers and the unique soul is

$$\mathcal{R}_{w(z)} = \left[ \underbrace{\bigcup_{\theta=-\infty}^{\infty} \left( \mathfrak{H}^+ \setminus (\overline{\infty 0} \cup \overline{e \infty} \cup \overline{e^{-1} e} \cup \overline{0 e^{-1}}) \cup \mathfrak{H}^- \setminus (\overline{\infty 0} \cup \overline{e \infty} \cup \overline{e^{-1} e} \cup \overline{0 e^{-1}}) \right)_{\theta}}_{\text{soul}} \right. \\ \left. \bigcup_{\theta=-\infty}^{\infty} \left( \underbrace{\mathcal{T}_-^{\circ}(\infty, 0)}_{\text{logarithmic tower}} \cup \underbrace{\mathcal{T}_+^{\times}(\infty, 0)}_{\text{logarithmic tower}} \right)_{\theta} \right] / \sim.$$

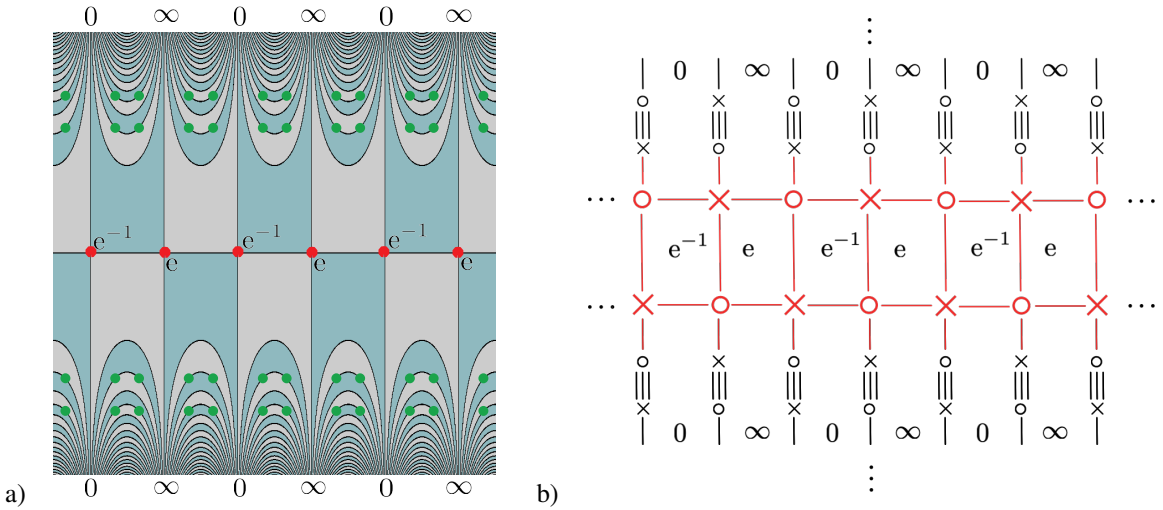


Figure 17: Speiser function  $w(z) = e^{\sin(z)}$ . (a) Speiser 4-tessellation  $(\mathcal{T}(w(z)^*\gamma), w(z)^*\mathcal{L}_\gamma)$  corresponding to  $\gamma = \mathbb{R} \cup \{\infty\}$  and  $w(z)$ , the green dots indicate the vertices of valence 2. (b) The corresponding Speiser graph of index  $q = 4$ . The nucleus is colored red and the logarithmic ends are colored black.

- c) For the tessellation with the cyclic order  $\mathcal{W}_4$ , it follows that  $\gamma = \mathbb{R} \cup \{\infty\}$  and its Speiser 4-tessellation is  $(\mathcal{T}(w(z)^*\gamma), w(z)^*\mathcal{L}_\gamma)$  which is shown in Figure 17.a. As can be appreciated, the tiles are topological 4-gons, with vertices of valence two represented by green dots (the cosingular points, with singular values  $w_1 = e$  and  $w_2 = e^{-1}$ ), only four “rows” are drawn, however there are an infinite number of them. There are an infinite number of vertices of infinite valence of the graph  $w(z)^*\gamma$ . These are the ideal points in the non Hausdorff compactification  $\mathbb{C}_z \cup \{\infty_{a_{1\pm}}, \infty_{a_{2\pm}}, \dots, \infty_{a_{\sigma\pm}}, \dots\}$  determined by the asymptotic values  $a_{\sigma\pm} = 0$  and  $a_{\sigma\pm} = \infty$ , for odd or even  $\sigma$  respectively.
- d) Its analytic Speiser graph of index 4 is drawn in Figure 17.b. In this case the Speiser graph has an infinite number of unbounded 0-faces and  $\infty$ -faces, which correspond to logarithmic singularities over the asymptotic values 0 and  $\infty$ , respectively. Moreover, it also has an infinite number of bounded  $e$ -faces and  $e^{-1}$ -faces. The bounded faces are 4-gons, thus they correspond to finitely ramified branch points of ramification index 2. Note that the nucleus consists of an infinite number of squares arranged in a horizontal line and an infinite number of “loose” edges (in red), surrounded by an infinite number of logarithmic ends (in black).

**Example 10.5.** Consider the function

$$w(z) = \sin(z) \exp(\sin(z)).$$

- a) The singular values are  $\mathcal{SV}_w = \{w_1, a_1, w_2, a_2\} = \{-e^{-1}, 0, e, \infty\}$ , where  $\{0, \infty\}$  are asymptotic values and  $\{-e^{-1}, e\}$  are critical values. It is thus a Speiser function, but not a finite Speiser function, since it has an infinite number of singularities of  $w^{-1}(z)$ :

- It has an infinite number of critical points  $\mathcal{CP}_w \doteq \{z_k = \frac{2k+1}{2}\pi \mid k \in \mathbb{Z}\}$  corresponding to the critical values  $\mathcal{CV}_w \doteq \{w_1, w_2\}$ ; for odd  $\sigma$  the critical values are  $w_1 = -e^{-1}$  with ramification index 4, and for even  $\sigma$  the critical values are  $w_2 = e$  with ramification index 2.
- It has an infinite number of logarithmic singularities  $\{U_{0,\sigma\pm}\}_{\sigma \in \mathbb{Z}}$  over the asymptotic value 0, and an infinite number of logarithmic singularities  $\{U_{\infty,\sigma\pm}\}_{\sigma \in \mathbb{Z}}$  over the asymptotic value  $\infty$ . The asymptotic paths are  $\alpha_{\sigma\pm}(\tau) = (2\sigma + 1)\frac{\pi}{2} \pm i\tau$ , for  $\sigma \in \mathbb{Z}$ ,  $\tau \in (0, \infty)$  associated to the asymptotic values

$$a_{\sigma\pm} = \begin{cases} 0_{\sigma\pm} = 0, & \text{for odd } \sigma, \\ \infty_{\sigma\pm} = \infty, & \text{for even } \sigma. \end{cases}$$

Moreover the points  $\{k\pi\}_{k \in \mathbb{Z}}$  are cocritical points with cocritical value 0. There are many more cocritical as will shortly be seen.

b) The Riemann surface has an infinite number of finitely ramified branch points

$$\circledcirc_k = \begin{cases} (z_k, -e^{-1}, 4), & \text{for odd } k, \\ (z_k, e, 2), & \text{for even } k, \end{cases} \quad k \in \mathbb{Z},$$

and an infinite number of infinitely ramified branch points

$$\circledcirc_{\sigma\pm} = \begin{cases} (\infty_{\sigma\pm}, 0, \infty), & \text{for odd } \sigma, \\ (\infty_{\sigma\pm}, \infty, \infty), & \text{for even } \sigma, \end{cases} \quad \sigma \in \mathbb{Z}.$$

The actual sheets that appear in  $\mathcal{R}_{w(z)}$  are:

$$\begin{aligned} \mathfrak{L}_{1,\theta_j} &= \widehat{\mathbb{C}} \setminus (\pi_2(\Delta_{\theta_j a_1 a_2})) = (\widehat{\mathbb{C}}_w \setminus \overline{0\infty})_{\theta_j}, \quad j = 1, 2, 3, 4, \\ \mathfrak{L}_{2,\theta_k} &= \widehat{\mathbb{C}} \setminus (\pi_2(\Delta_{\theta_k w_1 a_1}) \cup \pi_2(\Delta_{\theta_k a_1 a_2}) \cup \pi_2(\Delta_{\theta_k w_1 w_2}) \cup \pi_2(\Delta_{\theta_k w_2 a_2})), \\ &= (\widehat{\mathbb{C}}_w \setminus (\overline{-e^{-1}0} \cup \overline{0e\infty} \cup \overline{-e^{-1}0e} \cup \overline{e\infty}))_{\theta_k}, \quad \theta_k = 1, 2, 3, 4. \end{aligned}$$

The decomposition of  $\mathcal{R}_{w(z)}$  into maximal domains of single-valuedness is

$$\mathcal{R}_{w(z)} = \left[ \bigcup_{\theta_5 \in \mathbb{Z}} \left( \mathfrak{L}_{2,1} \cup \mathfrak{L}_{2,2} \cup \mathfrak{L}_{2,3} \cup \mathfrak{L}_{2,4} \cup \bigcup_{\theta_1=1}^{\infty} \mathfrak{L}_{1,\theta_1} \cup \bigcup_{\theta_2=1}^{\infty} \mathfrak{L}_{1,\theta_2} \cup \bigcup_{\theta_3=1}^{\infty} \mathfrak{L}_{1,\theta_3} \cup \bigcup_{\theta_4=1}^{\infty} \mathfrak{L}_{1,\theta_4} \right)_{\theta_5} \right] \sim .$$

Considering the cyclic order

$$\mathcal{W}_4 = [-e^{-1}, 0, e, \infty],$$

the decomposition of  $\mathcal{R}_{w(z)}$  into an infinite number of maximal logarithmic towers and the unique soul is

$$\begin{aligned} \mathcal{R}_{w(z)} = & \left[ \underbrace{\bigcup_{\theta_5 \in \mathbb{Z}} (\mathfrak{L}_{2,1} \cup \mathfrak{L}_{2,2} \cup \mathfrak{L}_{2,3} \cup \mathfrak{L}_{2,4})_{\theta_5} \cup}_{\text{soul}} \right. \\ & \left. \bigcup_{\theta_5 \in \mathbb{Z}} \left( \underbrace{\mathcal{T}_+^{\times}(0, \infty)}_{\substack{\text{left upper} \\ \text{logarithmic tower}}} \cup \underbrace{\mathcal{T}_-^{\circ}(0, \infty)}_{\substack{\text{left lower} \\ \text{logarithmic tower}}} \cup \underbrace{\mathcal{T}_-^{\circ}(0, \infty)}_{\substack{\text{right upper} \\ \text{logarithmic tower}}} \cup \underbrace{\mathcal{T}_+^{\times}(0, \infty)}_{\substack{\text{right lower} \\ \text{logarithmic tower}}} \right)_{\theta_5} \right] \sim , \end{aligned}$$

where for  $\theta_k = 1, 2, 3, 4$  the sheet  $\mathfrak{L}_{2,\theta_k}$  decomposes into half sheets

$$\mathfrak{L}_{2,\theta_k} = (\mathfrak{H}^+ \setminus (\overline{-e^{-1}0} \cup \overline{0\infty} \cup \overline{\infty - e^{-1}}) \cup \mathfrak{H}^- \setminus (\overline{-e^{-1}e} \cup \overline{e\infty} \cup \overline{\infty - e^{-1}}))_{\theta_k},$$

glued along the common boundary  $\overline{\infty - e^{-1}}$ .

c) For the tessellation, with the cyclic order  $\mathcal{W}_4$ , it follows that  $\gamma = \mathbb{R} \cup \{\infty\}$ . Its Speiser 4-tessellation  $(\mathcal{T}(w(z)^*\gamma), w(z)^*\mathcal{L}_\gamma)$  is shown in Figure 18.a. As can be appreciated, the tiles are topological 4-gons, with vertices of valence two represented by green dots (the cosingular points, with singular values  $a_1 = 0$  on the real axis,  $w_1 = e$ , and  $w_2 = e^{-1}$  on alternating rows symmetric with respect to the real axis), only a couple of “rows” are drawn, however there are an infinite number of them.

There are an infinite number of vertices of infinite valence of the graph  $w(z)^*\gamma$ . These are the ideal points in the non Hausdorff compactification

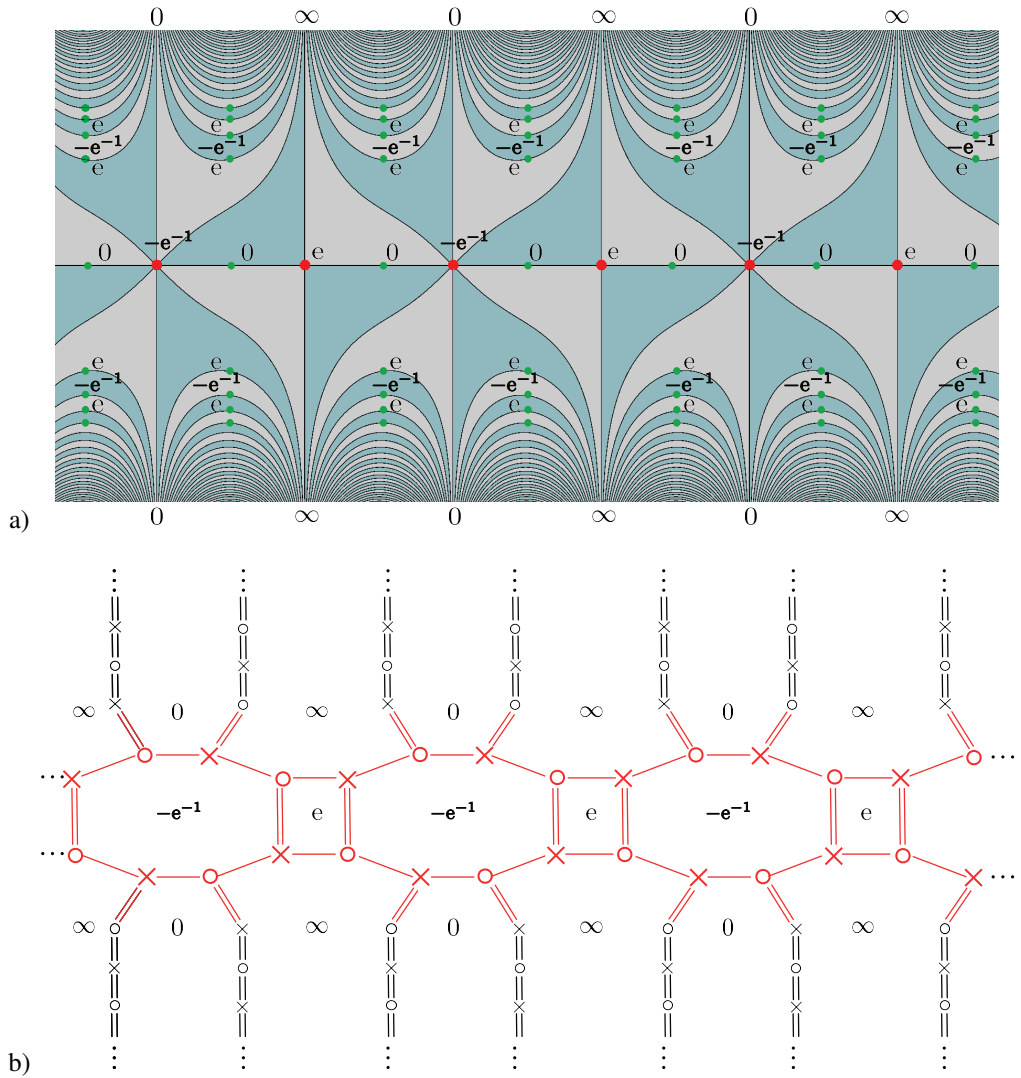


Figure 18: Speiser 4-tessellation and analytic Speiser graph of index  $q = 4$  for  $w(z) = \sin(z) \exp(\sin(z))$  with cyclic order  $\mathcal{W}_4 = [-\text{e}^{-1}, 0, \text{e}, \infty]$ . The nucleus is colored red and the logarithmic ends are colored black.

$$\mathbb{C}_z \cup \{\infty_{a_{1\pm}}, \infty_{a_{2\pm}}, \dots, \infty_{a_{\sigma\pm}}, \dots\}$$

determined by the asymptotic values  $a_{\sigma\pm} = 0$  and  $a_{\sigma\pm} = \infty$ , for odd or even  $\sigma$  respectively.

d) Its Speiser graph of index 4 is drawn in Figure 18.b. In this case the Speiser graph has an infinite number of unbounded 0-faces and  $\infty$ -faces, which correspond to logarithmic singularities over the asymptotic values 0 and  $\infty$ , respectively. Moreover, it also has an infinite number of bounded e-faces and  $-e^{-1}$ -faces. The bounded  $-e^{-1}$ -faces are 8-gons, thus they correspond to finitely ramified branch points of ramification index 4, while the bounded e-faces are 4-gons, thus they correspond to finitely ramified branch points of ramification index 2. Note that the nucleus consists of an infinite number of octagons and squares arranged in a horizontal line and an infinite number of “loose” edge bundles (in red), surrounded by an infinite number of logarithmic ends (in black).

**Example 10.6.** With Speiser graphs one can easily specify functions with “strange” behavior. For instance, consider the Speiser graph  $\mathfrak{S}_{EPH}$  of index 4 drawn in Figure 19.

- 1) On the ‘right subgraph’ of the Speiser graph  $\mathfrak{S}_{EPH}$ , we note a behavior similar to that of the Weirstrass  $\wp$ -function: a lattice with an infinite number of bounded faces that are not digons. These correspond to an infinite number of critical points of ramification index 2 with 4 distinct critical values  $\{w_1, w_2, w_3, w_4\}$ . This part of the graph has “elliptic conformal type behavior”.
- 2) On the ‘middle subgraph’ of the Speiser graph  $\mathfrak{S}_{EPH}$ , we observe a logarithmic end of the Speiser graph  $\mathfrak{S}_{EPH}$  consisting of an infinite sequence of digons with alternating labels 1 and 3. The logarithmic end is delimited by two unbounded faces labelled 2 and 4. This part of the graph has “parabolic conformal type behavior”.
- 3) On the ‘left subgraph’ of the Speiser graph  $\mathfrak{S}_{EPH}$ , we observe a tree structure with 4 edges on each vertex. Every face, of this part of the Speiser graph, is an unbounded face; thus we have an infinite number of unbounded faces. This part of the Speiser graph has “hyperbolic conformal type behavior”.

Of course, the actual conformal type of the associated function is hyperbolic.

Moreover, there are three “special” unbounded faces:

- the first one labelled 2, is delimited by the *bounded faces with labels 3 and 1*, of the lattice in (1) and of the logarithmic end in (2);
- the second one labelled 4, delimited by the *bounded faces with labels 3 and 1*, of the logarithmic end in (2), and by the *unbounded faces with labels 3 and 1*, of the tree in (3);
- the third one labelled 1, is delimited by the *unbounded faces with labels 2 and 4*, of the tree in (3), and by the *bounded faces with labels 2 and 4*, of the lattice in (1).
- Note that the nucleus (colored red) consists of all the Speiser graph minus the one logarithmic end (colored black) described in (2) above.

## References

- [1] W. P. Thurston, *What are the shapes of rational functions?*, mathoverflow, September 10, 2010. <https://mathoverflow.net/questions/38274/what-are-the-shapes-of-rational-functions>
- [2] S. Koch, T. Lei, *On balanced graphs, following W. Thurston*, D. P. Thurston (Ed.) in: What’s Next? The Mathematical Legacy of William P. Thurston, Princeton Univ. Press, 2020, pp. 213–231.
- [3] H. A. Schwarz, 1973. *Ueber diejenigen Fälle, in welchen die Gaussische hypergeometrische Reihe eine algebraische Function ihres vierten Elementes darstellt*, J. Reine Angewandte Mathematik, 75, 292–335. <http://eudml.org/doc/148203>
- [4] F. Klein, *Lectures on the Icosahedron*, Dover Phoenix Editions, USA, 2003.
- [5] A. Speiser, 1930. *Über Riemannsche Flächen*, Comment. Math. Helv. 2, 284–293.
- [6] R. Nevanlinna, *Analytic Functions*, Springer–Verlag, 1970.
- [7] E. Chislenko, Y. Tschinkel, 2007. *The Felix Klein Protocols*, Notices of the American Mathematical Society, 54, 8, 961–970. <https://www.ams.org/notices/200708/tx070800960p.pdf>

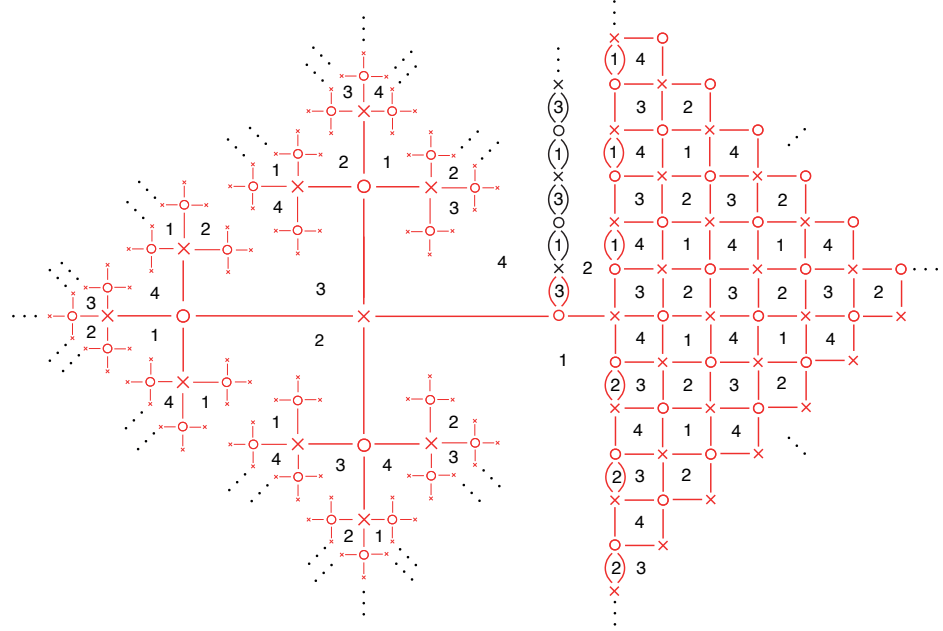


Figure 19: Speiser graph  $\Sigma_{EPH}$  of a function  $w(z)$  with  $q = 4$  distinct singular values that has an infinite number of bounded faces that are not digons, an infinite number of unbounded faces, and only one logarithmic tower. The function  $w(z)$  exhibits “behavior” associated to the three conformal types: elliptic, parabolic and hyperbolic. The nucleus is colored red and the unique logarithmic end is colored black.

- [8] L. J. González–Cely, J. Muciño–Raymundo, 2025. *Complex polynomials and tessellations on the Riemann sphere*, Results in Math. 80, 166, 1–28. <https://doi.org/10.1007/s00025-025-02473-8>
- [9] A. Alvarez–Parrilla, R. Gutiérrez–Soto, J. Muciño–Raymundo, 2025. *Tessellations of rational complex functions and the Riemann’s existence theorem*, <https://arxiv.org/abs/2510.21099>
- [10] A. A. Goldberg, I. V. Ostrovskii, *Value Distribution of Meromorphic Functions*, Trans. of the A.M.S., Vol. 236, Providence R. I., USA, 2008.
- [11] G. A. Jones, J. Wolfart, *Dessins d’Enfants on Riemann surfaces*, Springer, Switzerland, 2016.
- [12] A. Eremenko, S. Merenkov, 2025. *Nevanlinna functions with real zeros*, Illinois J. Math., 49, 4, 1093–1110. <https://doi.org/10.1215/ijm/1258138128>
- [13] R. Nevanlinna, 1932. *Über Riemannsche Flächen mit endlich vielen Windungspunkten*, Acta Math., 58(1), 295–373. <https://doi.org/10.1007/BF02547780>
- [14] W. Bergweiler, A. Eremenko, 1995. *On the singularities of the inverse to a meromorphic function of finite order*, Rev. Mat. Iberoamericana, 11, 2, 355–373. <http://dx.doi.org/10.4171/RMI/176>
- [15] A. Alvarez–Parrilla, J. Muciño–Raymundo, 2024. *Geometry of transcendental singularities of complex analytic functions and vector fields*, Complex Manifolds, 11, 1, 1–51. <https://doi.org/10.1515/coma-2024-0005>
- [16] M. Taniguchi, 2001. *Explicit representations of structurally finite entire functions*, Proc. Japan Acad. Ser. A Math. Sci., 77, 68–70. <https://projecteuclid.org/euclid.pja/1148393085>
- [17] M. Taniguchi, 2002. *Synthetic deformation space of an entire function*, Contemp. Math., 303, 107–136. <http://dx.doi.org/10.1090/conm/303/05238>

[18] A. Alvarez–Parrilla, J. Muciño–Raymundo, 2022. *Dynamics of singular complex analytic vector fields with essential singularities II*, J. Singul., 1–78. <https://www.journalofsing.org/volume24/article1.html>

[19] A. Alvarez–Parrilla, J. Muciño–Raymundo, S. Solorza, C. Yee–Romero, 2019. *On the geometry, flows and visualization of singular complex analytic vector fields on Riemann surfaces*, C. Cabrera et al. (Eds.) in: Proceedings of the 2018 Workshop in Holomorphic Dynamics, Instituto de Matemáticas, UNAM, México, Serie Papirhos, Actas 1, 21–109. <https://arxiv.org/abs/1811.04157>

[20] A. Alvarez–Parrilla, J. Muciño–Raymundo, 2017. *Dynamics of singular complex analytic vector fields with essential singularities I*, Conform. Geom. Dyn., 21, 126–224. <http://dx.doi.org/10.1090/ecgd/306>

[21] A. Alvarez–Parrilla, J. Muciño–Raymundo, 2021. *Symmetries of complex analytic vector fields with an essential singularity on the Riemann sphere*, Adv. Geom., 21, 4, 483–504. <http://dx.doi.org/10.1515/advgeom-2021-0002>

[22] F. Iversen, 1914. *Recherches sur les fonctions inverses des fonctions méromorphes*, Ph. D. Thesis, Helsingfords. <https://catalog.hathitrust.org/Record/007896919>

[23] A. Eremenko, 2021. *Singularities of inverse functions*, 1–16. <https://arxiv.org/abs/2110.06134>

[24] L. V. Ahlfors, L. Sario. *Riemann Surfaces*. Number 26 in Princeton Math. Series. Princeton University Press, Princeton, N.J., 1960.

[25] I. Richards, 1963. *On the classification of noncompact surfaces*, Trans. Amer. Math. Soc., 106, 1963, 259–269. <https://doi.org/10.1090/S0002-9947-1963-0143186-0>

[26] K. Strebel, *Quadratic Differentials*, Springer–Verlag, Berlin, 1984.

[27] J. Muciño–Raymundo, 2002. *Complex structures adapted to smooth vector fields*, Math. Ann., 229–265. <https://doi.org/10.1007/s002080100206>

[28] W. P. Thurston, *Three–Dimensional Geometry and Topology*, Vol. 1, Princeton University Press, USA, 1997.

[29] D. P. Sullivan. *Seminar on Conformal and Hyperbolic Geometry*. IHES Preprint, 1982.

[30] F. Pakovich, 2018. *On rational functions whose normalization has genus zero or one*, Acta Arithmetica, 182.1. <https://doi.org/10.4064/aa170113-28-8>

[31] D. Masoero, 2014. *Painleve I, coverings of the sphere and Belyi functions*, Constr. Approx., 39, 1, 43–74. <https://doi.org/10.1007/s00365-013-9185-3>

[32] P. G. Doyle, J. L. Snell, *Random walks and electric networks*, Carus Mathematical Monographs, 22, Math. Assoc. America, Washington, DC, 1984.

[33] W. Woess, *Random walks on infinite graphs and groups*, Cambridge Tracts in Mathematics, 138, Cambridge Univ. Press, Cambridge, 2000.

[34] R. D. Lyons, Y. Peres, *Probability on trees and networks*, Cambridge Series in Statistical and Probabilistic Mathematics, 42, Cambridge Univ. Press, New York, 2016.

[35] C. St. J. A. Nash–Williams, 1959. *Random walk and electric currents in networks*, Proc. Cambridge Philos. Soc., 55, 181–194. <https://doi.org/10.1017/S0305004100033879>

[36] P. M. Soardi, 1994. *Potential theory on infinite networks*, Lecture Notes in Mathematics, 1590, Springer, Berlin, 1994.

[37] R. J. Duffin, 1962. *The extremal length of a network*, J. Math. Anal. Appl., 5, 200–215.

[38] I. Benjamini, O. Schramm, 1997. *Every graph with a positive Cheeger constant contains a tree with a positive Cheeger constant*, Geom. Funct. Anal., 7, 3, 403–419. <https://doi.org/10.1007/PL00001625>

[39] J. Heinonen, P. Koskela, 1998. *Quasiconformal maps in metric spaces with controlled geometry*, Acta Math., 181, 1, 1–61. <https://doi.org/10.1007/BF02392747>

[40] Z.-X. He, O. Schramm, 1995. *Hyperbolic and parabolic packings*, Discrete Comput. Geom., 14, 2, 123–149. <https://doi.org/10.1007/BF02570699>

[41] K. Stephenson, *Introduction to circle packing*, Cambridge Univ. Press, Cambridge, 2005.

[42] J. Dodziuk, 1984. *Difference equations, isoperimetric inequality and transience of certain random walks*, Trans. Amer. Math. Soc., 284, 2, 787–794. <https://doi.org/10.1090/S0002-9947-1984-0743744-X>

[43] E. Drape, 1936. *Über die Darstellung Riemannscher Flächen durch Streckenkomplexe*, Deutsche Math., 1, 805–824.

[44] C. Blanc, 1937. *Les surfaces de Riemann des fonctions méromorphes*, Theses de l’entre-deux-guerres. <http://eudml.org/doc/192866>

[45] W. Lotz, 1951. *Zur Streckenkomplexdarstellung Riemannscher Flächen*, Mitt. Math. Sem. Giessen, 39, 25 pp.

[46] H. Habsch, 1952. *Die Theorie der Grundkurven und das Äquivalenzproblem bei der Darstellung Riemannscher Flächen*, Mitt. Math. Sem. Giessen, 42, i+51 pp. (13 plates).

[47] V. G. Tairova, 1962. *On “Streckenkomplexe” of closed Riemann surfaces of genus zero*, Izv. Vysš. Učebn. Zaved. Matematika, 4, 29, 155–160. <https://www.mathnet.ru/eng/ivm2089>

[48] V. G. Tairova, 1964. *“Streckenkomplexe” of a certain class of closed Riemann surfaces*, Sibirsk. Mat., Ž., 5, 929–951.

[49] L. Geyer, S. Merenkov, 2005. *A hyperbolic surface with a square grid net*, Journal D’analyse Mathematique, 96, 357–367. <https://doi.org/10.1007/BF02787835>

[50] R. Nevanlinna, V. Paatero, *Introduction to Complex Analysis*. Addison–Wesley, Reading, Massachusetts, 1969.

[51] J. Tomasini, 2015. *Realizations of branched self-coverings of the 2-sphere*, Top. and its Appl., 196, 31–53. <https://doi.org/10.1016/j.topol.2015.08.017>

[52] A. Schrijver, *Combinatorial optimization. Polyhedra and efficiency. Vol. A–C*, Algorithms and Combinatorics, 24,A–C, Springer, Berlin, 2003.

[53] L. Lovász, M. D. Plummer, *Matching theory*, corrected reprint of the 1986 original MR0859549, AMS Chelsea Publ., Providence, RI, 2009.

[54] L. R. Ford Jr., D. R. Fulkerson, *Flows in networks*, Princeton Univ. Press, Princeton, NJ, 1962.

[55] D. Gale, 1957. *A theorem on flows in networks*, Pacific J. Math., 7, 2, 1073–1082. [doi:10.2140/pjm.1957.7.1073](https://doi.org/10.2140/pjm.1957.7.1073)

[56] H. J. Ryser, 1957. *Combinatorial properties of matrices of zeros and ones*. Can. J. Math., 9, 371–377. [doi:10.4153/cjm-1957-044-3](https://doi.org/10.4153/cjm-1957-044-3)